

UNIVERSITY OF ESSEX

SCHOOL OF BIOLOGICAL SCIENCES

DATE OF SUBMISSION: OCTOBER 2016

Novel Techniques to Target Androgen Signalling in Prostate Cancer

A thesis submitted in accordance with the requirements of
the University of Essex for the degree of MSc by Dissertation
in Cell & Molecular Biology

By Angela Pine

SUPERVISOR: Dr Greg Brooke

Statement of Originality

Unless otherwise stated in the text, this thesis is the result of my own work.

Acknowledgements

I would like to thank my supervisor Dr Greg Brooke for all his help, support and guidance. I would additionally like to thank Dr Ralf Zwacka, as my MSD supervisory board member, who provided me with further insight and useful feedback during supervisory meetings. Special thanks are given to Dr Antonio Marco who designed the computational programme to enable the effective design of DNAzymes, and to Amna Allafi for her practical help with siRNA screen knockdown. Without the assistance of other members of the Brooke Group: Rosie Bryan and Mohammad Alkheilewi much of this work would not have been possible.

Lastly, I wish to thank everyone else who encouraged and inspired me throughout the completion of this research project. In this respect, I would especially like to thank my parents for their emotional and financial support. I would also like to thank my grandfather, who kindly provided me with inheritance that greatly helped to cover my tuition fees and living costs, enabling me to complete this MSD.

Abstract

Prostate cancer (PCa) is currently the second highest cause of male cancer related death in the UK. The majority of aggressive cases of PCa spread outside of the organ to areas such as the bone where it becomes difficult to treat. Current treatment options focus on targeting androgens, the male sex hormones. Reducing the levels or activity of androgens can shrink tumours significantly, however resistance is inevitable. Multiple mechanisms of resistance have been described, but often the tumours appear to remain dependent upon androgen signalling for growth. In these cases, a novel therapeutic approach is required.

This project aimed to develop novel methods to target the androgen signalling axis. Specifically, this project aimed to identify target key metabolic proteins driving PCa growth and to design DNAzymes (single stranded antisense molecules constructed of DNA) to down-regulate androgen receptor (AR) expression. We identified a DNAzyme, AM-3 that can degrade AR RNA and inhibit the proliferation of the LNCaP PCa cell line. A program was also developed by our collaborator, Dr Antonio Marco that could predict the efficiency of DNAzymes based on their target RNA. We demonstrated that DNAzymes generated by the program are more efficient compared to a published DNAzyme (DT99), known to cleave the same RNA.

We have also looked to expand on the knowledge gained by previous studies demonstrating that the AR regulates multiple metabolic enzymes to promote PCa growth. Hence an siRNA screen targeting 237 different genes involved in metabolism and cell traffic was performed in order to identify novel metabolic targets to inhibit PCa growth. LNCaP cells were transfected with the siRNAs and proliferation measured via crystal violet assays. A total of

15 potential target genes reduced LNCaP proliferation by more than 75%. The screen identified several previously characterized targets such as COX-2 and FASN, as well as novel targets AZIN2, STX8 and ALAS2 that have not been associated with PCa previously.

Abbreviations

1^o: Primary

2^o: Secondary

ACSL1: Acyl-CoA Synthetase Long-Chain Family Member 1

ADC: Antizyme Inhibitor 2

AF-1: Activation Function 1

AF-2: Activation Function 2

ALAS2: 5'-Aminolevulinate Synthase 2

AMD1: Adenosylmethionine Decarboxylase 1

AONs: Anti-sense oligonucleotides

APMAP: Adipocyte Plasma Membrane Associated Protein

AR: Androgen receptor

AZIN2: Antizyme Inhibitor 2

ARE: Androgen Response Element

BPH: Benign Prostatic Hyperplasia

CA7: Carbonic Anhydrase 7

CA13: Carbonic Anhydrase 13

cDNA: Complementary DNA

COX-2: Prostaglandin-Endoperoxide Synthase 2

CRPC: Castrate Resistant Prostate Cancer

C-Terminal: Carboxyl-Terminal

DBD: DNA Binding Domain

ddH₂O: Double distilled water

DEPC: Diethylpyrocarbonate

DHT: Dihydrotestosterone

DMSO: Dimethyl Sulphoxide

DNA: Deoxyribonucleic acid

dNTPs: Deoxyribonucleotides

dp: Decimal place

DZ: DNAzyme

E. coli: Escherichia coli

EDTA: Ethylenediaminetetraacetic acid

EP: E-type prostaglandin receptor

EtOH: Ethanol

FASN: Fatty Acid Synthase

FBS: Foetal bovine serum

FKBP11: FK506 Binding Protein 11

FSD1L: Fibronectin Type III And SPRY Domain Containing 1 Like

GUCY1A2: Guanylate Cyclase 1, Soluble, Alpha 2

HCl: Hydrochloric acid

HPV: Human Papilloma Virus

HRP: Horseradish peroxidase

HSP: Heat Shock Protein

kDa: Kilodaltons

LB: Luria Broth

LBD: Ligand Binding Domain

LH: Luteinizing Hormone

LHRH: Luteinizing Hormone Releasing Hormone

LNA: Locked Nucleic Acid

MIB: Mibolerone

Min/s: Minute/s

mL: Millilitre

NaCl: Sodium Chloride

nm: Nanometre

N-Terminal: Amino-Terminal

Nt: nucleotides

PBS: Phosphate Buffered Saline

PCa: Prostate Cancer

PCR: Polymerase Chain Reaction

PDILT: Protein disulphide isomerase-like protein of the testes

PORCN: Porcupine Homolog

PSA: Prostate Specific Antigen

PVDF: Polyvinylidene difluoride

RNA: Ribonucleic acid

Rpm: Revolutions per minute

RPMI: Roswell Park Memorial Institute

RT: Room temperature

RT-PCR: Real Time PCR

SDS: Sodium Dodecyl Sulphate

SDS-PAGE: Sodium Dodecyl Sulphate Polyacrylamide gel electrophoresis

siRNA: small interfering RNA

STX8: Syntaxin 8

TAE: Tris/Acetic acid/EDTA

TBE: Tris/Boric Acid/EDTA

TE: Tris/EDTA

T_m: Melting temperature

TNM: Tumour, Nodes & Metastasis

Tris-HCl: Tris-Hydrochloric Acid

UROD: Uroporphyrinogen Decarboxylase

UV: Ultra violet

μL: micro litre

μg: micro gram

Table of Contents

STATEMENT OF ORIGINALITY	2
ACKNOWLEDGEMENTS	2
ABSTRACT	3
ABBREVIATIONS	5
TABLE OF CONTENTS	9
LIST OF TABLES AND FIGURES	12
CHAPTER 1: INTRODUCTION	13
1.1 PROSTATE CANCER	13
1.1.1 NORMAL PROSTATE	13
1.1.2 PROSTATE CANCER	14
1.2 ANDROGEN HORMONES & THE ANDROGEN RECEPTOR (AR)	18
1.2.1 ANDROGEN HORMONE PRODUCTION	18
1.2.2 THE ANDROGEN RECEPTOR - GENE, STRUCTURE AND FUNCTION	19
1.3 TREATMENT OF PROSTATE CANCER	23
1.3.1 TREATMENT OPTIONS FOR PROSTATE CANCER	23
1.3.2 CASTRATE RESISTANT PROSTATE CANCER & RESISTANCE TO HORMONE THERAPIES	24
1.3.3 THE ROLE OF THE ANDROGEN RECEPTOR IN CRPC	26
1.4 NOVEL/ALTERNATIVE APPROACHES TO THE TREATMENT OF PROSTATE CANCER	29
1.4.1 TARGETING THE ANDROGEN RECEPTOR	29
1.4.2 ALTERNATIVE TECHNOLOGIES - DNAZYMES	31
1.4.3 ALTERNATIVE MECHANISMS TO TARGET THE AR PATHWAY	34
1.5 PROJECT OBJECTIVES	35
1, IDENTIFICATION OF DNAZYMES TO DOWN-REGULATE AR EXPRESSION.	36
2, TEST A COMPUTER MODEL AND SOFTWARE PROGRAM DEVELOPED TO AIDE WITH DNAZYME DESIGN	36
3, IDENTIFICATION OF METABOLIC PROTEINS THAT ARE ESSENTIAL FOR PCA PROLIFERATION.	36
CHAPTER 2: MATERIALS AND METHODS	37
2.1 REAGENTS, BUFFERS AND SOLUTIONS	37
2.2 BACTERIAL CULTURES, TRANSFORMATIONS, DNA PREPARATION AND <i>IN VITRO</i> TRANSCRIPTION OF RNA FOR USE IN DNAZYME EXPERIMENTS	38
2.2.1 POLYMERASE CHAIN REACTION (PCR)	38
2.2.2 AGAROSE GEL ELECTROPHORESIS	39
2.2.2.1 DNA Gel Electrophoresis	39
2.2.2.2 RNA Gel Electrophoresis	39
2.2.3 LIGATION OF PCR PRODUCTS INTO pGEM T-EASY VECTOR	40
2.2.4 TRANSFORMATION OF COMPETENT CELLS	40
2.2.5 INOCULATION OF LB BROTH FOR EXTRACTION OF PLASMID DNA	40
2.2.6 EXTRACTION OF PLASMID DNA	41
2.2.6.1 Mini preparation	41
2.2.6.2 Maxi preparation	41
2.2.7 ANALYZING SUCCESS OF PLASMID PRODUCTION	42
2.2.7.1 NanoDrop® ND-1000 UV/VIS Spectrophotometer	42

2.2.7.2 Plasmid verification by diagnostic digest and sequencing	43
2.2.8 <i>IN VITRO</i> TRANSCRIPTION OF RNA FOR DNAZYME CLEAVAGE REACTIONS	44
2.3 DNAZYME CLEAVAGE REACTIONS	44
2.4 VISUALISATION OF DNAZYME CLEAVAGE	45
2.4.1 DENATURING AGAROSE GELS	45
2.4.2 UREA PAGE	45
2.4.2.1 Diamond Stain	45
2.4.2.2 Methylene Blue Stain	46
2.4.2.3 Silver Staining	46
2.4.2.4 FAM labelled RNA	46
2.5 MAMMALIAN CELL CULTURE TECHNIQUES	47
2.5.1 CELL PASSAGING	47
2.5.2 CELL COUNTING AND PLATING	47
2.5.3 FREEZING AND DEFROSTING CELLS	48
2.6 TRANSIENT TRANSFECTION OF MAMMALIAN CELLS	48
2.6.1 siRNA KNOCKDOWN FOR SCREEN	48
2.6.2 TRANSFECTION OF AM-3 INTO MAMMALIAN CELL LINES	49
2.7 PROLIFERATION ASSAYS	49
2.7.1 CRYSTAL VIOLET ASSAY	49
CHAPTER 3: GENE THERAPY BY WAY OF DNAZYMES	51
<hr/>	
3.1 INTRODUCTION	51
3.1.1 DNAZYME DESIGN	51
3.1.2 A COMPUTATIONAL APPROACH TO DNAZYME DESIGN	51
3.2 RESULTS	52
3.2.1 <i>IN VITRO</i> TRANSCRIPTION OF RNA FOR USE IN CLEAVAGE REACTIONS	52
3.2.2 VISUALISATION OF RNA	55
3.2.2.1 Silver Staining	55
3.2.2.2 Methylene Blue Staining	57
3.2.2.3 Diamond Staining	58
3.2.4 DNAZYME CLEAVAGE REACTION OPTIMISATION – MgCl ₂ CONCENTRATION IN REACTION BUFFER	61
3.2.5 TESTING THE PROGRAM: DNAZYMES AGAINST THE ANDROGEN RECEPTOR	64
3.2.5.1 DNazyme AM-3 efficiency against AR RNA	66
3.2.6 TESTING THE PROGRAM: DNAZYMES AGAINST HPV16 RNA	72
3.3 DISCUSSION	76
3.3.1 COMPUTER MODEL AND SOFTWARE DESIGNED DNAZYMES AGAINST HPV16 RNA ARE MORE EFFICIENT THAN PREVIOUSLY PUBLISHED DT99	76
3.3.2 THE COMPUTER MODEL AND SOFTWARE CAN BE USED TO DESIGN EFFICIENT DNAZYMES AGAINST AR RNA	78
3.4 SUMMARY	79
CHAPTER 4: FINDING NOVEL METABOLIC TARGETS FOR THE TREATMENT OF CRPC	81
<hr/>	
4.1 INTRODUCTION	81
4.1.1 TARGETING METABOLIC PROTEINS FOR THE TREATMENT OF CRPC	81
4.2 RESULTS	81
4.2.1 OPTIMISATION OF AN siRNA SCREEN TO IDENTIFY NOVEL METABOLIC TARGETS FOR THE TREATMENT OF PROSTATE CANCER	81
4.2.1.1 Optimisation of Positive Control for use in siRNA screen	82
4.2.2 IDENTIFICATION OF METABOLIC TARGETS USING AN siRNA SCREEN	83
4.3 DISCUSSION	86
4.3.1 FATTY ACID BIOSYNTHESIS	86
4.3.1.1 The fatty acid biosynthesis pathway	86

4.3.1.2 The role of fatty acid biosynthesis in cancer	88
4.3.1.3 Blocking Fatty Acid Synthesis via inhibition of FASN & ACSL1	90
4.3.2 ARACHIDONIC ACID & PROSTAGLANDIN BIOSYNTHESIS	92
4.3.2.1 The arachidonic acid & prostaglandin bioynthesis pathway	92
4.3.2.2 The role of arachidonic acid & prostaglandin bioynthesis in cancer	93
4.3.2.3 Blocking prostaglandin bioynthesis via COX-2 inhibitors	94
4.3.3 POLYAMINE BIOSYNTHESIS	94
4.3.3.1 The polyamine biosynthesis pathway	94
4.3.3.2 The role of polyamine biosynthesis in cancer and its inhibition	97
4.3.4 OTHER TARGETS IDENTIFIED IN THE SIRNA SCREEN	98
4.3.4.1 FK506 Binding Protein 11 (FKBP11)	98
4.3.4.2 Guanylate Cyclase 1, Soluble, Alpha 2 (GUCY1A2)	98
4.3.4.3 Adipocyte Plasma Membrane Associated Protein (APMAP)/C20orf3	99
4.3.4.4 Syntaxin 8 (STX8)	99
4.3.4.5 Porcupine Homolog (PORCN)	100
4.3.4.6 Fibronectin type III and SPRY domain containing 1 like (FSD1L)	100
4.3.4.7 5'-Aminolevulinate Synthase 2 (ALAS2) & Uroporphyrinogen Decarboxylase(UROD)	100
4.3.4.8 Carbonic Anhydrases	101
4.3.5 Protein disulphide isomerase-like protein of the testes (PDILT)	102
4.4 SUMMARY	103
CHAPTER 5: CONCLUSION	104
BIBLIOGRAPHY	105

List of Tables and Figures

<u>TABLE 1.1 – THE TUMOUR, NODES AND METASTASIS (TNM) STAGING SYSTEM FOR PCA.</u>	<u>17</u>
<u>TABLE 2.1 – REACTION CONDITIONS FOR PCR</u>	<u>39</u>
<u>TABLE 2.2 - RESTRICTION ENZYMES AND DNA FRAGMENT SIZES PRODUCED BY DIGESTION</u>	<u>44</u>
<u>TABLE 3.1 – DNAZYMES AGAINST AR RNA AS PREDICTED BY THE COMPUTER MODEL AND SOFTWARE. * + = POOR EFFICIENCY, ++ = AVERAGE EFFICIENCY, +++ = GOOD EFFICIENCY</u>	<u>60</u>
<u>TABLE 3.2 – DNAZYMES AGAINST HPV16 RNA AS PREDICTED BY THE COMPUTER MODEL AND SOFTWARE. * + = POOR EFFICIENCY, ++ = AVERAGE EFFICIENCY, +++ = GOOD EFFICIENCY</u>	<u>73</u>
<u>TABLE 4.1 – TARGET GENES OF INTEREST INDICATED BY SIRNA KNOCK-DOWN SCREEN RESULTS.</u>	<u>85</u>

Chapter 1: Introduction

1.1 Prostate Cancer

1.1.1 Normal Prostate

The prostate is a secretory gland found only in males. It is located at the bottom of the bladder, wrapped around the urethra (Figure 1.1). The prostate consists of both glandular and muscular tissue and is divided into three zones, the transition zone, the central zone and the peripheral zone (Muruve, 2015). The transition zone is an area consisting of 10% glandular tissue. This zone has three regions which when enlarged can lead to urinary tract symptoms. The central zone surrounds the ejaculatory ducts and consists of 25% glandular tissue whilst the peripheral zone encompasses the lateral and posterior region of the prostate and is made up of 70% glandular tissue (Muruve, 2015). This tissue produces secretions that are known as prostatic fluid, which contains factors to nourish sperm as well as proteases that can digest the seminal clot.

The prostate gland is contained within a capsule composed of collagen, elastin and large amounts of smooth muscle, which contracts upon ejaculation forcing the prostatic fluid into the urethra. The size of the prostate gland is approximately 4 cm long and 2 cm wide however this can vary as males get older due to abnormalities of the prostate such as benign prostatic hyperplasia or cancer (Seeley *et al.*, 2006).

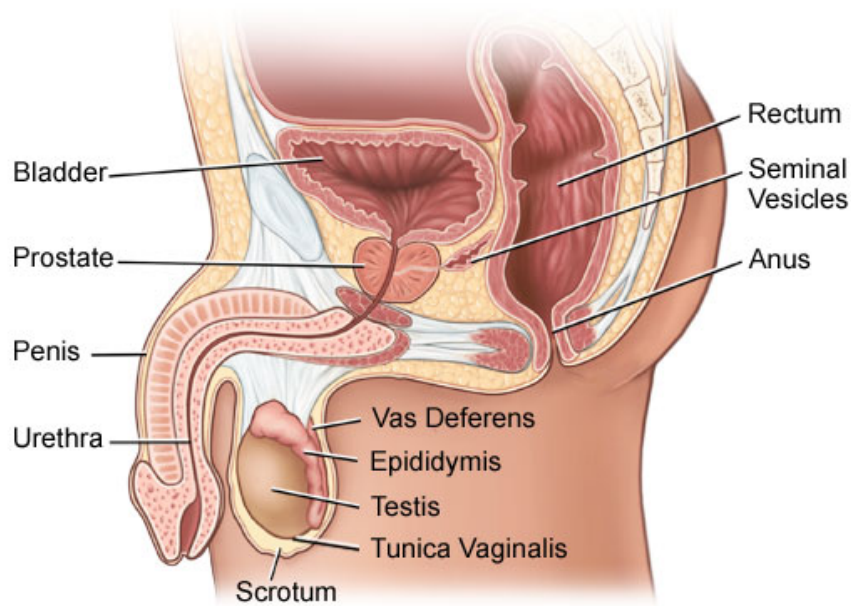


[Figure 1.1 - The male reproductive tract.](#)

The prostate is located at the base of the bladder, wrapped around the urethra (image taken from (Muruve, 2015)).

1.1.2 Prostate Cancer

Prostate Cancer (PCa) is the most common cancer among men in the UK, with over 40,000 cases diagnosed per annum, accounting for a quarter of all new cancer diagnoses (CRUK, 2014b). More than 10,000 men die from PCa in the UK per year, accounting for 13% of all male cancer deaths, making it the 2nd most common cause of cancer-related death behind only lung cancer.

There are several known statistically significant risk factors associated with PCa including ethnicity, family history of the disease and ageing (Giovannucci *et al.*, 2007), with over 75% of all PCa cases diagnosed in men over 65 years of age (CRUK, 2014b). Other factors such as cigarette smoking history, physical activity, body mass index, and height are associated with increased risk of fatal disease (Giovannucci *et al.*, 2007).

The most common form of PCa is adenocarcinoma which makes up 90% of all cases (NCI, 2015). Adenocarcinomas arise from the glandular tissue of the prostate, with 70% originating in the peripheral zone, 20% in the transition zone and only 1-5% in the central zone. Other cancers of the prostate make up the other 5% and are very rare and include small cell carcinoma, squamous cell carcinoma and transitional cell carcinoma (NCI, 2015).

Men presenting with symptoms such as difficulty passing urine, will have their prostates assessed via a digital rectal examination (DRE). Any inconsistency found upon examination, such as lumps or enlargement, would warrant further examination in order to diagnose and/or stage PCa (Seeley *et al.*, 2006). If abnormalities are found, then biopsies will be taken from six different regions of the prostate and a diagnosis is made based on the abnormality of the cells seen. When diagnosing PCa the histopathologist will grade the disease using the Gleason score system, which assigns a histological grade to the pattern of the tumour based on the differentiation of glandular cells in the tissue (numbered 1-5) (Figure 1.2). The two most common grades seen across the biopsies will be added together and to give the final Gleason score. The extent of the disease is determined based upon the Gleason score and the spread of the disease throughout the body. The tumour, nodes and metastasis (TNM) classification system is then used to stage the disease (Figure 1.3 & Table 1.1) (NCI, 2015). T records the primary tumour stage. The stages range from TX or T0 where no primary tumour can be seen to T4 where the tumour is invading nearby tissues or organs. The N or node records the presence of metastasis in lymph nodes and M records distant metastases up to M1c, which signifies the involvement of bone metastasis and the most severe stage of the disease.

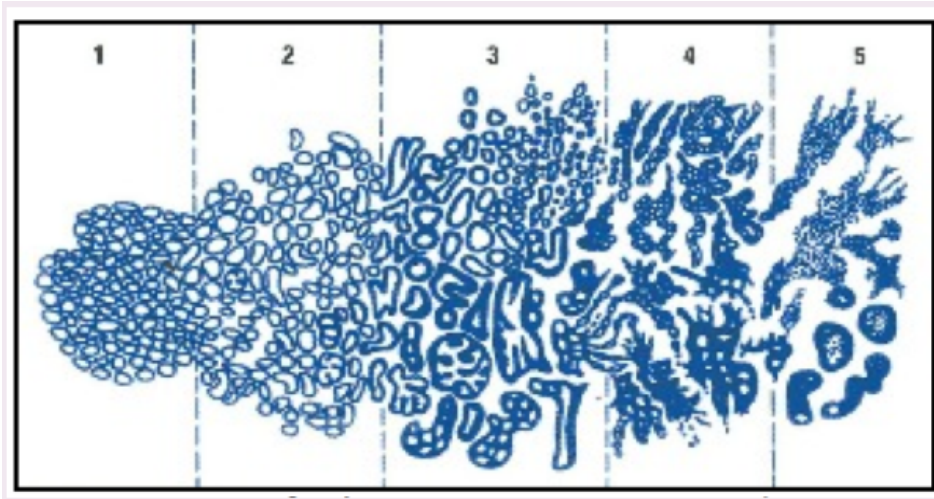


[Figure 1.2 - The Gleason scoring system.](#)

Cells are scored based on the degree of abnormality 1 being the lowest, 5 being the highest. The grades of the two most common patterns of cells are added together to give a score between 2 to 10. The higher the score the more aggressive the cancer (Figure taken from (Prostate, 2016b)).

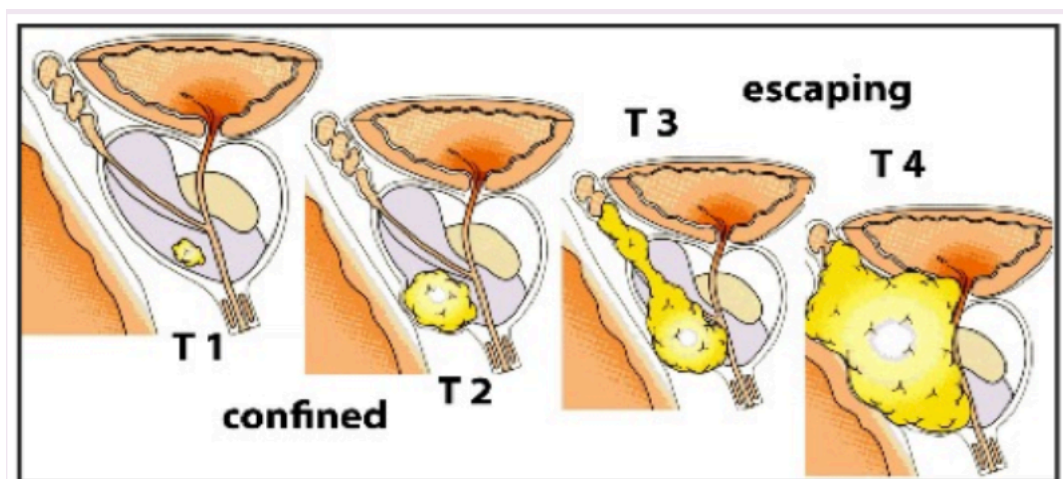


[Figure 1.3 - The TNM system.](#)

The current system for staging PCa. There are 4 stages (T1 to T4) where the tumour (in yellow) develops and spreads outside the prostate (grey) to other areas of the body (Figure taken from (Prostate, 2016a))

Table 1.1 – The Tumour, Nodes and Metastasis (TNM) Staging System for PCa.

Primary tumor (T)	
TX	Primary tumor cannot be assessed
T0	No evidence of primary tumor
T1	Clinically inapparent tumor not palpable or visible by imaging
T1a	Tumor incidental histologic finding in ≤5% of tissue resected
T1b	Tumor incidental histologic finding in >5% of tissue resected
T1c	Tumor identified by needle biopsy (because of elevated prostate specific antigen [PSA] level)
T2	Tumor confined within prostate; tumors found in 1 or both lobes by needle biopsy but not palpable or reliably visible by imaging
T2a	Tumor involves one-half of 1 lobe or less
T2b	Tumor involves more than one-half of 1 lobe but not both lobes
T2c	Tumor involves both lobes
T3	Tumor extends through the prostatic capsule; invasion into the prostatic apex, or the prostatic capsule is classified not as T3 but as T2
T3a	Extracapsular extension (unilateral or bilateral)
T3b	Tumor invading seminal vesicle(s)
T4	Tumor fixed or invades adjacent structures other than seminal vesicles (eg, bladder, levator muscles, and/or pelvic wall)
Pathologic (pT)*	
pT2	Organ confined
pT2a	Unilateral, involving one-half of 1 lobe or less
pT2b	Unilateral, involving more than one-half of 1 lobe but not both lobes
pT2c	Bilateral disease
pT3	Extraprostatic extension
pT3a	Extraprostatic extension or microscopic invasion of the bladder neck
pT3b	Seminal vesicle invasion
pT4	Invasion of the bladder and rectum
Regional lymph nodes (N)	
<i>Clinical</i>	
NX	Regional lymph nodes were not assessed
N0	No regional lymph node metastasis
N1	Metastasis in regional lymph node(s)
<i>Pathologic</i>	
PNX	Regional nodes not sampled
pN0	No positive regional nodes
pN1	Metastases in regional nodes(s)
Distant metastasis (M)*	
M0	No distant metastasis
M1	Distant metastasis
M1a	Nonregional lymph nodes(s)
M1b	Bone(s)
M1c	Other site(s) with or without bone disease

1.2 Androgen Hormones & The Androgen Receptor (AR)

1.2.1 Androgen Hormone Production

The development of PCa is dependent upon male hormones known as androgens (Pine, 2016). Androgens are steroid hormones responsible for the normal growth of male characteristics. The most common androgens are testosterone (T) and dihydrotestosterone (DHT) which are produced under the control of the hypothalamo-pituitary gonadal axis (Figure 1.4). Androgen production is stimulated when luteinizing hormone releasing hormone (LHRH) is released from the hypothalamus inducing the release of gonadotrophins such as luteinising hormone (LH) and adrenocorticotrophic hormone (ACTH) from the anterior pituitary gland ((Lonergan and Lonergan PE, 2011; Lonergan and Tindall, 2011). The LH then acts on the leydig cells of the testes to stimulate the release of testosterone. The testes are responsible for 95% of all testosterone released with the other 5% coming from the adrenal glands (Tsao *et al.*, 2016). Testosterone is converted to DHT (the more active androgen) by 5 α -reductase, and both can act as ligands for the AR (Schalken and Fitzpatrick, 2016). Androgens have multiple target sites in males such as the testes, seminal vesicles, bone marrow and the prostate which it stimulates to grow and function via the AR (Dart, 2013).

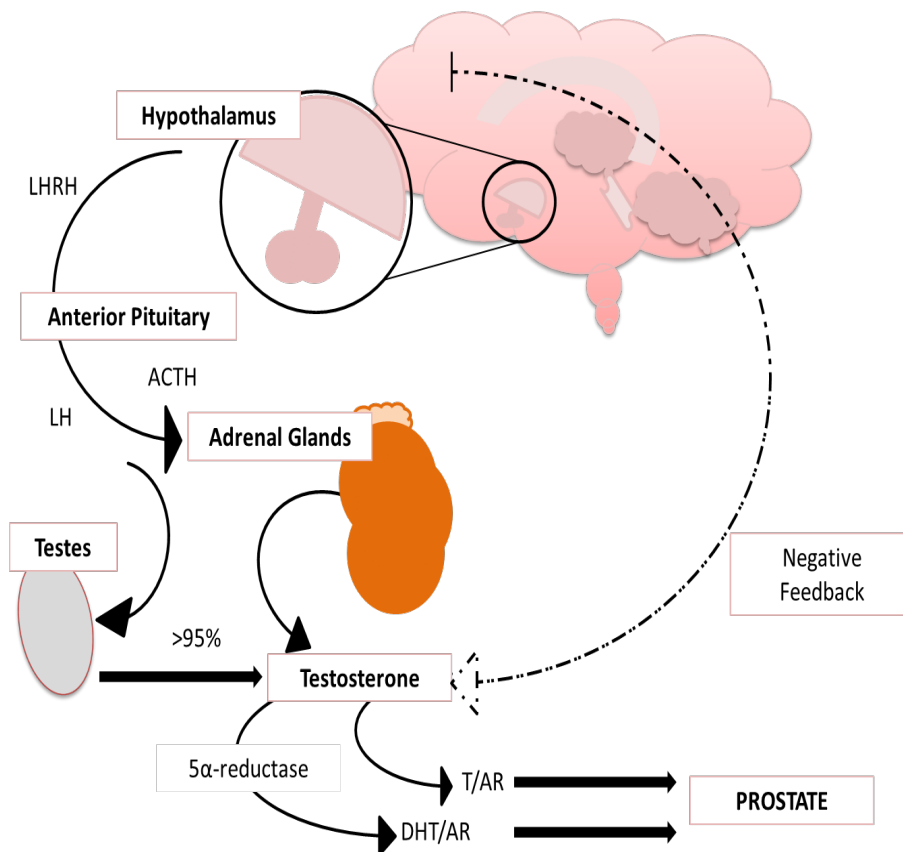


[Figure 1.4 - The hypothalamo-pituitary-gonadal axis.](#)

This axis and the feedback loop is responsible for prostate growth. Luteinizing hormone releasing hormone (LHRH) is released from the hypothalamus inducing the release of gonadotrophins such as luteinizing hormone (LH) and adrenocorticotrophic hormone (ACTH) from the anterior pituitary gland. The LH then acts on the leydig cells of the testes to stimulate the release of testosterone. Testosterone (T) is converted to DHT by 5 α -reductase. These androgens then act on their target sites, such as the prostate (adapted from (Lonergan and Tindall, 2011)).

1.2.2 The Androgen Receptor - Gene, Structure and Function

The AR is a ligand activated transcription factor responsible for mediating the effects of the hypothalamo-pituitary-gonadal axis on prostate growth and function. It is a member of the steroid hormone receptor family and the gene is located at Xq11-12 (Figure 1.5) (Schalken and Fitzpatrick, 2016).

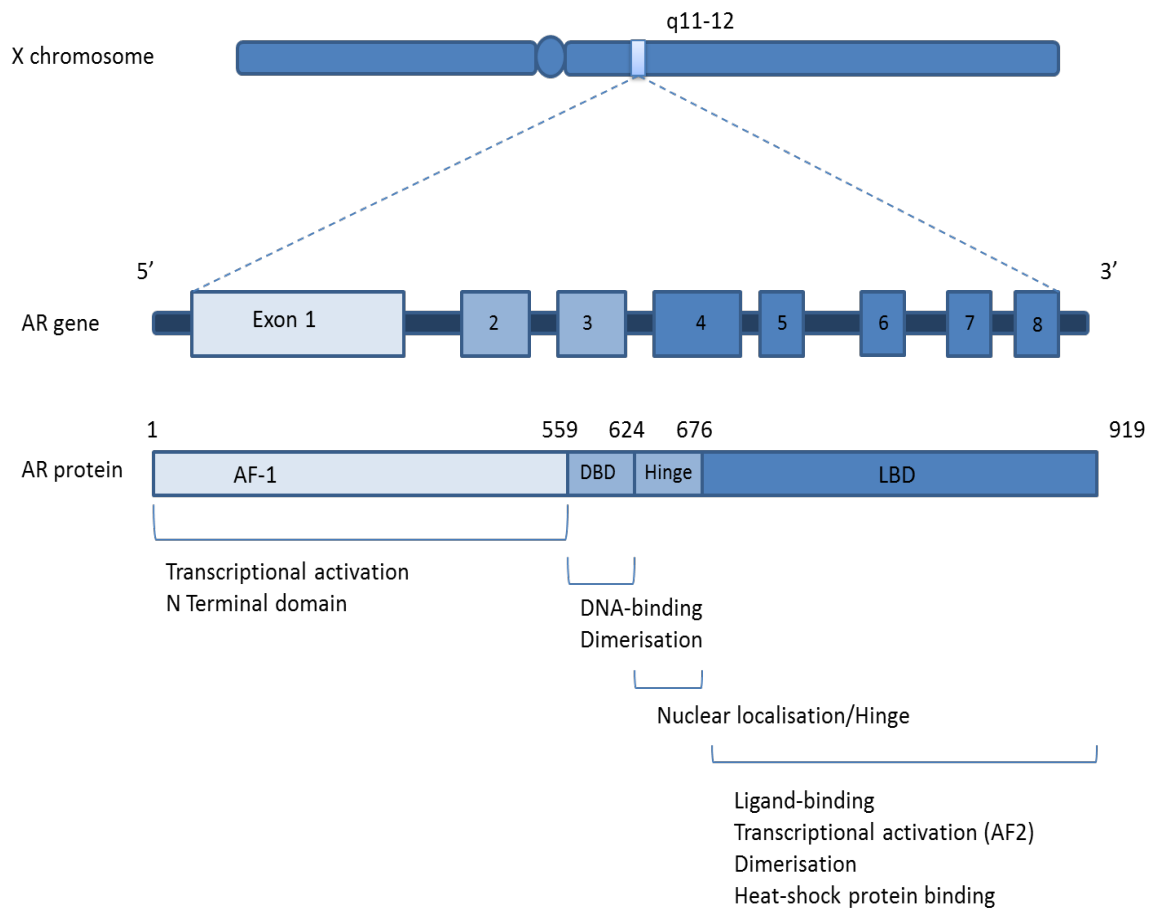


[Figure 1.5 - Schematic representation of the AR gene and its location on the X chromosome \(q11-12\).](#)

The AR gene comprises 8 exons. The AR is a modular protein consisting of two activation function sites (AF1 located between amino acids 1 and 559, and AF2), an N terminal domain, a DNA binding domain (DBD) for dimerisation and DNA binding (located between amino acids 559 and 624), a hinge region (624 – 676) and a ligand binding domain (LBD) (676-919) (adapted from (Schalken and Fitzpatrick, 2016)).

The general structure of the AR was first described in 1988 by Evans (Evans, 1988). The AR consists of four functional domains; two activation functions, AF-1 is located in the N-terminus and the AF-2, which is the weaker of the two domains located in the C-Terminus in the ligand binding domain (LBD). These AF domains bind the activators of transcription (co-activators) (Figure 1.5). There is a central DNA binding domain (DBD) through which the receptor interacts with DNA, and the LBD into which androgen binds (Brooke *et al.*, 2014).

The unliganded receptor is predominantly located in the cytoplasm, bound to heat shock proteins (HSPs) (Figure 1.6). These HSPs stabilise the structure of the AR and hold the receptor in a ligand-binding competent state. Once androgen binds to the AR, the HSPs dissociate promoting receptor dimerisation, tyrosine kinase phosphorylation and translocation of the AR to the nucleus (Mostaghel *et al.*, 2014; Taplin, 2007). Once in the nucleus the AR binds to androgen response elements (ARE) which are located in the promoter and enhancer regions of target genes, and via the recruitment of co-regulatory proteins, forms an active transcription complex (Figure 1.6). Co-activators containing histone acetyltransferase (HAT) activity, or that have recruited proteins with HAT activity, relax the chromatin structure to a more transcriptionally active form allowing the basal transcription machinery to bind and subsequently initiate transcription. In contrast, co-repressors such as the silencing mediator of retinoid and thyroid (SMRT) and nuclear receptor co-repressor (NCOR) mediate chromatin condensation and promote gene silencing (Mostaghel *et al.*, 2014; Taplin, 2007).

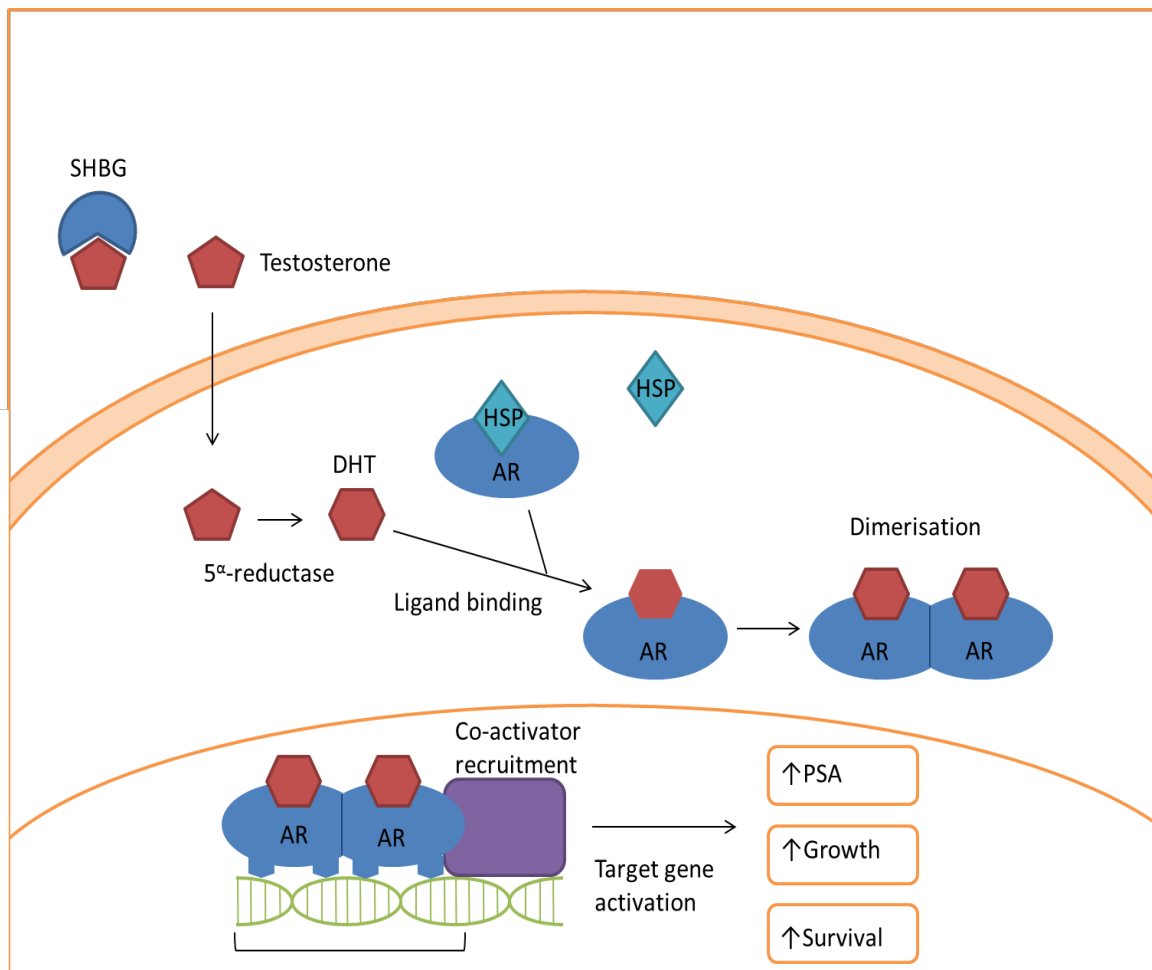


[Figure 1.6 – Schematic representation of the AR pathway.](#)

Testosterone is bound to sex-hormone-binding globulin (SHBG) and albumin (not shown) in the blood. Free testosterone exchanges with this and enters the cell where it is converted to dihydrotestosterone (DHT) by 5 α -reductase. DHT binds to the AR promoting the dissociation of heat shock proteins (HSPs) and receptor phosphorylation. The AR dimerises and binds to androgen response elements. Co-activators and co-repressors are recruited to the AR complex leading to alterations in gene expression (adapted from (Schalken and Fitzpatrick, 2016; Universitet, 2016b)).

Studies using tools such as DNA microarray, chromatin immunoprecipitation-on-chip (ChIP-on-chip) and chromatin immunoprecipitation sequencing (ChIP-seq) have identified the AR transcriptional network in PCa (Chng and Cheung, 2013; Lamb *et al.*, 2014; Takayama and Inoue, 2013; Takayama *et al.*, 2007). Such studies have demonstrated that of the genes regulated in response to androgen signalling, genes involved in metabolism appear to be

enriched. For example, in a study conducted by Massie *et al.* it was found that the AR regulates a number of genes involved in metabolism. Up-regulated expression of key steps in glucose uptake and glycolysis were seen and it was predicted that the AR may therefore facilitate cell growth by promoting glucose uptake and anabolic metabolism (Massie *et al.*, 2011).

1.3 Treatment of Prostate Cancer

1.3.1 Treatment Options for Prostate Cancer

The treatment given to patients with PCa will depend on the grade and stage of the disease. Low grade tumours tend to grow slowly so patients, especially if they are older tend to be monitored rather than treated (termed watchful waiting). PCa that is contained within the capsule can be removed via surgery or treated using radiotherapy. For PCa that has spread outside of the capsule then hormone therapy is the most common option (CRUK, 2014a).

Androgen hormones have been shown to drive prostate tumour growth, and as such therapies often target the androgen-signalling pathway. Androgen ablation drugs were first described over 60 years ago by Huggins and Hodges in the form of androgen deprivation therapy (ADT) (Huggins and Hodges, 1941). These drugs known as hormone therapies aim to block the production and/or action of androgens (Goktas and Crawford, 1999; Heidenreich *et al.*, 2014). Hormone therapy can be divided into two main categories: anti-androgens that bind to and inhibit the receptor and LHRH analogues that aim to inhibit androgen production. LHRH analogues work via the hypothalamo-pituitary axis (Figure 1.4) and block the production of androgens (Brooke and Bevan, 2009) however, these do not affect the concentrations of adrenally produced androgen precursors which can be converted to dihydrotestosterone in the prostate itself (Brooke and Bevan, 2009). Anti-

androgen therapies such as bicalutamide also target the androgen signalling axis. Antiandrogens bind to the AR and hold it in an inactive state thereby preventing the binding of ligand (androgens). Some, such as enzalutamide, bind with higher affinity than androgens themselves and block translocation of the AR into the nucleus (Ammannagari and George, 2016). The exact mechanism of action of antiandrogens is unclear, however it has been found that they can act, in part, by recruiting co-repressors to regulatory regions of target genes (Brooke and Bevan, 2009). Despite this, AR expression does not correlate with prognosis and the duration of response to ADT, as is the case with oestrogen and progesterone receptors in breast cancer (de Vere White *et al.*, 1997).

1.3.2 Castrate Resistant Prostate Cancer & Resistance to Hormone Therapies

Hormone therapy is initially successful in increasing patient survival in the majority of patients, however it is not curative as in 2009 it was noted that only 5-10% of patients survive more than 10 years after the start of treatment (Harris *et al.*, 2009; Tangen *et al.*, 2003). Patients that initially respond to hormone therapy also invariably relapse with tumours becoming unresponsive to therapy and recurring within 1-3 years (Katsogiannou *et al.*, 2015). This often leads to tumours progressing to the aggressive castrate resistant stage (castrate resistant prostate cancer (CRPC)) in which patients have a mean survival period of just 13.5 months (Hirst *et al.*, 2012). Despite an 11% decrease in mortality rates over the last 14 years (CRUK, 2014b), drug resistance remains a significant issue in the clinical management of the disease (Semenas *et al.*, 2012) and few therapeutic options exist for this stage of the disease.

Once hormone therapy fails patients are often withdrawn from the treatment and in approximately 30% of cases the tumour will stop growing or even shrink for some months

(CRUK, 2014a). This is known as the Anti-Androgen Withdrawal Response (AAWR), which is thought to occur as a result of the AR acquiring somatic mutations that reduce ligand specificity and enable antagonists such as anti-androgens to work as agonists (Penning, 2015). Few therapeutic options are available for CRPC. Drugs that are available include docetaxel, cabazitaxel, abiraterone, enzalutamide, estramustine and the steroids prednisone, and mitoxantrone. Docetaxel has been shown to have a response in some patients (Petrylak, 2003), as has cabazitaxel (post docetaxel treatment) but both require combination with steroids and only increase mean survival by 2-8 months (Berthold *et al.*, 2008; de Bono *et al.*, 2010; Petrylak *et al.*, 2004; Tannock *et al.*, 2004).

In recent years two treatments have been approved that appear to have value for this stage of the disease; enzalutamide, (previously known as MDV3100) is a second-generation AR inhibitor. After Phase III clinical trials enzalutamide showed a 4.8 month survival benefit (Ramadan *et al.*, 2015).

Abiraterone acetate (AA) is an androgen biosynthesis inhibitor which works by inhibiting CYP17 (an enzyme required for androgen biosynthesis) (Dinh *et al.*, 2016), thus blocking the synthesis of adrenal androgens into the more potent DHT. Abiraterone decreases serum and tissue androgen levels and has led to the increased survival of CRPC patients by on average 3 months (Mostaghel *et al.*, 2014). AA has been approved for use in the UK in combination with prednisone to reduce side effects. However, patients can only be prescribed AA in the UK once they have become resistant to chemotherapy and/or hormone therapy (NICE, 2014).

Despite the promise of these new therapies, resistance to these has also been described. For example the AR F876L mutation has been associated with enzalutamide resistance (Korpal *et al.*, 2013b). Korpal *et al.* discovered that this mutation switches the functionality of enzalutamide from that of an antagonist to an agonist (Korpal *et al.*, 2013a). Novel methods to target the AR signalling axis are therefore required for the treatment of the disease.

1.3.3 The Role of the Androgen Receptor in CRPC

Much evidence exists to suggest that the AR continues to drive CRPC, even in the androgen-depleted environment. The mechanisms responsible for the development of CRPC include; increased AR sensitivity (hypersensitive AR) due to amplified AR, or increased levels of DHT. AR over-expression is found in approximately 40% of resistant tumours and hyper-sensitises the pathway to low levels of androgens (Feldman and Feldman, 2001). Another mechanism is ligand independent activation (ligand independence) of the AR as a result of kinase signalling such as tyrosine kinase Ack1, which has been shown to phosphorylate the AR and regulate AR activity in the absence of ligand (Mahajan *et al.*, 2010). AR activity can also be affected by over expression of co-activators and reduced levels of co-repressors (Figure 1.7). Finally AR mutations (Feldman and Feldman, 2001) and variants (Guo and Qiu, 2011) have been shown to play a vital role in CRPC.

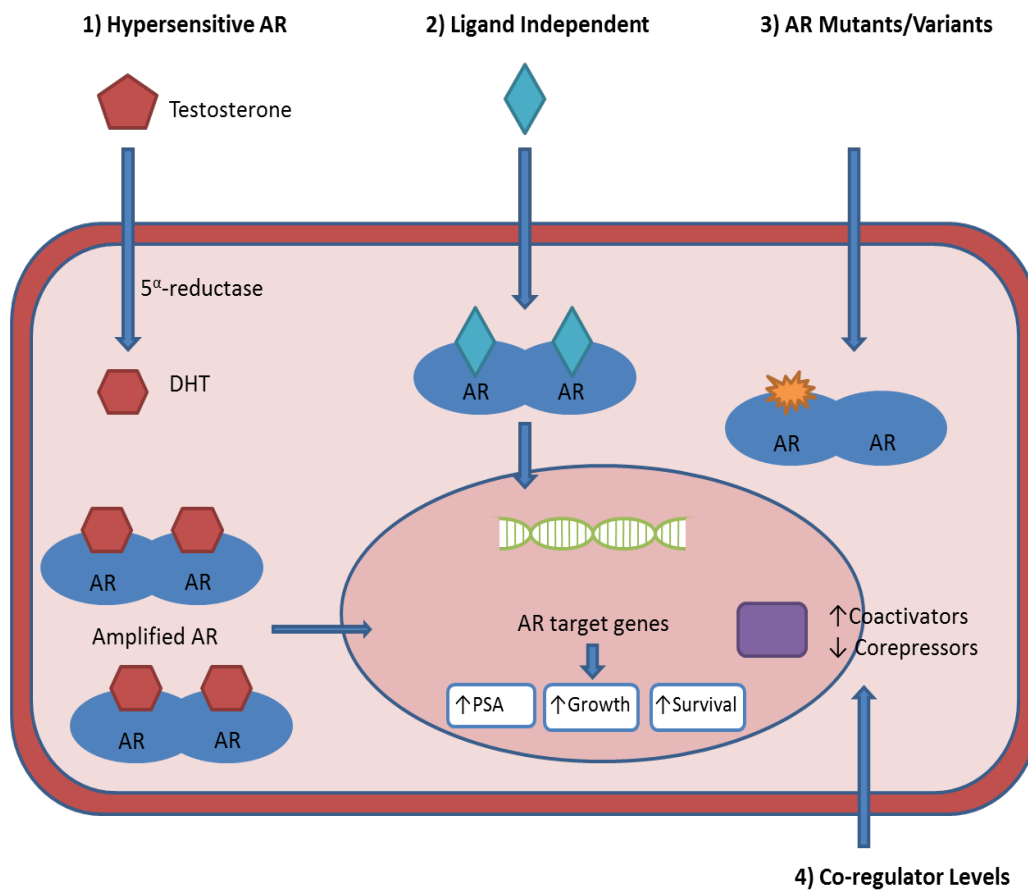


[Figure 1.7 - Schematic of possible mechanisms of CRPC.](#)

The hypersensitive pathway, the ligand independent pathway and the effect of altered co-regulator levels on the AR (adapted from (Schalken and Fitzpatrick, 2016).

AR mutations are very rare in early PCa but their frequency increases up to 50% in cases of CRPC (Brooke and Bevan, 2009). The majority of mutations associated with PCa are found in the AR LBD (Brooke and Bevan, 2009; Chan *et al.*, 2015) and many appear to alter ligand binding specificity, allowing other ligands (e.g. other hormones) to bind to the receptor and induce an active conformation. This means that molecular AR-modifications are often responsible for resistance to androgen deprivation treatment (Steinestel *et al.*, 2015).

AR variants (AR-Vs) have also been shown to be important in therapy resistance. These variants (AR-Vs) are generated by splicing and 7 variants have been identified in CRPC (Guo and Qiu, 2011) (Figure 1.8). These variants include the most common variant found in CRPC, an AR splice variant referred to as AR3/AR-V7. Such variants have been shown to drive androgen-independent cell proliferation and promote therapy resistance. This means that AR-Vs are attractive targets for novel therapies of CRPC.

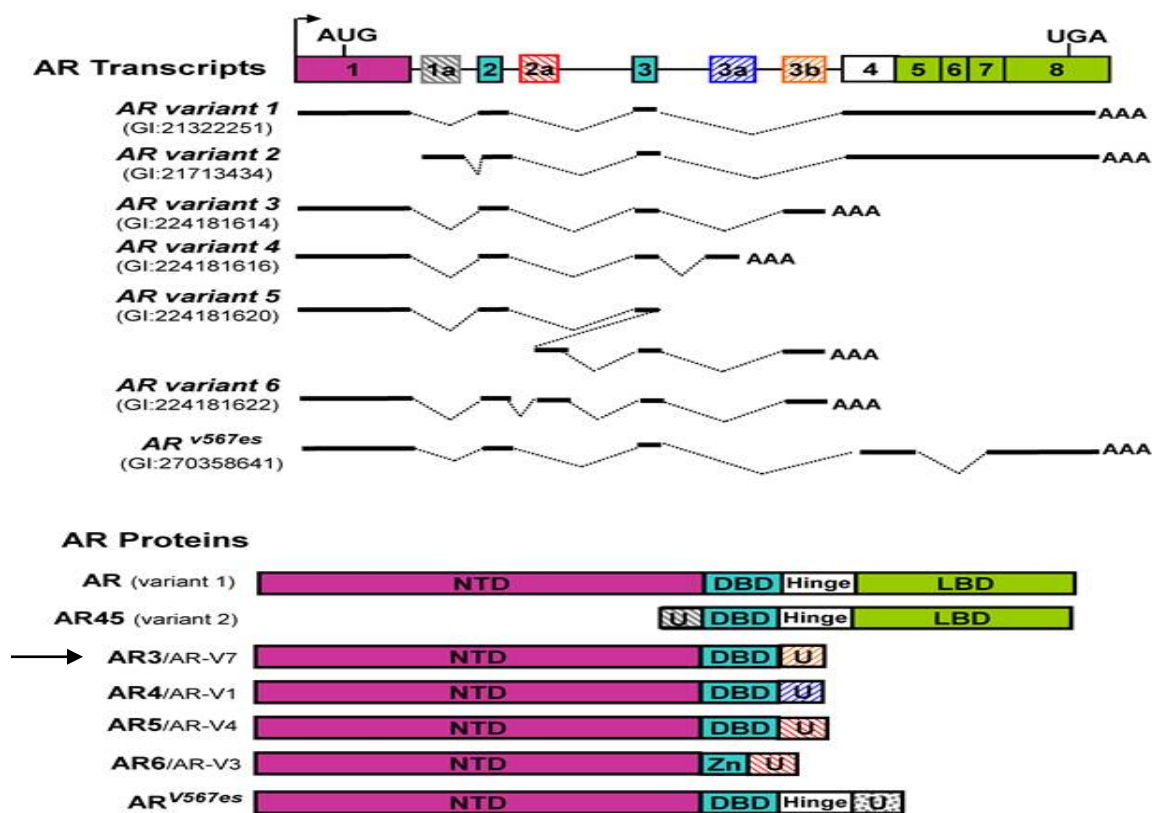


Figure 1.8 – Common AR variants found in castrate resistant PCa.

The N Terminal domain (NTD) remains unchanged in all variants except variant 2, as is the DNA binding domain (DBD), which is changed in AR6/AR-V3. Zn = zinc domain, U = uracil. (taken from (Guo and Qiu, 2011).

1.4 Novel/Alternative Approaches to the Treatment of Prostate Cancer

1.4.1 Targeting the Androgen Receptor

Due to androgen signalling remaining active in CRPC (Semenas *et al.*, 2012), the AR remains a valid target for the treatment of this stage of the disease. The development and introduction of the two drugs enzalutamide and abiraterone acetate are examples of progress still being made in the development of anti-androgens. Despite promising results resistance to these drugs is an issue, meaning that other treatments are still under development for the continued treatment of CRPC (Li *et al.*, 2013).

Therapeutics still under development that have showed promise include inhibitors of the LBD (ARN-509 & ODM-201) and androgen synthesis inhibitors (TOK-001/Galeterone (CYP17 lyase inhibitor), VT-464 (CYP17,20 lyase inhibitor)). The LBD inhibitors ARN-509 and ODM-201 have a similar mechanism of action to enzalutamide, inhibiting AR nuclear translocation and DNA binding. Both ARN-509 and ODM-201 have been shown to have improvements over previous agents since that have reduced adverse side effects, such as seizures, due to a lower dose requirement (Clegg *et al.*, 2012; Proverbs-Singh *et al.*, 2015). Androgen synthesis inhibitors that have been developed are similar to AA in that they inhibit CYP lyase enzymes. TOK-001 and VT-464 have both shown to be effective in clinical trials, with TOK001 even displaying AR antagonist properties alongside it's CYP17 inhibitor status, towards both wild-type and mutant AR, even degrading AR protein (Njar and Brodie, 2015). VT464 has shown a greater effect on the AR pathway reducing DHT and testosterone more than AA in clinical trials (Toren *et al.*, 2015).

AR-Vs mean there is a need to develop therapies that do not depend on the availability of a LBD (Antonarakis *et al.*, 2014), as such targeting the AR axis via new methods is an evolving

field and anti-androgens are not the only method being pursued. New ways of targeting the AR pathway are constantly being sought such as; N terminal targeting, “engineered repressors” and down-regulation of the AR by way of antisense oligonucleotides, to name just a few (Brooke *et al.*, 2014; Yamamoto *et al.*, 2015). Targeting the N terminal of the AR has been achieved by EPI-001 a small molecule antagonist that inhibits protein-protein interactions and thereby blocks transcriptional activity of the AR. This results in reduced growth of tumours in xenograft models (Myung *et al.*, 2013). The anti-angiogenic drug endostatin has been investigated for an anti-tumour effect in CRPC cells in culture. It has been observed in preclinical studies that endostatin is structurally similar to the AR. Endostatin binds to the AF-2 region of the AR specifically by way of a protein-protein interaction thereby reducing expression of AR regulated genes and demonstrating an AR dependent effect. The study showed that cells treated with endostatin also exhibited significantly lower levels of AR (Lee *et al.*, 2015).

Engineered repressors inhibit AR activity by way of an interaction motif that binds to the AR LBD fused to repression domains. Brooke *et al* (2014) described these repressors and studied their mechanism in preclinical trials. They demonstrated that they do inhibit the growth of PCa cells, however further work is needed to design a delivery method for such a therapy (Brooke *et al.*, 2014).

The use of antisense oligonucleotides (AONs) is not a new concept and these short fragments of nucleic acid have been under clinical development since the early 1990's. The approval of the first AON for therapeutic use against cytomegalovirus retinitis in patients with AIDs came in 1998 (Roehr, 1998). However, the use of an AON against cancer has been slow to be realised. AON's are single stranded oligonucleotides that induce RNA

degradation. One such AON has been developed for use in CRPC, ENZ-4176. ENZ-4176 is a third generation AON that utilises a locked structure to target mRNA with greater binding affinity despite reduced oligonucleotide length (Gleave and Monia, 2005). The AON specifically binds to the complementary region of the mRNA leading to destruction of the target and ultimately reducing protein expression. ENZ-4167 is designed to target AR mRNA binding at exon 4 in the hinge region. ENZ-4167 reached phase Ia clinical trials however, results showed minimal activity of the AON at the doses tested and further development of the compound has been halted due to business reasons (Bianchini *et al.*, 2013).

1.4.2 Alternative Technologies - DNAzymes

Recent advances in genomics and molecular oncology mean that personalised treatments and targeted cancer therapy has been seen to be on the horizon. Alternative technologies such as AONs, small interfering RNA, ribozymes and DNAzymes are under development as novel cancer therapies (Beale *et al.*, 2003; Dass *et al.*, 2008; Wu *et al.*, 1999). DNAzymes are single stranded antisense molecules, however these are constructed from DNA. DNAzymes were first discovered in 1994 by Professor Ronald R. Breaker (Breaker and Joyce, 1994). The '10-23' DNAzyme was described by Santoro and Joyce in 1997 (Santoro and Joyce, 1997). This DNAzyme contains a catalytic core of 15 nucleotides and substrate binding arms of variable length and sequence that interact with target RNA via Watson-Crick based interactions and confer specificity (Figure 1.9). The 10-23 DNAzyme cleaves RNA between an unpaired purine (A, G) and a paired pyrimidine (U, C) in the presence of Mg^{+2} via a de-esterification reaction (Figure 8) (Dass *et al.*, 2008).

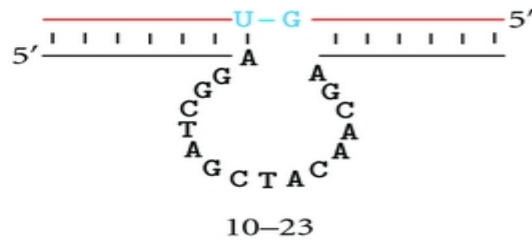


[Figure 1.9 - The general structure of a 10-23 DNAzyme.](#)

The DNAzyme (black) consists of two substrate recognition arms containing an unpaired purine and paired pyrimidine flanking the 15 nucleotide catalytic core (image taken from (Dass *et al.*, 2002)).

DNAzymes are both flexible in cleavage site selectability and specific at the same time. Their substrate specificity is flexible in that they can cleave at any purine:pyrimidine junction in any RNA, however a single base mismatch in the substrate binding arm significantly decreases their cleavage activity (Babunageswararao, 2011). Ensuring the DNAzyme is stable is important. DNAzymes like other oligonucleotides are susceptible to nuclease attack within the intracellular environment. In order to stabilize the molecules modifications, such as the incorporation of a 3'-3' inverted nucleotide at the 3' terminus of the DNAzyme, prevents exonuclease degradation and can increase the duration that the molecule remains functionally active in serum (Dass *et al.*, 2002; Reyes-Gutierrez and Alvarez-Salas, 2009).

Ever since the inception of the 10-23 DNAzyme by Santoro and Joyce in 1997, DNAzymes have been derived by what is fundamentally hand design. Each DNAzyme recognizes nucleotide residues within the target RNA via complementary binding arms, resulting in phosphodiester bond cleavage of the target and generation of two RNA fragments. DNAzymes are ranked according to their cleavage efficiency. Identifying the most efficient DNAzyme can be a labour intensive process as each DNAzyme has to be tested *in vitro*. The

cleavage efficiency for each DNAzyme varies based on properties of the target, such as secondary structure (and therefore cleavage site accessibility) and on properties of the DNAzyme itself such as the four potential cleavage sites offered by the 10-23 DNAzyme; GU, GC, AU and AC purine:pyrimidine junction pairings which can be cleaved with different efficiencies (Santoro and Joyce, 1997).

DNAzymes are being assessed for many applications. To date DNAzymes currently undergoing clinical trials include: Sterna Biologicals DNAzyme hgd40, a GATA-3 antagonist for the treatment of Th2-driven asthma (completed phase IIa clinical trials) (NIH, 2012), ulcerative colitis (due to complete phase II clinical trials in March 2016) (NIH, 2014a) and atopic eczema (due to complete phase IIa clinical trials) (NIH, 2014b). Results for these trials are yet to be published. The aim of these therapies is to target the transcription factor GATA-3. It is known that GATA-3 plays a key role in the immune responses driven by Th2 and thus the production of cytokines as well as interleukins 4, 5 and 3. The DNAzyme hgd40 has been designed to cleave GATA-3 mRNA reducing specific cytokine and interleukin production and thereby reducing localised inflammation (Dicke *et al.*, 2012).

Another DNAzyme that has completed phase II clinical trials is DZ1 (DNAzyme targeting EBV-LMP1), developed for the treatment of nasopharyngeal carcinoma. Nasopharyngeal carcinoma is common in southern China and in 90% of cases Epstein-Barr virus-encoded latent membrane protein 1 (EBV-LMP1) has been detected (Lu *et al.*, 2008). This oncoprotein is involved in many signalling pathways, that when constitutively activated increases proliferation and decreases apoptosis (Morris *et al.*, 2009). It has also been linked to the up-regulation of VEGF (Wang *et al.*, 2010) an important factor in angiogenesis, and therefore also plays a role in the development of tumour vasculature.

Another attractive target for the application of DNAzymes is the human papilloma virus (HPV). HPV is the main etiological agent of cervical cancer (zur Hausen, 1996) and HPV16 encodes 2 oncogenes E6 & E7 which are associated with the onset and progression of the disease (Munger *et al.*, 1989; Pirisi *et al.*, 1987). HPV16 E6 & E7 control cell proliferation and lifespan of the cell via inactivation of p53 and retinoblastoma proteins (Dyson *et al.*, 1989; Werness *et al.*, 1990). They have been extensively validated as a therapeutic target for cervical carcinoma (Alvarez-Salas *et al.*, 1999; Alvarez-Salas *et al.*, 1998; Jiang and Milner, 2002; Tan and Ting, 1995) and the DNAzyme DT99 has been demonstrated to successfully degrade HPV16 mRNA (Cairns *et al.*, 1999).

1.4.3 Alternative Mechanisms to Target the AR Pathway

It is understood that cancer cells alter their metabolic activity in order to maintain their heightened energy requirements, with biological processes such as aerobic glycolysis (the Warburg effect) and lipid synthesis increasing (Vander Heiden *et al.*, 2009). The Warburg effect was first described in the 1930's by Otto Warburg (Oliveira *et al.*, 2015). He reported that cancer cells alter the metabolism of glucose by converting it to lactate even when there are sufficient levels of oxygen present to support mitochondrial oxidative phosphorylation. This means that there are considerable differences in the metabolism of cancer cells compared with that of normal cells that will only produce lactate under anaerobic conditions, meaning that cancer cells obtain their energy from aerobic glycolysis rather than mitochondrial oxidative phosphorylation (Oliveira *et al.*, 2015).

The Warburg effect usually supplies the means of cancer detection via ¹⁸F-deoxyglucose positron emission tomography (18F-FDG-PET). 18F-deoxyglucose or 2-deoxy-2-(¹⁸F)fluoro-D-glucose (18F-FDG), is a glucose analog containing a positron-emitting fluorine-18. 18F-

FDG is taken up by tissues in the body undergoing glucose metabolism, and as a result of increased glucose metabolism in tumours, it accumulates in affected regions. As a result, ¹⁸F-FDG is a major clinical tool in detecting cancers. However, PCa is characterized by slow glycolysis and therefore the uptake of ¹⁸F-FDG by tumours for the purpose of PET scans makes it impossible to distinguish benign and malignant tumours (Sahin *et al.*, 2015). This example highlights the need for a better understanding of the metabolic profile of PCa, and especially CRPC.

The pathways responsible for metabolic activity, and the enzymes within these core metabolic pathways, have been shown to contribute to cancer cell proliferation and survival. For example, serine biosynthesis has recently been shown to be an important metabolic pathway in the development of breast cancer (Possemato *et al.*, 2011). Studies carried out by the Brooke group (Brooke *et al.* 2015) and others have identified that multiple proteins involved in metabolism are regulated in response to androgen such as, fructose-bisphosphate aldolase A (ALDOA), fatty acid synthase (FASN), and ATP citrate lyase (Meehan and Sadar, 2004; Ros *et al.*, 2012; Rowland *et al.*, 2007). By identifying proteins regulated by the AR it is possible that inhibition of PCa growth could be achieved by targeting these key proteins downstream of the AR.

1.5 Project Objectives

The AR appears to drive CRPC and is therefore a therapeutic target for the treatment of this stage of the disease. The aim of this project is to investigate and develop novel therapeutic strategies for the treatment of this stage of the disease:

1, Identification of DNazymes to down-regulate AR expression.

DNazymes were identified that worked at physiological $MgCl_2$ concentration. Lead DNazymes were transfected into the AR positive cell line LNCaP, and cell proliferation measured using crystal violet assays.

2, Test a computer model and software program developed to aide with DNzyme design

The program developed to aide DNzyme design was tested by performing cleavage reactions on program designed DNazymes alongside the published DT99 against HPV16 RNA. Data was then compared to the predicted efficiency of each DNzyme from the program in order to optimize the program.

3, Identification of metabolic proteins that are essential for PCa proliferation.

To identify metabolic enzymes important in PCa, an siRNA screen was performed in the LNCaP cell line. A total of 15 targets genes were identified by the screen.

Chapter 2: Materials and Methods

2.1 Reagents, buffers and solutions

Name	Description
------	-------------

Bacterial work

Ampicillin	1 g sodium ampicillin, ddH ₂ O to 10 mL
Luria Broth (LB)	10 g Sodium chloride (NaCl), 10 g bactotryptone, 5 g yeast extract per 1 litre of RO water. Autoclaved prior to use. Supplemented if required using 50 µg / mL of ampicillin (Sigma).
Luria Broth Agar (LB Agar)	LB broth and 1.25 g of Bactoagar. Autoclaved prior to use and poured to make agar plates whilst still warm. 4 µL IPTG (200 mg/mL) and 40 µL Xgal (20 mg/mL) can be added where necessary by spreading once the plate has set.
SOC Medium	4 g tryptone, 1 g yeast extract, 0.1168 g 10 mM NaCl, 0.0372 g 2.5 mM KCl, ddH ₂ O to 200 ml, 0.1904 g 10 mM MgCl ₂ , 0.7206 g 20mM glucose

DNA agarose gel electrophoresis

Agarose Gel (1%)	1 g agarose dissolved in 100 mL of 1 X Tris Acetic acid Ethylenediaminetetraacetic acid (EDTA) (TAE) via boiling and 5µL of ethidium bromide (1 µg/mL).
Tris Acetic acid EDTA (TAE) (1X)	40 mM Tris, 20 mM acetic acid and 1 mM EDTA.

RNA denaturing agarose gel electrophoresis

Denaturing Agarose Gel	1 g agarose, ddH ₂ O to 72 ml. Dissolve. Add 10 mL 10x MOPS buffer and mix. Allow to cool to 60 °C. Add 18 mL 37% formaldehyde (in fume hood) and mix. Run using 1x MOPS buffer (10x MOPS buffer diluted in TAE)
10x TBE	96.88 g Tris, 49.44 g boric acid, 5.92 g EDTA. Dilute to 800 mL with ddH ₂ O and autoclave.

DNAzyme Cleavage Reactions

DNAzyme Cleavage Reaction Buffer	50 mM Tris-HCl (pH 7.5), 10 mM MgCl ₂ , 150 mM NaCl and 0.01% SDS
----------------------------------	--

Urea PAGE

Urea PAGE gel (12 %)	4.2 g urea, 1 mL 10x TBE, 4 mL 30 % acrylamide, 2 mL DEPC water. Filter sterilise. 8 µL TEMED, 70 µL APS. Allow to set. Pre run gel for 30 mins.
DEPC water	0.8 mL DEPC, ddH ₂ O to 800 mL. Autoclave.
Running buffer (1x TBE)	100 mL 10x TBE & 900 mL ddH ₂ O

Silver Staining RNA

Fixative Solution	5 ml glacial acetic acid, 100 ml EtOH & 1000 ml ddH ₂ O
Silver Stain	High concentration: 0.1 g silver nitrate & 100 ml ddH ₂ O Lower concentration: 0.25 g silver nitrate & 60 ml ddH ₂ O
Development Solution (Sodium Carbonate)	Must be made up fresh and kept at 8°C. 3 g sodium carbonate, 100 ml ddH ₂ O. Avoid clumping by adding powder gradually whilst stirring. Add to it 50 ul sodium thiosulphate solution.
Development Solution (Sodium hydroxide & formaldehyde)	Sodium hydroxide (3.0%) & formaldehyde 37%.
Sodium Thiosulphate Solution	0.2 g sodium thiosulphate & 50 ml ddH ₂ O

2.2 Bacterial cultures, transformations, DNA preparation and *In vitro* transcription of RNA for use in DNase experiments

2.2.1 Polymerase Chain Reaction (PCR)

Polymerase Chain Reaction (PCR) was conducted on complementary DNA (cDNA) samples generated from LNCaP. Phire Hot Start II DNA polymerase (Thermo Fisher) was used and the reactions consisted of 4 µL of 5 X Phire Green Reaction Buffer; 200 µM each of deoxyribonucleotides (dNTPs); 0.5 µM of both the forward and reverse primers for the appropriate region of the AR; 100 ng of DNA template; 0.4 µL of Phire Hot Start II DNA

polymerase; and autoclaved ddH₂O to a total volume of 20 µL. The reaction conditions are displayed in Table 2.1. PCR products were visualized using agarose gel electrophoresis.

[Table 2.1 – Reaction conditions for PCR](#)

STAGE NUMBER	DESCRIPTION OF STAGE	TEMPERATURE	LENGTH OF TIME	NUMBER OF CYCLES
1	Initial denaturation	98 °C	30 seconds	1
2	Denaturation	98 °C	5 seconds	25 – 35 (Normally 30)
3	Annealing	60 °C *	5 seconds	
4	Extension	72 °C	15 seconds / kb	
5	Final Extension	72 °C	60 seconds	1
		4 °C	hold	

2.2.2 Agarose Gel Electrophoresis

2.2.2.1 DNA Gel Electrophoresis

Agarose gel electrophoresis was conducted to assess the size and quality of DNA obtained from different sources. The composition of the gel is described in Section 2.1. Gel electrophoresis was performed in 1x TAE (see Section 2.1) and the bands visualized using the Alphamager EP MultiImage I system (Alpha Innotech).

2.2.2.2 RNA Gel Electrophoresis

Denaturing agarose gel electrophoresis was conducted to assess RNA cleavage during DNazyme experiments. The composition of the gel is described in Section 2.1. Gel electrophoresis was performed in 1x MOPs buffer (Lonza) and the bands visualized using the Alphamager EP MultiImage I system (Alpha Innotech).

2.2.3 Ligation of PCR products into pGEM T-easy Vector

Ligation reactions were performed following the manufacturers guidelines (Promega). In brief, 5 μ l 2X Rapid ligation buffer, 1 μ l of pGEM vector (50 ng), 1 μ l PCR product (diluted to permit a 1:3 ratio with vector DNA), 1 μ l of T4 DNA ligase and ddH₂O to a final volume of 10 μ l were added to the ligation mix. The reaction was mixed by pipetting and incubated overnight at 4 °C.

2.2.4 Transformation of competent cells

Escherichia coli XL-1 cells were transformed using the standard protocol outlined by Promega. In brief, 50 μ L of cells were thawed on ice and gently mixed with 2 μ l of ligation reaction. The mixture was then incubated on ice for 30 min before heat shocking at 42 °C for 45 seconds. The cells were immediately incubated on ice for a further 2 mins, 950 μ L of SOC medium added (Section 2.1) and incubated at 37 °C for 1.5 hours with shaking at 150 rpm. 100 μ L of this cell suspension was spread onto an LB agar plate containing 10 % ampicillin, IPTG (Sigma) and Xgal (Sigma) (Section 2.1). Plates were incubated at 37 °C overnight.

2.2.5 Inoculation of LB broth for extraction of plasmid DNA

A single white bacterial colony white was picked using a sterile pipette tip. This was incubated in 5 mL of fresh LB broth supplemented with 10 % ampicillin at 37 °C for 12 hours (or overnight) with shaking at 225 rpm. 4.5 mL of the bacterial cells were then collected via centrifugation at 8,000 rpm at RT for 1 minute.

2.2.6 Extraction of plasmid DNA

2.2.6.1 *Mini preparation*

Small scale isolation of plasmid DNA was conducted using the GeneJET Plasmid Miniprep Kit (Thermo Scientific), following the standard protocol. In brief, the transformed cells were re-suspended thoroughly with 250 μL of the Resuspension Solution using a vortex. 250 μL of Lysis solution was added and the resulting mixture mixed thoroughly by inverting the tube 4 – 6 times. Following this, 350 μL of the Neutralization Solution was added and the tube inverted a further 4 – 6 times to mix. The mixture was centrifuged at 13,000 rpm for 5 mins and the supernatant transferred to a GeneJET spin column. This was centrifuged for 1 min at 13,000 rpm, and the flow-through discarded. The collected DNA was washed twice by centrifuging with 500 μL of the Wash Solution for 1 min, each time discarding the flow-through. The column was then centrifuged for an additional 1 min to ensure the removal of the Wash Solution. This column was transferred into a fresh 1.5 mL Eppendorf tube. The plasmid DNA was subsequently eluted by incubation of the column with 50 μL of Elution Buffer at RT for 2 mins, and subsequent centrifugation at 13,000 rpm for 2 mins. DNA concentration and quality was assessed using a Nanodrop (Thermo Scientific) (see Section 2.2.7.1).

2.2.6.2 *Maxi preparation*

Isolation of plasmid DNA was conducted on a larger scale using the EndoFree Plasmid Purification Maxi Kit (Qiagen), according to the standard protocol. In brief, 0.5 mL of a starter culture was used to inoculate 200 mL of fresh LB broth containing 10% ampicillin at 1 $\mu\text{l}/\text{mL}$. This was incubated at 37 $^{\circ}\text{C}$ for 12 hours with shaking at 250 rpm. The cells were collected via centrifugation at 6,000 rpm for 15 mins at 4 $^{\circ}\text{C}$. The pellet was re-suspended in

10 mL of Buffer P1 via vortexing. 10 mL of Buffer P2 was added and the tube inverted 6 times prior to incubation at RT for 5 mins. Following this, 10 mL of pre-chilled Buffer P3 was added, and the tube inverted again 4 – 6 times, prior to adding the sample to the QIAfilter Cartridge and incubating at RT for 10 mins. The lysate was filtered through the QIAfilter Cartridge and 2.5 mL of Buffer ER added. The sample was mixed thoroughly via inverting the tube 10 times, prior to incubation on ice for 30 mins. Whilst the lysate was incubated, the QIAGEN-tip 500 column was equilibrated with 10 mL of Buffer QBT. Once Buffer QBT had passed through the QIAGEN-tip 500 completely, the filtered lysate was added and allowed to bind to the resin by gravity flow. The QIAGEN-tip was washed twice with 30 mL of Buffer QC and DNA eluted using 15 mL of Buffer QN. The DNA was precipitated by the addition of 10.5 mL of isopropanol followed by centrifugation at 13,000 rpm for 30 minutes at 4 °C. The resulting pellet was washed with 5 mL of 70 % ethanol and re-spun at 13,000 rpm for 10 mins. The supernatant was carefully discarded and the pellet air dried for 5 – 10 mins and re-dissolved in 150 – 300 µL of Buffer TE. DNA concentration and quality was assessed using a Nanodrop (Thermo Scientific) (see Section 2.2.7.1).

2.2.7 Analyzing success of plasmid production

2.2.7.1 NanoDrop® ND-1000 UV/VIS Spectrophotometer

The NanoDrop® ND-1000 UV/VIS Spectrophotometer (Nanodrop, Thermo Scientific) was used to quantify the DNA concentration and purity, according to the manufacturer's guidelines. To assess the quality of the DNA, the ratio of the absorbance at 260 nm over that at 280 nanometres (nm) (260/280) was observed. A ratio of value larger than 1.8 was accepted for use, as below this could indicate protein contamination. The ratio of the absorbance at 260 nm over that at 230 nm (260/230) was also observed. For this, values

larger than 1.8 were accepted for use, as below this value could indicate the presence of other contaminants such as polysaccharides. The Nanodrop was additionally used to measure the concentration of RNA, according the manufacturer’s guidelines.

2.2.7.2 Plasmid verification by diagnostic digest and sequencing

Cloning success was initially verified by diagnostic digest using fast digestion restriction enzymes (Thermo Scientific). Restriction enzyme sites were identified in the pGEM plasmid (Figure 2.1). The restriction enzymes and the fragment sizes expected to be produced from the digestion reaction are displayed in Table 2.2. 1 µg of plasmid DNA was digested utilizing 1 µL of each enzyme with 2 µL of Buffer Green Fast Digest (Thermo Scientific). This reaction was made up to a total of 20 µL using sterile ddH₂O, and the digestion was conducted at 37 °C for 30 mins. Reactions were visualised alongside undigested plasmid DNA using 1 % agarose gel electrophoresis. Successful cloning was confirmed using Sanger Sequencing (Source Bioscience).

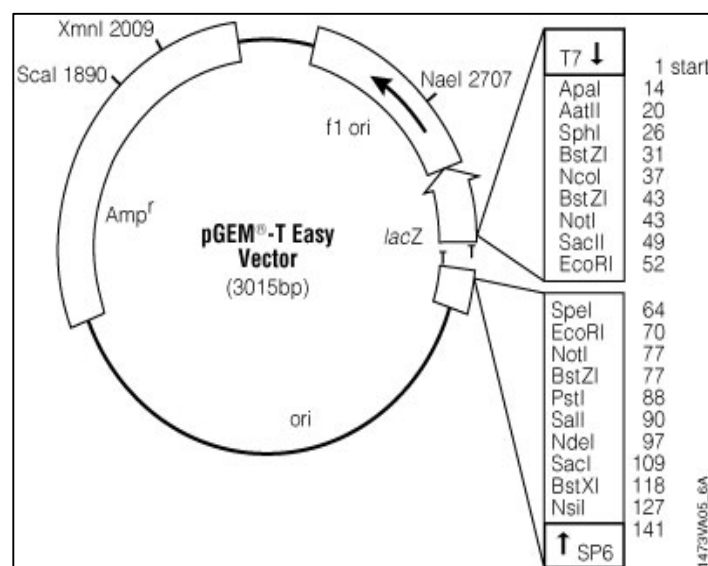


Figure 2.1 - Plasmid map of pGEM T Easy Vector.

[Table 2.2 - Restriction enzymes and DNA fragment sizes produced by digestion](#)

Plasmid	Restriction Enzyme Used For Digestion	Sizes of fragments produced by digestion
pGEM Easy T	<i>SacI</i>	2.7kb, 360bp

2.2.8 *In vitro* Transcription of RNA for DNAzyme Cleavage Reactions

In vitro transcription of RNA was carried out using the TranscriptAid T7 High Yield Transcription Kit (ThermoFisher Scientific) according to the manufacturers guidelines. In brief, the total reaction volume of 20 μ l was made using DEPC-treated water, 4 μ l of 5X TranscriptAid reaction buffer, 8 μ l of NTP solutions (in equal volumes), 1 μ g of template DNA and 2 μ l of TranscriptAid enzyme. This was then mixed thoroughly by vortexing and briefly spun. The reaction was incubated for 2 hours at 37 °C, for transcripts of <100nt the incubation period was extended to 4-8 hours at 37 °C. A control reaction was carried out at the same time using 2 μ l of control DNA at 0.5 μ g/ μ l.

The integrity, length and yield of the RNA transcripts >500nt was evaluated using an agarose gel. Shorter transcripts were evaluated using denaturing agarose gels (see Section 2.1). 2X RNA loading dye (ThermoFisher Scientific) containing ethidium bromide and RiboRuler RNA ladder were used. The Nanodrop (Thermo Scientific) (Section 2.2.7.1) was additionally used to measure the concentration of RNA, according the manufacturer's guidelines

2.3 DNAzyme Cleavage Reactions

RNA was diluted to a final concentration of 0.2 μ M, and DNAzymes were diluted to a final concentration of 1 μ M, in DNAzyme buffer (Section 2.1). An uncut RNA negative control was also used that corresponded to the section of RNA being cleaved by the DNAzyme. The

RNA and DNAzyme mixes were pre-equilibrated at 37 °C separately for 10 mins before being combined to form a final reaction volume of 20 µl. Reactions were left to proceed for the desired time before being terminated by the addition of 2X RNA loading dye and being snap frozen on dry ice. Samples were then boiled at 70 °C prior to loading on the appropriate gel for visualisation.

2.4 Visualisation of DNAzyme Cleavage

Cleaved RNA was visualized via several different techniques.

2.4.1 Denaturing Agarose Gels

In vitro transcribed RNA was visualized using denaturing agarose gels (Section 2.1). Reactions were loaded (already in 2X RNA loading dye) along with RiboRuler and uncut RNA negative control. Gels were run in 1X MOPS buffer (Section 2.1). Prior to visualization using the AlphaImager EP Multimage I system (Alpha Innotech).

2.4.2 Urea PAGE

Unlabelled RNA that had been *in vitro* transcribed was initially visualized using different staining techniques. In all cases samples containing 2X RNA loading dye were loaded subsequent to incubating at 70 °C for 10 mins and cooling on ice for 2 mins. Uncut RNA negative control was also loaded along with RiboRuler into a urea PAGE gel (Section 2.1). Electrophoresis was conducted at 120-150 V for 1 hr. Gels were stained with Diamond Stain (Promega), methylene blue stain (Sigma), or a silver stain.

2.4.2.1 Diamond Stain

The stain was used according to the manufacturer's instructions and visualized using the AlphaImager EP Multimage I system (Alpha Innotech).

2.4.2.2 Methylene Blue Stain

The stain was diluted to 0.02% and the urea PAGE gel left to develop until bands became visible. The gel was then de-stained using ddH₂O in order to remove unnecessary background staining.

2.4.2.3 Silver Staining

The gel was placed in fixative solution (Section 2.1) for 10 mins on a rocker and washed three times with ddH₂O (2 mins per wash, rocking). 15% formaldehyde solution was added and the gel was incubated for 10 mins with rocking. Silver solution (Section 2.1) was added, 1:240 or 1:1000 silver nitrate, and left to stain for 10-20 mins. The gel was then washed rapidly with ddH₂O ensuring the water did not stay on the gel for longer than 15 seconds. The development solution (Section 2.1) was then added. The gel was incubated in sodium hydroxide and formaldehyde development solution (Section 2.1) for less than 1 minute. Sodium carbonate development solution was left for less than 3 mins in order to reduce background staining. The development reaction was then stopped in 7.5% acetic acid at 4 °C for 5-10 mins.

2.4.2.4 FAM labelled RNA

In order to visualize FAM labelled RNA cleavage urea PAGE gels were used. RiboRuler was loaded along with each sample including an uncut RNA negative control. Electrophoresis was conducted at 120-150 V for approximately 1 hour. Gels were removed and visualized using the Fusion FX imager (Vilber Lourmat) using the GFP protocol.

2.5 Mammalian Cell Culture Techniques

The adherent human PCa cell line LNCaP (ATCC) was utilised as a model of androgen-dependent PCa.. Cells were grown in Roswell Park Memorial Institute (RPMI) 1640 growth medium containing the components: 2 mM L-Glutamine, 10 % streptomycin and Phenyl Red (PSG); supplemented with 10% fetal bovine serum (FBS) (Biosera). Cells were cultured under incubation conditions of 37 °C and 5 % Carbon Dioxide (CO₂).

2.5.1 Cell Passaging

Once the cell confluence reached approximately 70 – 80 %, cell passaging was performed. Prior to passaging, fresh RPMI 1640 medium, PBS and trypsin/EDTA (Sigma) were warmed. Medium was aspirated from the flask, and cells washed with PBS. The cells were incubated with Trypsin/EDTA for the required length of time for them to detach from the flask (approximately 5 mins, depending on the cell line properties). Medium was added to dilute the trypsin-EDTA and the desired volume of cell suspension was added to a new flask containing fresh medium.

2.5.2 Cell Counting and Plating

After trypsinisation, 10 µL of the cell suspension was removed and viewed on the haemocytometer. To calculate the approximate concentration of cells x 10⁴ per mL in the cell suspension, an average was taken of the number of cells in the ten 1 mm² squares. This value was converted into the number of cells x 10⁵ and used to calculate the volume of cell suspension and fresh medium required to seed the desired cell concentration in a 6 or 12 well plate (Thermo Scientific).

2.5.3 Freezing and Defrosting Cells

To make frozen cell stocks, cells were passaged, and the cell pellet re-suspended in freezing mixture, consisting of 10 % Dimethyl Sulphoxide (DMSO, Sigma) and 90 % FBS. The mixture was transferred into a cryotube, wrapped in insulating material and maintained at -80 °C. Cells intended for storage longer than 2 – 3 months were transferred to liquid nitrogen for storage.

To defrost frozen stocks, cells were rapidly defrosted in the cryotube in warm water. They were transferred into 10 mL of pre-warmed medium. The resulting cell suspension was centrifuged at 2,000 rpm for 5 mins, the supernatant removed and the cells re-suspended in 10 mL of fresh pre-warmed medium. The cell suspension was transferred to a 75 cm² culture flask and more medium was added to result in a total of 24 mL. Cells were incubated under previously stated conditions and passaged as required.

2.6 Transient Transfection of Mammalian Cells

2.6.1 siRNA Knockdown for Screen

LNcaP cells were transiently transfected with small interfering RNA (siRNA) to specifically knockdown the expression of genes involved in Metabolism and Cell Traffic/Signalling.

For the siRNA transfections conducted during this study, RNAiMax transfection reagent (Invitrogen) was utilized. In brief, 24 hours prior to conducting transfections, 4×10^4 cells were seeded in 100 µL of medium per well in a 96-well plate. Per well, 0.2 µl 10 µM of on-target and control siRNA were diluted in 9.8 µl Optimem (Invitrogen) and in a separate tube 0.075 µL of RNAiMax was diluted in 9.925 µL of Optimem. The two tubes were combined and gently mixed prior to incubating at RT for 5 mins. Following this, 20 µL of each

transfection mix was then added per well, resulting in a final concentration of 20 nM siRNA per well.

For a 6-well plate, 3×10^5 cells were seeded in 1 ml of medium per well. Per well, 10 μ l of 10 μ M on-target and control siRNA were diluted in 90 μ l of Optimem. In a separate tube 2.27 μ l of RNAiMax was diluted in 97.73 μ l of Optimem. The two tubes were combined and gently mixed prior to incubating at RT for 5 mins. Following this, 200 μ l of transfection mix was added per well, resulting in a final concentration of 50 nM siRNA per well. Successful knock-down was confirmed using Western blotting and RT-qPCR (Sections 2.9.2 and 2.8.3.2).

2.6.2 Transfection of AM-3 into Mammalian Cell Lines

For the DNazyme transfections conducted during this study, RNAiMax transfection reagent was used. In brief, 24 hours prior to conducting transfections, 4×10^4 cells were seeded in 100 μ L of medium per well in a 96 well plate. 0.44 μ l of appropriate DNazyme (stock at 100 μ M) was diluted in 2.92 μ l Optimem, in a separate tube 1.25 μ L of RNAiMax was diluted in 2.92 μ L of Optimem. The two tubes were combined and gently mixed prior to incubating at RT for 5 mins. Following this, 5 μ L of each transfection mix was then added per well.

2.7 Proliferation Assays

2.7.1 Crystal Violet Assay

In order to measure the relative proliferation of the cells after transfection crystal violet assays were performed. Cells in 96 well plates were fixed by adding 100 μ l 4 % paraformaldehyde and left to incubate at RT for 1 hour. Three washes with PBS were performed and the plate left to air-dry at RT. 50 μ l of 0.08 % crystal violet stain was added

to each well including the control wells, containing no cells, and incubated at RT for 1 hour. The plate was washed with ddH₂O three times and left to air-dry once more at RT. Crystal violet stain was resolubilised using 100 µl 10 % acetic acid on a rocking platform for 1 hour. The plate was read at 490 nm and readings were adjusted for background staining by subtracting the average OD for the control wells (without cells).

Chapter 3: Gene Therapy by way of DNAzymes

3.1 Introduction

3.1.1 DNAzyme Design

Traditionally DNAzymes have been designed by hand. Substrate binding arms of the 10-23 DNAzyme are matched to regions of the gene of interest randomly. Any one gene can have tens to hundreds of possible cleavage sites for a DNAzyme depending on their size and sequence, meaning design by hand is “hit and miss”. Conventionally large arrays or RNase H activity assays have been used to map sites of RNA hybridization in large antisense oligodeoxynucleotides. In the case of hammerhead ribozymes (a single-folded strand of RNA that undergoes self-cleavage), RNA molecules that can be designed to target and cleave mRNA, target site selection has been performed using large pools of molecules with randomized hybridizing arms (Lieber and Strauss, 1995). Only once cleavage reactions are carried out can the effectiveness of any hand designed DNAzyme be quantified. Thanks to our collaborator, Dr Antonio Marco (University of Essex), a computational approach can now be taken using a program that can predict the cleavage efficiency and specificity of all DNAzymes for a particular gene. Here we test a selection of predicted DNAzymes and compare them to the most effective counterparts published in the literature. For this we focused on the human papilloma virus gene E6/E7 and the published DNAzyme, DT99 (Cairns *et al.*, 1999).

3.1.2 A Computational Approach to DNAzyme Design

A computer model and associated software was developed by Dr Antonio Marco in order to design DNAzymes. Dr Marco theorized that the computational treatment of DNAzymes was similar to that of predicting small RNA regulators and their targets, being based on the

“Nearest-Neighbour” thermodynamic model. This model suggests that the identity and orientation of nucleic acids positioned neighbouring each other form base pair interactions that provide stability, this is rather than treating DNA or RNA as a string of interactions between base pairs (SantaLucia, 1998).

The output of the program was assessed by building upon thermodynamic models of nucleic acid interactions and assessing various criteria for DNAzyme efficiency and specificity. These criteria, or parameters, were; Delta G, hairpin formation of the DNAzyme, dimer formation of the DNAzyme, off target effects, and accessible sites. The Delta G is the Gibbs free energy, whereby a negative value would indicate the reaction would proceed spontaneously due to the change in total entropy being non-negative where reaction conditions, temperature and pressure, being held constant. Gibbs free energy and total entropy must always move in opposite directions for a reaction to proceed spontaneously due to the second law of thermodynamics.

3.2 Results

3.2.1 *In vitro* transcription of RNA for use in cleavage reactions

Initially RNA was *in vitro* transcribed for use in cleavage reactions. To begin a section of the AR gene (1300 bp – 2000 bp) was PCR amplified and cloned into the pGEM vector after being checked via gel electrophoresis and gel extracted.

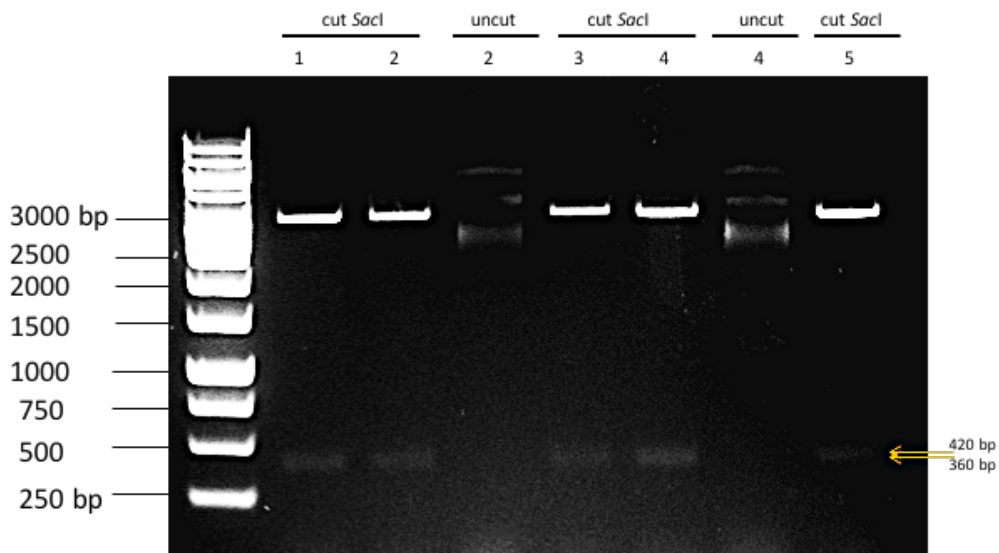


[Figure 3.2 - Diagnostic digest of AR gene \(1300-2000 bp\) in pGEM indicating the correct orientation of insert.](#)

Bacterial cultures were grown overnight and minipreps performed. The resulting DNA was digested using the *SacI* restriction enzyme to digest the pGEM AR₁₃₀₀₋₂₀₀₀ plasmid. Gel electrophoresis was performed and Prior to *in vitro* transcription the plasmid was linearised with the 3' *Sall* site. *In vitro* transcription was then performed using the pGEM-AR₁₃₀₀₋₂₀₀₀ plasmid (Figure 3.3) and a 700 bp fragment of AR RNA was created.

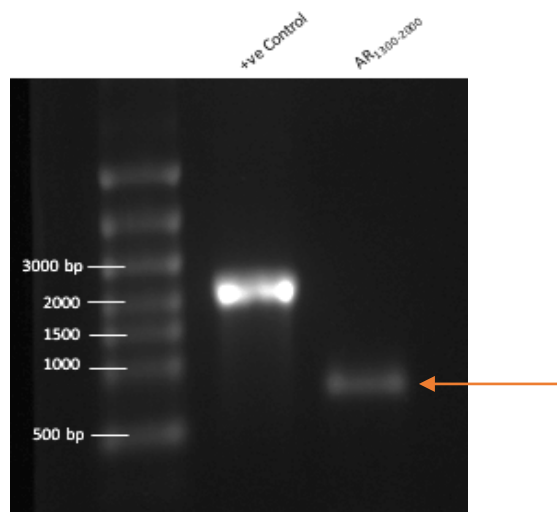


[Figure 3.3 - In vitro transcription of AR₁₃₀₀₋₂₀₀₀.](#)

In vitro transcription was performed using the DNA from colony number 1 in the diagnostic digest. Gel electrophoresis was performed using a denaturing agarose gel and the bands from the control and AR₁₃₀₀₋₂₀₀₀ visualised.

3.2.2 Visualisation of RNA

A number of staining techniques were performed in order to visualize the RNA in cleavage reaction samples. Initially RNA was visualized using ethidium bromide in the loading dye of the samples (as shown in Figures 3.3), however the signal from the *in vitro* transcribed RNA was weak due to the low concentration of RNA used in the cleavage reactions. Alternative methods of visualization were therefore attempted.

3.2.2.1 Silver Staining

In order to stain the RNA, the silver staining technique was performed on urea PAGE gels containing RNA ladder only (Figure 3.4). Silver staining was originally developed to stain proteins separated in PAGE gels, however it has since been developed to visualize other molecules such as nucleic acids (Boulikas and Hancock, 1981; Somerville and Wang, 1981).

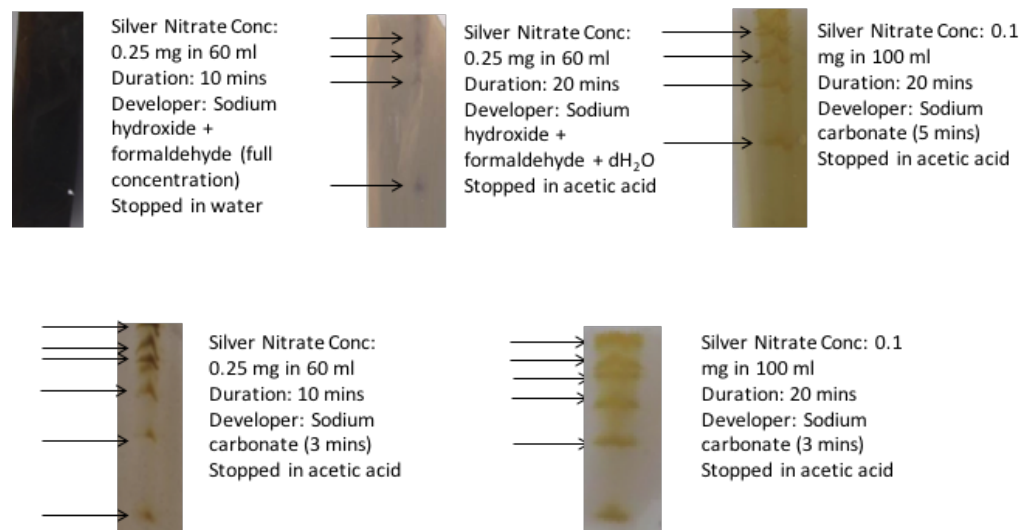


[Figure 3.4 – A comparison of silver staining of RNA in urea PAGE gels.](#)

RNA was loaded into urea PAGE gels and run prior to staining using different variables in silver staining technique. Silver nitrate concentration was either 0.25 g in 60 mL ddH₂O (1:240) or 0.1 mg in 100 mL ddH₂O (1:1000). Stain incubation varied from 10-20 minutes. Either a sodium carbonate (incubation of 3-5 mins) or sodium hydroxide and formaldehyde developer was used. Reactions were either stopped in ddH₂O or acetic acid.

Several variations of silver staining techniques were attempted with alterations in: the concentration of silver nitrate (either 1:240 or 1:1000), the duration of incubation in silver nitrate solution (10-20 minutes), the type of developer used (either sodium hydroxide and formaldehyde or sodium carbonate) and finally whether the development of the stain was stopped using acetic acid or water. Figure 3.4 shows the staining results of each different variation on the protocol. The least efficient method of staining is shown to be one where the sodium hydroxide and formaldehyde development solution was used. The best staining technique for RNA visualization appeared with either the higher concentration of silver nitrate left for just 10 minutes or the lower concentration left for 20 minutes, both developed using sodium carbonate for 3 minutes and stopped with acetic acid.

The most efficient staining protocol was performed on the cleavage reaction samples (Figure 3.5). No cleavage could be seen in the samples and even uncut RNA was difficult to visualize due to background staining that could not be removed. The staining protocol was deemed to be too unpredictable so an alternative visualization technique was performed.

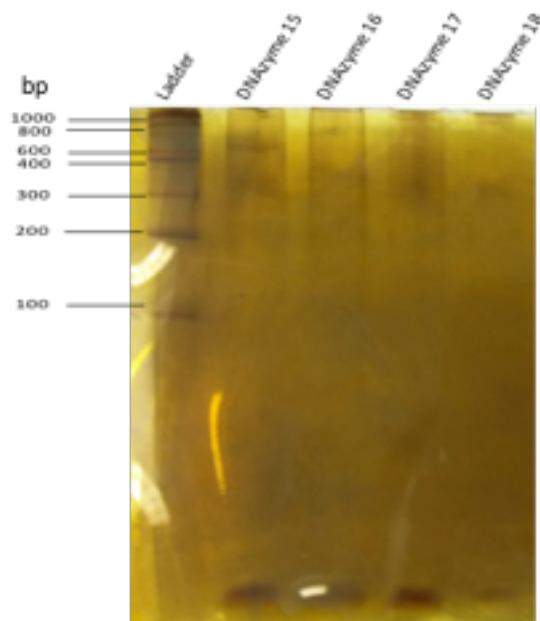


[Figure 3.5 - Silver staining of cleavage reaction samples in urea PAGE gel does not allow for clear RNA visualisation due to background staining.](#)

Sample RNA was stained using 1:240 (0.25 mg/60 mL) concentration of silver nitrate and developed with sodium carbonate for 3 minutes. The development was stopped with acetic acid.

3.2.2.2 Methylene Blue Staining

Methylene blue is a positively charged dye that binds to negatively charged nucleic acids with facilitates visualisation in the PAGE gel (Figure 3.6). Staining of the RNA ladder was still weak with the methylene blue method. Longer incubation times resulted in over-staining and this could not be removed sufficiently with de-staining techniques. It was presumed to be too difficult to visualize lower concentrations of RNA using this technique.

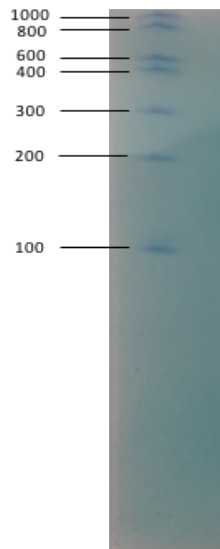


[Figure 3.6 - Methylene blue staining in urea PAGE gel is weak at high concentrations of RNA.](#)

RNA was run on urea PAGE gel prior to staining with 0.02% methylene blue until bands became visible. De-staining was performed with ddH₂O.

3.2.2.3 Diamond Staining

Diamond staining was also performed which enabled clearer visualization of RNA (Figure 3.7). However, it was discovered that *In vitro* transcribed RNA was not stable and would degrade very quickly, making visualization even more difficult. In order to overcome this issue, AR 5'FAM labelled RNA fragments were ordered which could be visualized without the need for any staining and would remain stable for longer periods stored at -80 °C (Figure 3.7). It was therefore decided that all DNAzyme cleavage reactions would be performed on FAM-labelled RNA.

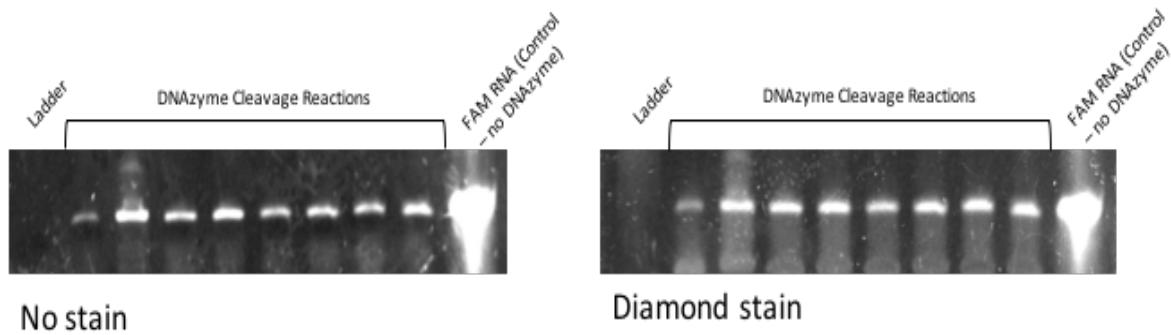


[Figure 3.7 - Diamond staining of RNA in urea PAGE gel is less efficient than 5'FAM labelled RNA.](#)

RNA was run on urea PAGE gels prior to staining with Diamond stain or no staining.

3.2.3 Use of a new computer model and software to design efficient DNAzymes

Initially DNAzymes were designed by hand to target AR RNA. These DNAzymes were tested *in vitro* and *in vivo* by way of cleavage reactions and transfections. None of the original DNAzymes would cleave AR RNA to any degree and none reduced LNCaP proliferation following transfection (Figure 3.8).

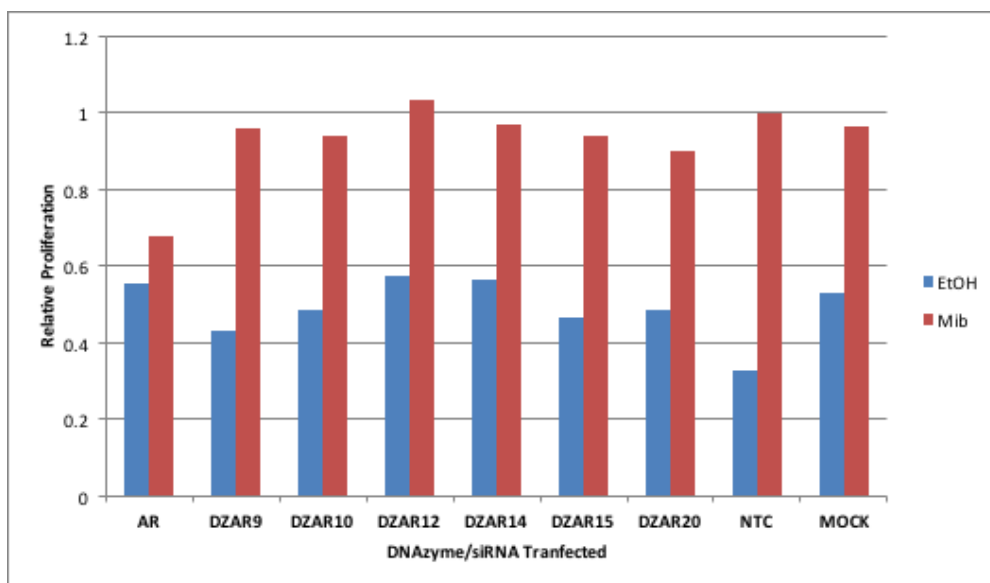


[Figure 3.8 – Transfection into LNCaP cells of original AR RNA DNAzymes designed prior to the program shows no effect on cell proliferation.](#)

LNCaP cells were transfected using RNAiMax as per the standard DNAzyme transfection protocol. Single repeat.

In order to design successful and efficient DNAzymes against the AR we enlisted the assistance of Dr Antonio Marco. He in turn generated a computer model and software program that, it was hoped, would generate possible DNAzymes that would cleave RNA efficiently.

The computer model and software predicted the five DNAzymes in Table 3.1 to be efficient against AR RNA. Each DNAzyme was predicted by the program to have varying cleavage efficiency ranging from poor to good (as indicated in Table 3.1). The program assesses the efficiency of DNAzymes based on the parameters: binding energy (delta G – Gibbs free energy), the probability of hairpins forming within the DNAzyme, the probability of DNAzymes forming dimers with each other, off target effects (i.e. the DNAzyme base pairing to RNA other than that of the target RNA), and accessible sites (the number of bases that the program predicts the DNAzyme will be able to access and bind due to RNA secondary structure).

[Table 3.1 – DNAzymes against AR RNA as predicted by the computer model and software. * + = poor efficiency, ++ = average efficiency, +++ = good efficiency](#)

DNAzyme	Binding position on RNA (bp)	Predicted Efficiency*	Parameters					Accessible Sites	Sequence
			Delta G	Hairpin (< 3.6)	Dimer (< 8.5)	Off Target	Off Target		
AM1	669-687	+++	-24.24	-2.9	-6.5	0	16	CTGCGGCTGGGCTAGCTACAAC GAGAAGGTTGC	
AM2	1348- 1366	++	-22.93	-1.72	-8.4	0	15	GAGACAGGGGGCTAGCTACAA CGAAGACGGCAG	
AM-1	657-675	+	-21.51	-4	-4.2	0	3	AGTTGCTGGGCTAGCTACAAC GATCCTCATCC	
AM-2	1341- 1359	+	-20.28	-3.3	-10.7	0	13	GGTAGACGGGGCTAGCTACAAC GAAGTTCAAGT	

AM-3	1353-1371	+	-18.66	-3.8	-7.2	0	3	GTAGAGAGAGGCTAGCTACAAC GAAGGGTAGAC
------	-----------	---	--------	------	------	---	---	---------------------------------------

3.2.4 DNAzyme Cleavage Reaction Optimisation – MgCl₂ concentration in reaction buffer

In order to test the validity of the program, DNAzyme cleavage reactions were performed using 5'FAM labelled RNA that was between 40-50 nt in length (Figure 3.9). Negative control DNAzymes were used that had an inverted catalytic core, which inactivates their ability to cleave target RNA (Dass *et al.*, 2008).

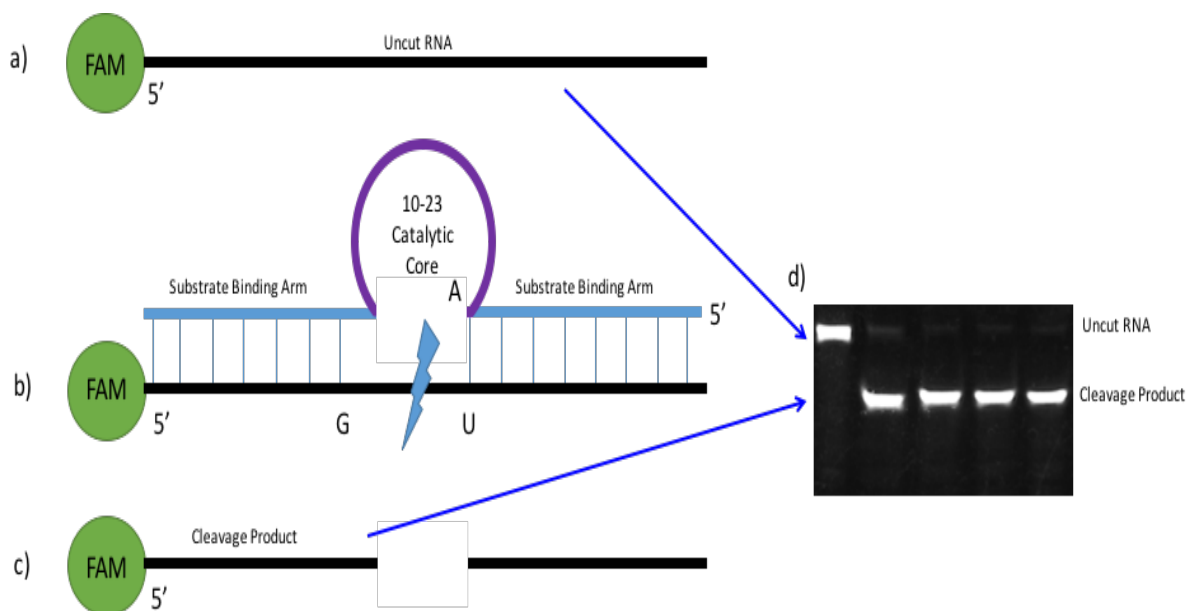


[Figure 3.9 - 10-23 DNAzyme cleavage reaction carried out using 5'FAM labelled target RNA.](#)

5'FAM labelled RNA and the DNAzyme were incubated separately in DNAzyme buffer for 10 minutes at 37 °C. These were then combined and incubated at 37 °C for the desired period of time. Reactions were stopped with RNA loading dye and snap frozen. The samples were boiled prior to loading on urea PAGE gels and bands visualised.

DNAzyme cleavage reaction protocols differ in literature. The initial experiments utilized 10 mM MgCl₂ and cleavage efficiency was investigated over a time course (Figure 3.10). Here we found that only 50% cleavage could be achieved with the DNAzyme targeting the AR

RNA over 16 hours, and even less cleavage was seen with DT99 over this period. It is important to note that it appears as uncleaved RNA does not reduce in amount over time, this is due to the level of exposure required to visualize small concentrations of RNA in the cleavage product at shorter time points (i.e. 2 hours). Without this level of exposure, no cleavage would be apparent.

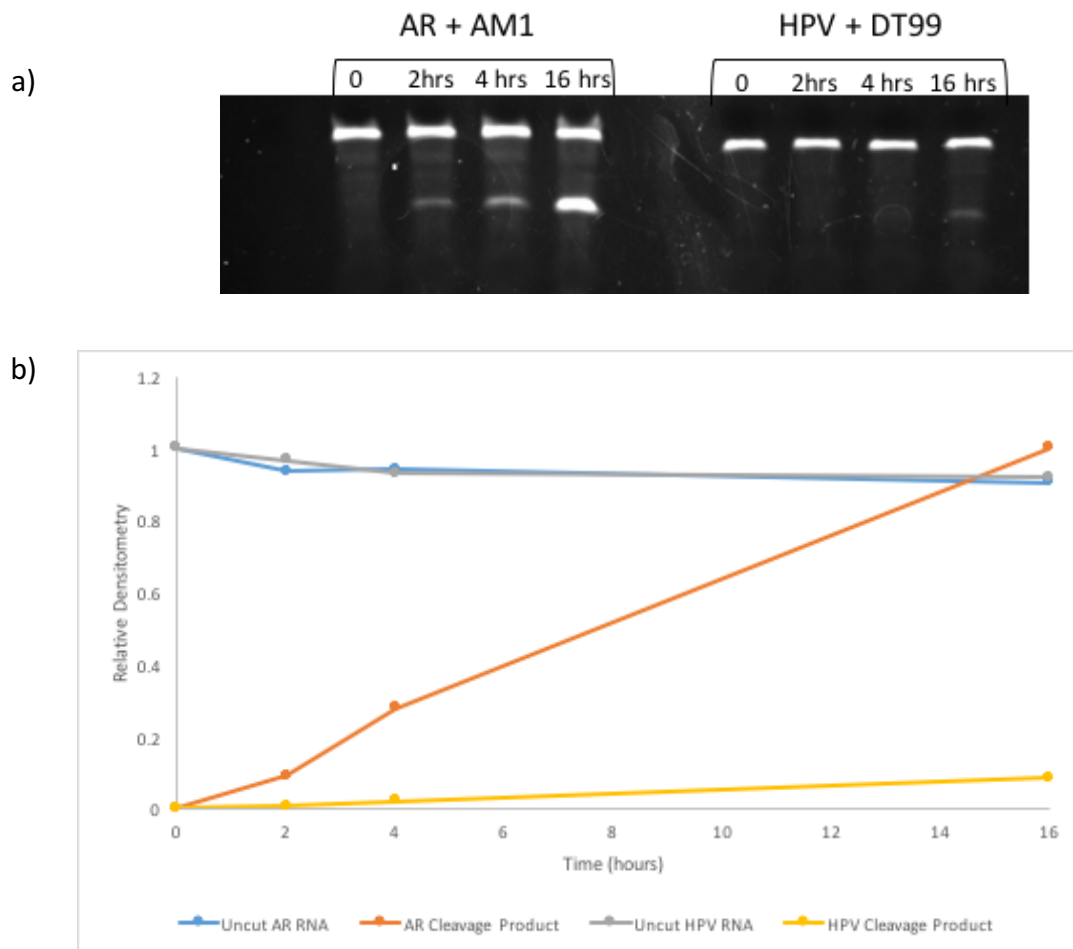


[Figure 3.10 – RNA cleavage over 16 hours is incomplete with DNAzyme buffer containing 10 mM MgCl₂.](#)

The usual DNAzyme cleavage reaction protocol was followed with DNAzyme buffer containing 10 mM MgCl₂. Cleavage reactions were stopped after 16 hours and a) samples run on a urea PAGE gel and bands visualised. b) ImageJ was used to measure densitometry of bands and a graph of relative densitometry produced (bottom). Single repeat.

The optimal concentration of $MgCl_2$ in DNAzyme buffer was confirmed by performing cleavage reactions with increasing concentrations of $MgCl_2$. All reactions were stopped by the addition of loading dye after 16 hours. The cleavage efficiency was found to increase between 10 – 40 mM of $MgCl_2$, and maximum cleavage occurred at ≥ 30 mM therefore the highest concentration was chosen for future experiments.

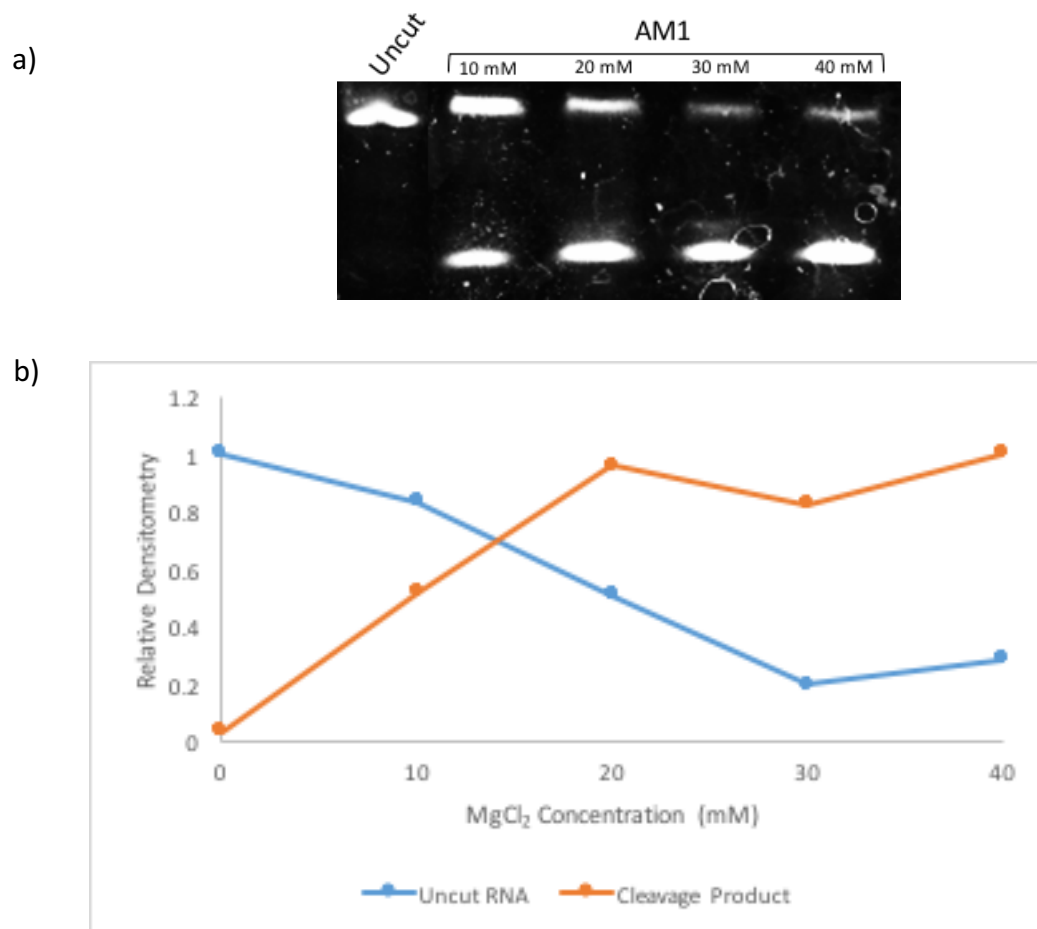


[Figure 3.11 - Cleavage reaction carried out using DNAzyme reaction buffer with increasing \$MgCl_2\$ concentrations \(10 mM to 40 mM\). 40 mM \$MgCl_2\$ gave the highest relative cleavage of AR RNA after 16 hours.](#)

DNAzyme AM1 against AR RNA was used to optimise the concentration of $MgCl_2$ in DNAzyme cleavage reaction buffer. Cleavage reactions performed as per the standard protocol. All reactions were stopped after 16 hours and a) bands visualised on a urea PAGE gel. b) ImageJ was used to measure densitometry of bands and a graph of relative densitometry produced (bottom). Single repeat.

3.2.5 Testing the Program: DNAzymes against the Androgen Receptor

The computer model was utilized to design new DNAzymes against the AR in the hope that these would cleave effectively. The aim was to also find the most efficient DNAzyme and identify its properties in order to adjust the parameters used by the software to rank the DNAzymes. To do this, we used *in vitro* cleavage reactions to test the 5 lead DNAzymes designed by the program (Figure 3.12).

A 16-hour cleavage reaction was performed on each DNAzyme against AR RNA. All 5 of the program designed DNAzymes (Table 3.1) cleaved in this timeframe (Figure 3.12). All 3 DNAzymes against AR RNA cleaved with minimal amount of intact RNA remaining. DNAzyme AM2 cleaved almost all the RNA and DNAzymes AM1 and AM-1 both less RNA at approximately 30-40% respectively. Negative control DNAzymes with an inverted catalytic core were also investigated under the same cleavage conditions and no cleavage was seen.

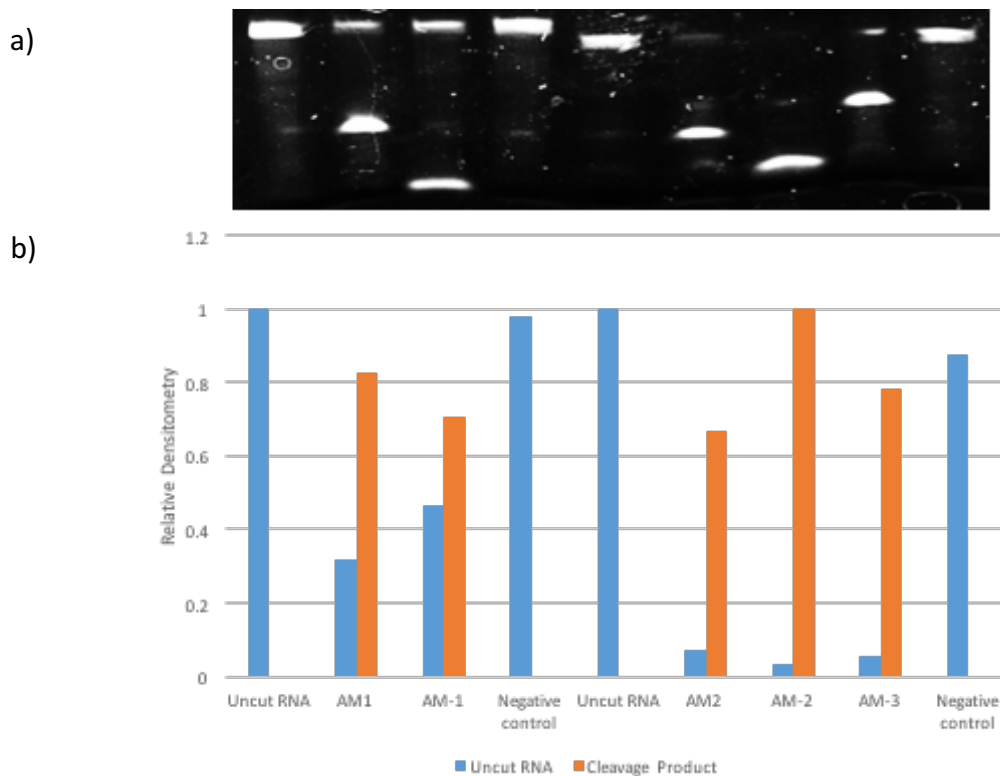


[Figure 3.12 – 16-hour cleavage reaction performed on AR RNA DNAzymes designed by the computer model and software indicates that all DNAzymes cleave AR RNA efficiently.](#)

Cleavage reactions were carried out as per the standard protocol using 40 mM MgCl₂. Reactions were stopped by the addition of loading dye and snap freezing prior to boiling and a) loading on a urea PAGE gel to visualise bands. b) ImageJ was used to measure densitometry of bands and a graph of relative densitometry produced. Single repeat.

To test the efficiency of the program DNAzymes at cleaving AR RNA, cleavage reaction time courses were performed for each DNAzyme. Aliquots of the reactions were taken and stopped at 30, 120 and 240 minutes (Figure 3.13).

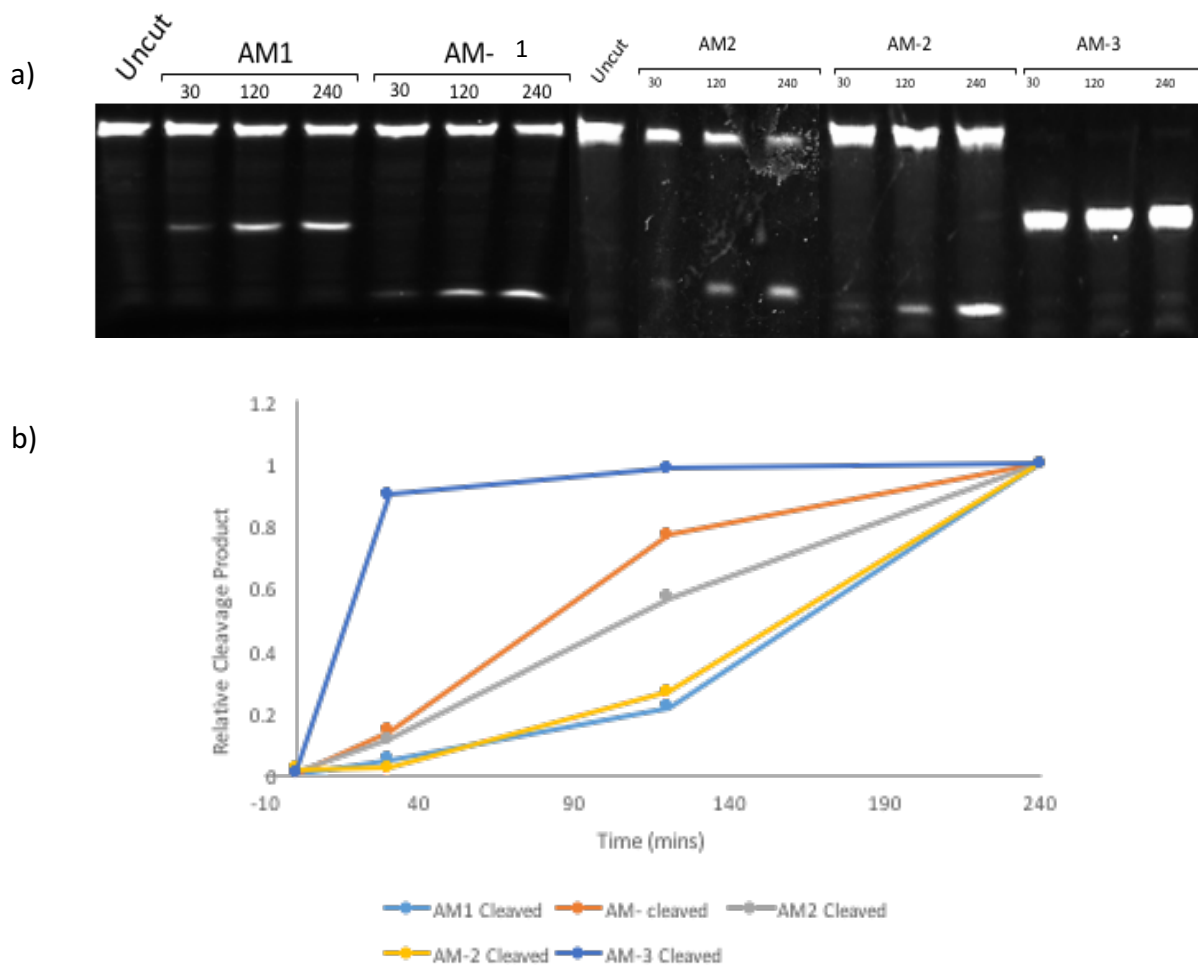


[Figure 3.13 - Cleavage reaction time course performed on AR RNA DNazymes designed by the computer model and software. The most efficient DNzyme is AM-3 with complete cleavage achieved after 30 minutes.](#)

Cleavage reactions were performed as per the standard protocol with aliquots taken at 30, 120 and 240-minute time points. Reactions were stopped by the addition of loading dye and snap freezing prior to boiling and a) loading on a urea PAGE gel to visualise bands. b) ImageJ was used to measure densitometry of bands and a graph of relative densitometry of the cleavage product produced. Single repeat.

3.2.5.1 DNzyme AM-3 efficiency against AR RNA

The complete cleavage of the AR RNA by AM-3 after 30 minutes indicates that this DNzyme is the most efficient at cleaving AR RNA *in vitro* under standard cleavage reaction conditions. In order to test the efficiency of this DNzyme further, a shorter cleavage reaction time course was carried out with aliquots taken at 5, 10, 15, 20, 25 and 30 minutes

(Figure 3.14). Cleavage reaction buffer $MgCl_2$ concentration remained at 40 mM. Almost complete cleavage was achieved within 5-minutes reaction time.

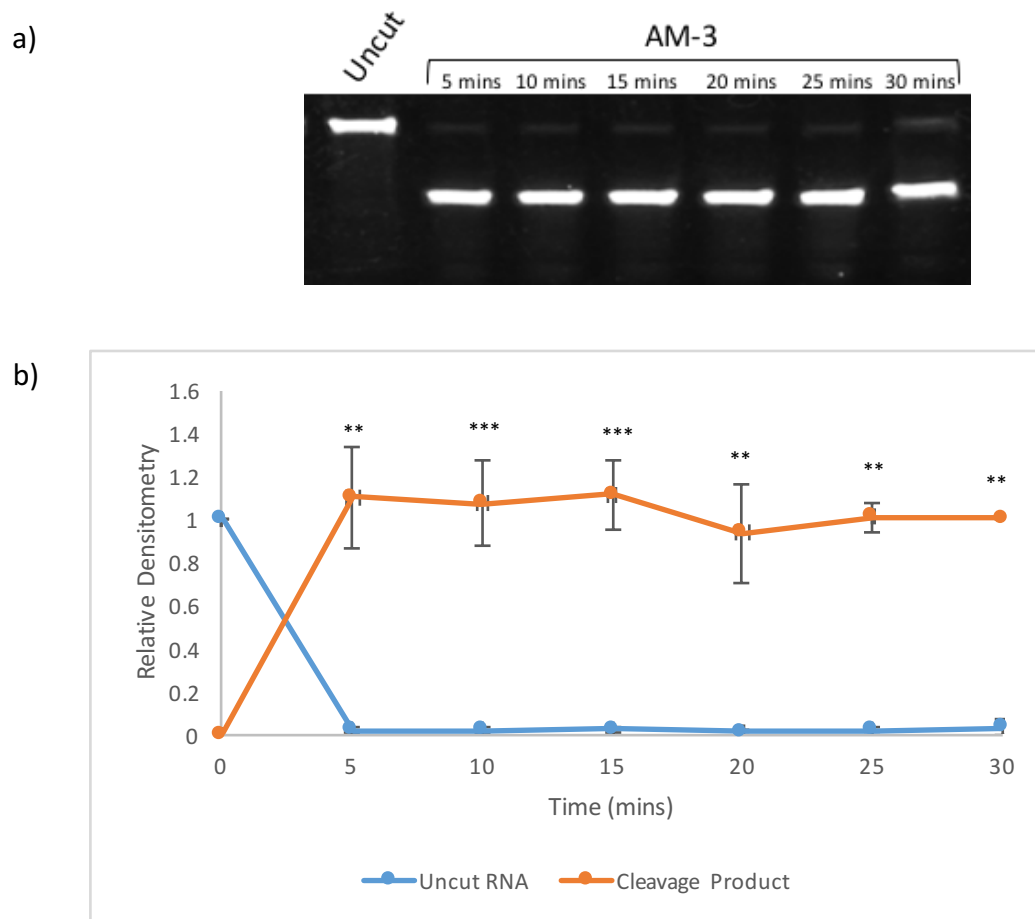


[Figure 3.14 - Cleavage reaction time course performed on AM-3 against AR indicates complete cleavage can still be seen after only 5-minute reaction time](#)

Cleavage reaction buffer contained 40 mM $MgCl_2$. Aliquots were taken after 5, 10, 15, 20, 25 and 30 minutes. Reactions were stopped by the addition of loading dye and snap freezing prior to boiling and a) loading on a urea PAGE gel to visualise bands. b) ImageJ was used to measure densitometry of bands and a graph of relative densitometry produced. Mean of 3 independent repeats. One-way ANOVA - ** $p < 0.005$, *** $p < 0.0005$.

A further experiment on DNAzyme AM-3 was performed to investigate if cleavage efficiency was affected by the $MgCl_2$ concentration in the reaction buffer (Figure 3.15). The

experiment indicated that AM-3 could still completely cleave AR RNA after 10 minutes in the presence of 10 mM MgCl₂.

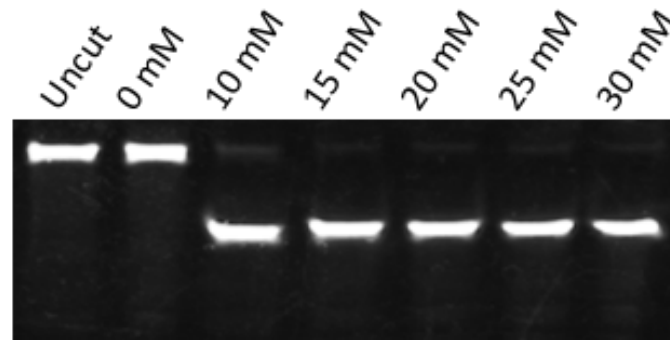
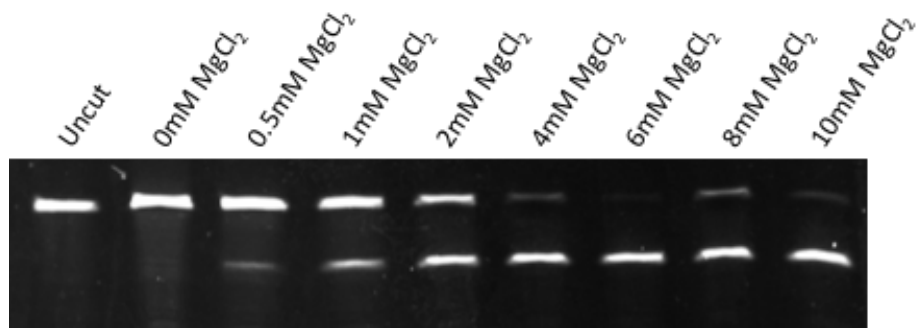


[Figure 3.15 - Cleavage reaction performed on AM-3 against AR with decreasing concentrations of MgCl₂ indicates that complete cleavage can still be seen after 10 mins at 10 mM MgCl₂.](#)

Cleavage reaction buffer containing 0, 10, 15, 20, 25 or 30 mM MgCl₂. Reactions were stopped after 10 minutes by the addition of loading dye and snap freezing prior to boiling and loading on a urea PAGE gel to visualise bands. 3 individual repeats performed all indicating total cleavage at 10 mM.

Further investigation of this DNAzyme was therefore required to test the MgCl₂ concentration range over which AM-3 is functional. To test this, lower concentrations of MgCl₂ were tested in a range that covered physiological conditions (whereby MgCl₂ is usually close to 2 mM) (Figure 3.16). The experiment indicated that at a concentration of 4 mM AM-3 could still cleave almost all the AR RNA after 10 minutes, and at physiological concentration (2 mM) approximately 50% of AR RNA was cleaved ($p < 0.0005$).

a)



b)

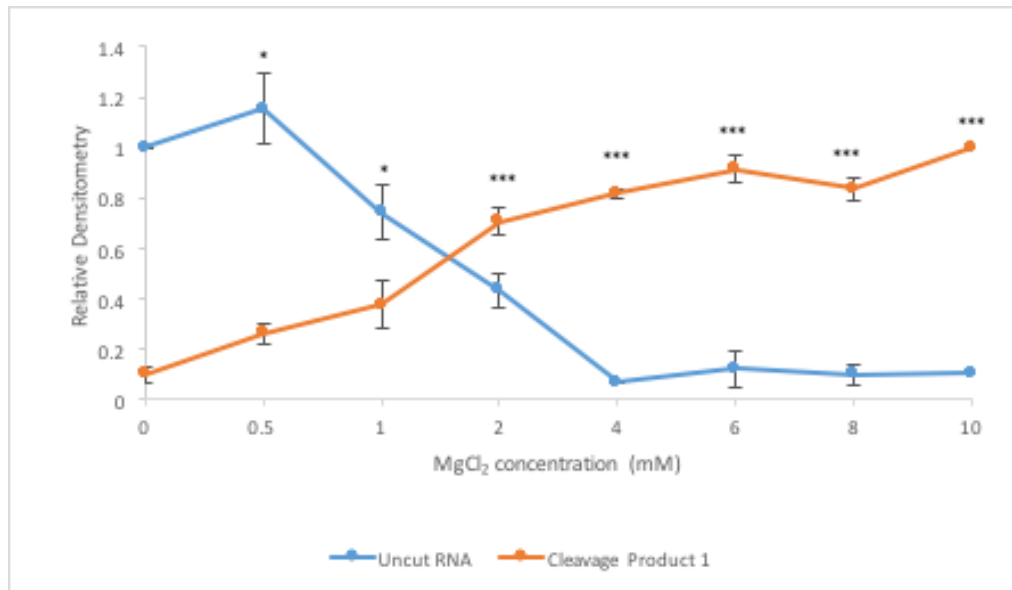


[Figure 3.16 - Cleavage reaction performed on AM-3 against AR with decreasing concentrations of MgCl₂. Approximately 50% cleavage can still be seen with 2 mM \(physiological concentration\) of MgCl₂ after 10 minutes.](#)

Cleavage reaction buffer containing 0, 0.5, 1, 2, 4, 6, 8 and 10 mM MgCl₂. All reactions stopped after 10 minutes by the addition of loading dye and snap freezing prior to boiling and a) loading on a urea PAGE gel to visualise bands. b) ImageJ was used to measure densitometry of bands and a graph of relative densitometry produced. Mean of 3 independent repeats ±1 SE. T-test - *p<0.05, ***p<0.0005.

To further investigate the activity of AM-3 at the physiologically relevant concentration of MgCl₂, a time course was performed (Figure 3.17). Here we could see that total cleavage was achieved after 30 minutes.

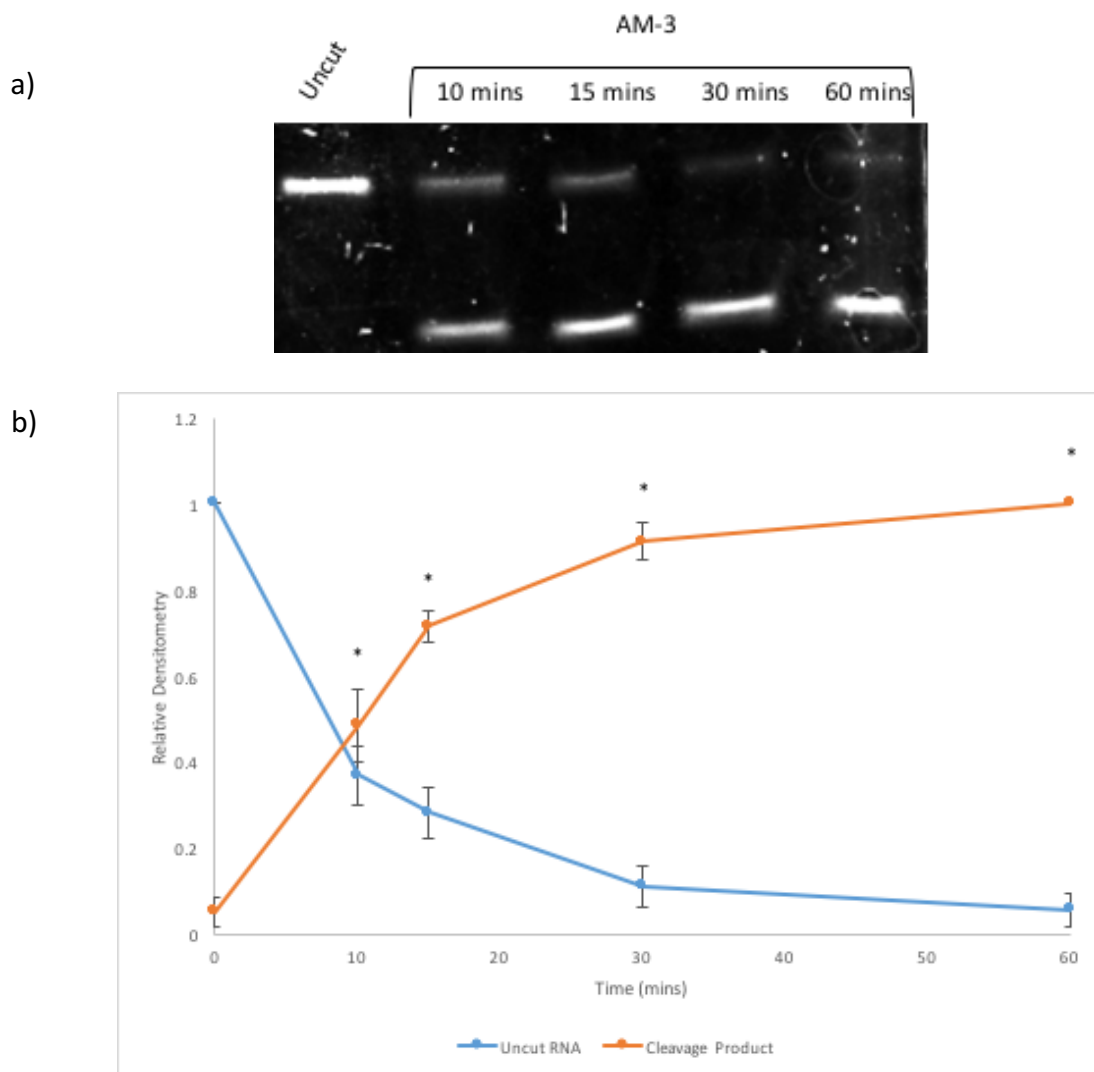


[Figure 3.17 - Time course of cleavage reaction performed using AM-3 against AR with 2 mM concentration of MgCl₂ indicates that 60% cleavage can be achieved after only 10 minutes and total cleavage after 30 minutes.](#)

Cleavage reaction buffer containing 2 mM MgCl₂. Aliquots taken at 10, 15, 30 and 60 minutes. Reactions were stopped by the addition of loading dye and snap freezing prior to boiling and a) loading on a urea PAGE gel to visualise bands. b) ImageJ was used to measure densitometry of bands and a graph of relative densitometry produced. Mean of 3 independent repeats ± 1 SE. One-way ANOVA - * $p < 0.0005$.

To investigate the ability of AM-3 to cleave AR RNA in cultured cells the DNAzyme was transfected into the androgen dependent PCa cell line, LNCaP (Figure 3.18). Other studies have shown that DNAzymes are not able to efficiently diffuse into cells so the transfection

reagent RNAiMax was used (Reyes-Gutierrez and Alvarez-Salas, 2009). Cell proliferation was then measured via crystal violet assays. A significant inhibition of proliferation was seen when AM-3 was transfected into LNCaP cells when compared to cells transfected with a negative control DNAzyme (inverted catalytic core). We have therefore identified a DNAzyme that can efficiently cleave AR RNA at physiologically relevant $MgCl_2$ concentrations and significantly inhibit LNCaP proliferation.

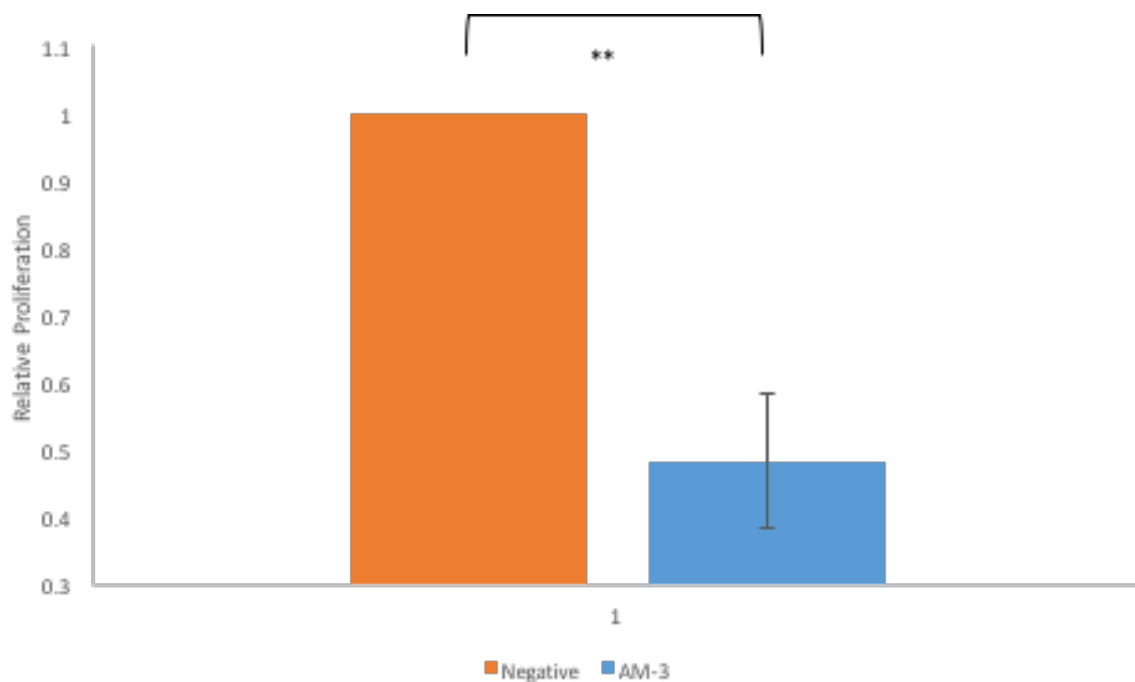


[Figure 3.18 – LNCaP Proliferation inhibited by approximately 50% by AM-3](#)

LNCaP cells were transfected with AM-3 or a negative control DNAzyme (inverted catalytic core) and grown in full media. Proliferation was assessed using crystal violet assays and proliferation expressed relative to the negative control. Mean of 2 independent repeats ± 1 SE. T-test - ** $p < 0.005$.

All AR DNAzymes designed by the program were then transfected into LNCaP cells and proliferation measured via crystal violet assays. After 3 repeats, it can be seen that AM-3 completely abolishes androgen-induced growth (Figure 3.19).

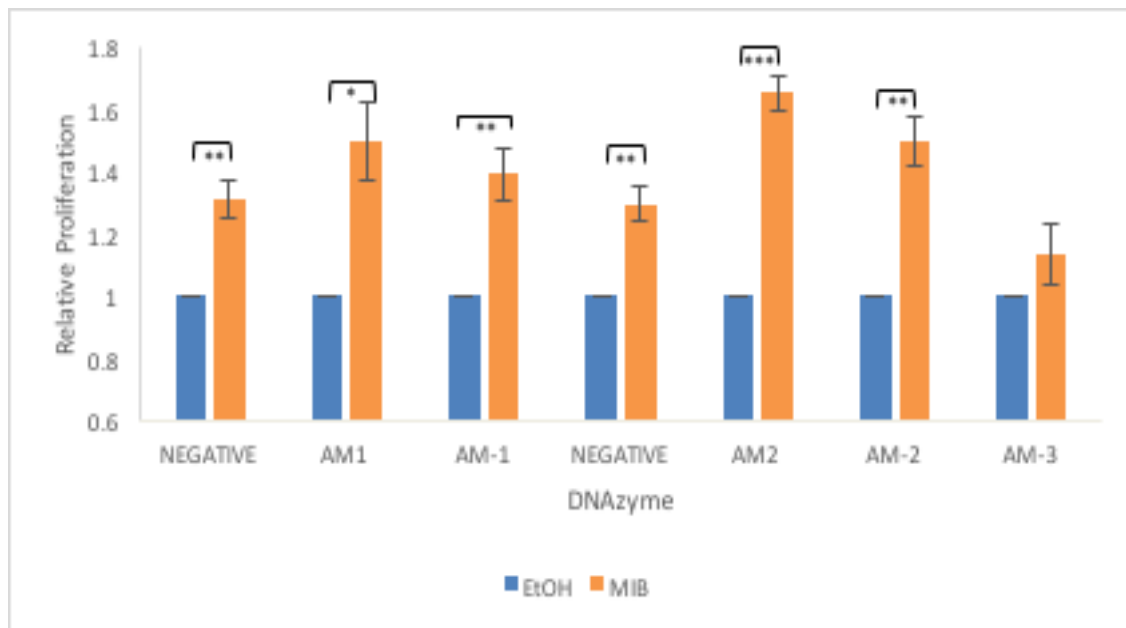


[Figure 3.19 – Program designed DNAzymes against AR RNA transfected into LNCaP cells indicates AM-3 abolishes androgen induced growth.](#)

LNCaP cells were transfected with DNAzymes against the AR. Proliferation was assessed using crystal violet assays and proliferation expressed relative to the negative controls. Mean of 3 independent repeats ± 1 SE. T-test - * $p < 0.05$, ** $p < 0.005$, *** $p < 0.0005$.

3.2.6 Testing the Program: DNAzymes against HPV16 RNA

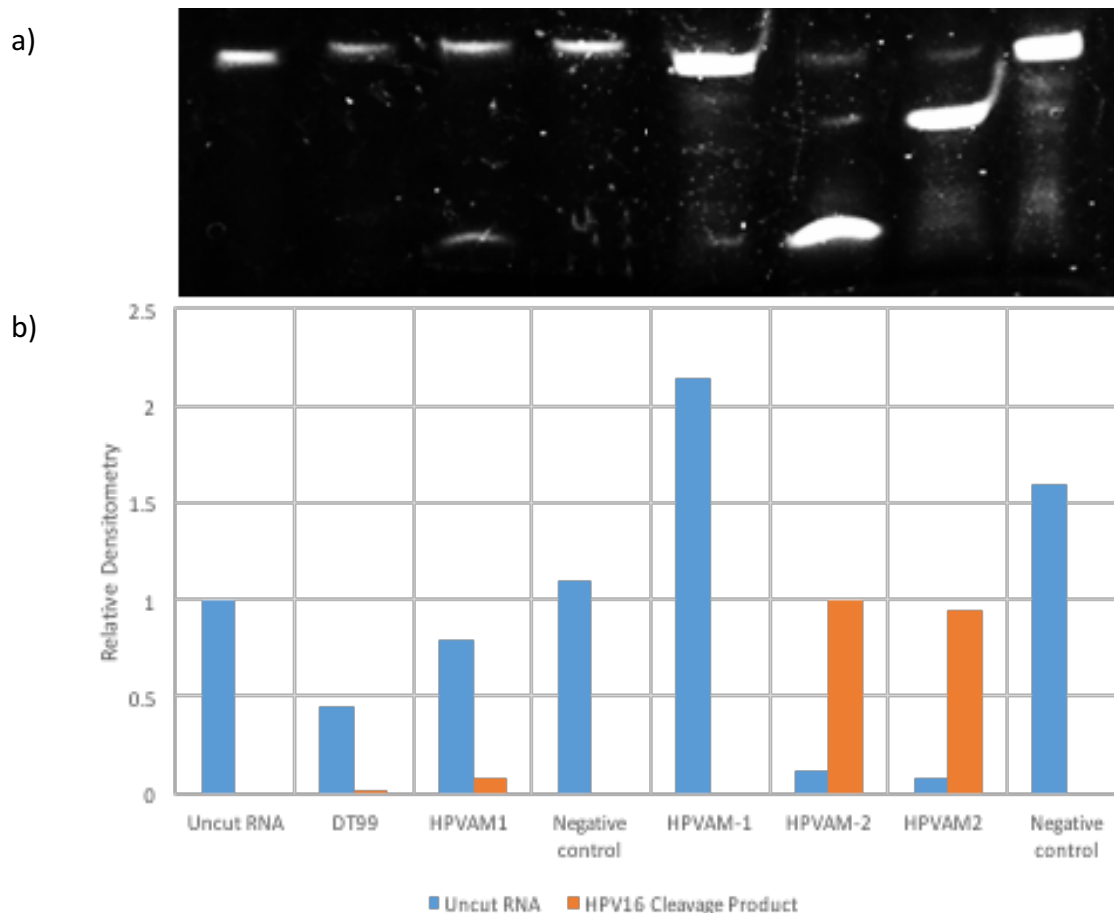
Although the primary aim of this study was to investigate a therapeutic option for the treatment of CRPC, the development of a new tool to design efficient DNAzymes became a secondary focus. In order to test the effectiveness of the computer model we asked it to predict DNAzymes that would target HPV16 RNA in order that we could compare them to the published DNAzyme DT99 (Cairns *et al.*, 1999). The four DNAzymes in Table 3.2 were predicted by the program to have varying cleavage efficiency ranging from poor to good.

Table 3.2 – DNAzymes against HPV16 RNA as predicted by the computer model and software.

* + = poor efficiency, ++ = average efficiency, +++ = good efficiency

DNAzyme	Binding position on RNA (bp)	Predicted Efficiency*	Parameters					Sequence
			Delta G	Hairpin (< 3.6)	Dimer (< 8.5)	Off Target	Accessible Sites	
HPVAM1	445-463	++	-19.24	-3.6	-4.2	1	16	CTCTACGTGGGCTAGCTACAAC GATCTTGATGA
HPVAM-1	389-407	+	-14.56	-1.6	-5	0	11	CTTATATTAGGCTAGCTACAAC GAGGAATCTTT
HPVAM-2	392-410	+	-16.85	-2.9	-6.74	0	10	CCCCTTATAGGCTAGCTACAAC GATATGGAATC
HPVAM2	405-423	+++	-24.37	-4.8	-4.8	0	7	CCGGTCCAGGCTAGCTACAACG ACGACCCCTT

In order to test the efficiency of these DNAzymes we performed cleavage reactions of all four DNAzymes alongside that of DT99. An overnight cleavage reaction was carried out on 5' FAM labelled HPV16 RNA. This indicated which DNAzymes were least/most efficient. The gel image and ImageJ densitometry results shown in Figure 3.20 indicate that the computationally designed HPVAM1, HPVAM-2 and HPVAM2 are all more efficient at cleaving HPV16 RNA than the previously published DT99. In comparison to DT99, which cleaved less than 1% of HPV16 RNA in this experiment HPVAM1 provides nearly 8% cleavage, HPVAM2 94% and HPVAM-2 total cleavage after 16 hours.



[Figure 3.20 - Cleavage reaction carried out overnight using DNAzymes against HPV16 RNA. DT99 is the second least efficient DNAzyme.](#)

Cleavage reactions performed as per the standard protocol with 40 mM MgCl₂ concentration in the DNAzyme buffer. All reactions stopped after 16 hours with loading dye and snap frozen prior to boiling and a) loading on gel in order to visualise bands. b) ImageJ was performed to measure densitometry of bands and a graph of relative densitometry produced. Single repeat.

In order to further investigate efficiency, a time course was performed over 240 minutes (Figure 3.21). Here we can see that all DNAzymes that were designed computationally to target HPV16 RNA are more efficient than DT99 at cleaving over this time course. HPVAM1 and DT99 were unable to cleave the RNA within 240 minutes. HPVAM-1 does appear to show cleavage after 30 minutes in this experiment however, which was not seen in the previous cleavage reaction (Figure 3.20). HPVAM-2 is shown to be the most efficient

DNAzyme in this time course, however both HPVAM-2 and HPVAM2 are efficient in cleaving RNA within 4 hours with approximately 50% cleavage achieved by both in this time.

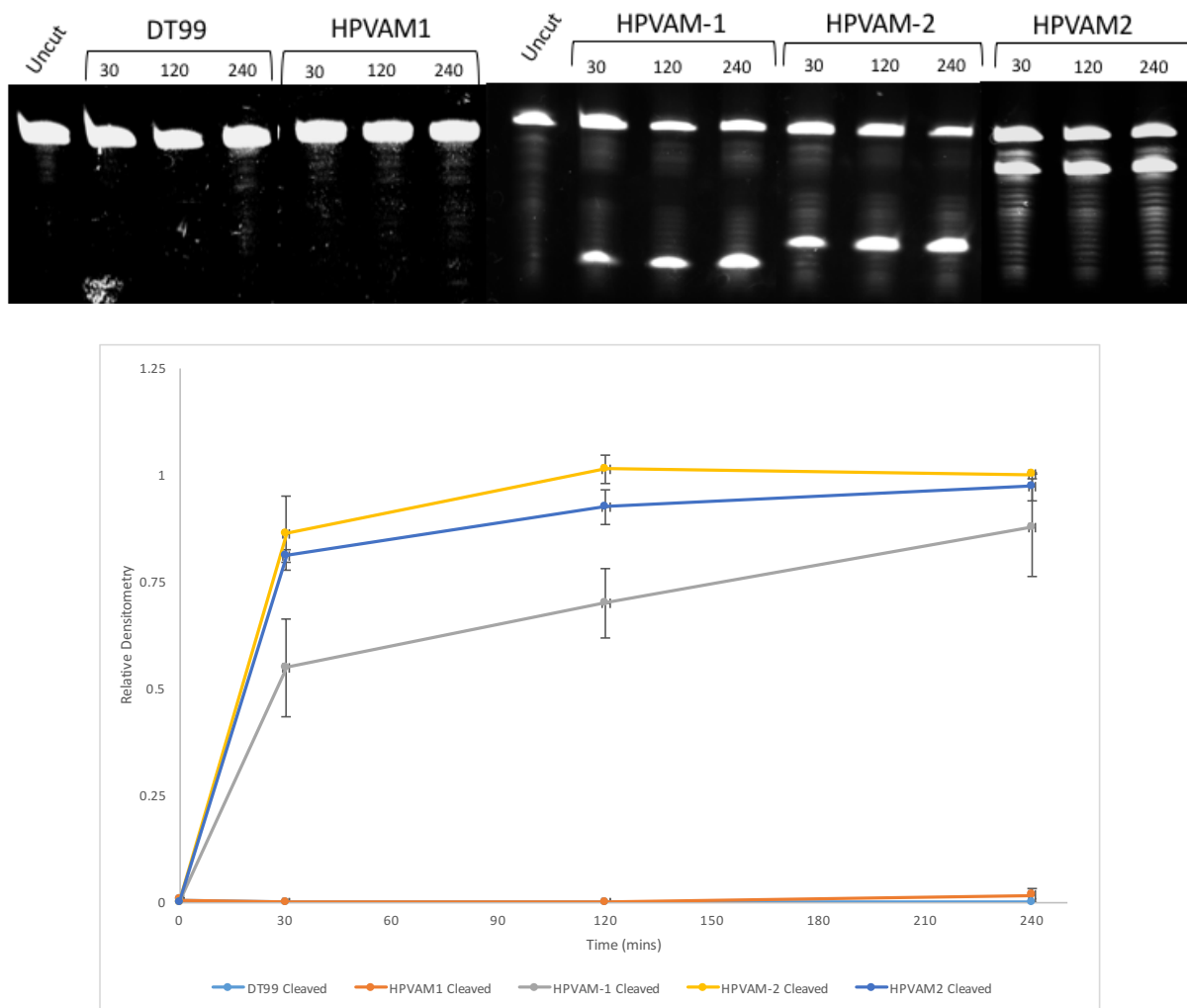


[Figure 3.21 - Cleavage reaction time course performed using DNAzymes against HPV16 RNA. Program DNAzymes cleave HPV RNA more efficiently than the published DT99.](#)

Cleavage reactions performed as per the standard protocol with 40 mM MgCl₂ concentration in the DNAzyme buffer. Aliquots of reactions taken at 30, 120 and 240 minutes. a) All reactions stopped with loading dye and snap frozen prior to boiling and loading on gel in order to visualise bands. b) ImageJ was used to measure densitometry of bands and graphs of relative densitometry produced for cleavage product. Mean of 2 independent repeats (DT99 & HPVAM1) 3 independent repeats (all other DNAzymes) ±1 SE. Two-way ANOVA – p<0.0001.

3.3 Discussion

DNAzymes are being developed as therapeutic tools for many diseases such as cancer and to halt viral infections (Beale *et al.*, 2003; Dass *et al.*, 2008; Sood *et al.*, 2007; Wu *et al.*, 1999) and they offer promise as novel therapeutics in the treatment of castrate resistant PCa. In this study I provide evidence of the effective development and implementation of a computer model and software program to design DNAzymes effective at cleaving target RNA efficiently.

3.3.1 Computer model and software designed DNAzymes against HPV16 RNA are more efficient than previously published DT99

DT99 has been shown to be an efficient DNAzyme against HPV16 RNA (Cairns *et al.*, 1999). In order to investigate the efficiency of DT99 in comparison to HPV16-targetting DNAzymes designed by the computer model, cleavage reactions were performed. Reactions used either *in vitro* transcribed RNA or 5'FAM labelled RNA and differing visualization techniques performed to find the optimal method for visualizing and quantifying both un-cleaved and cleaved RNA. Utilising 5'FAM labelled RNA and urea PAGE for visualization provided the best resolution images of cleavage reactions. Here RNA remained stable and did not degrade, which was an issue with the *in vitro* translated RNA.

Most nucleic acid enzymes such as DNAzymes require metal ions for catalytic functions (Li *et al.*, 2000), thus making them a form of metalloenzyme (Lan and Lu, 2012). For this reason, it was necessary to perform cleavage reactions using differing concentrations of MgCl₂. Higher concentrations of MgCl₂ (≥ 30 mM) did increase cleavage efficiency, it was also noted that MgCl₂ concentration and cleavage efficiency was very much dependent on the DNAzyme in question. However, AM-3 efficiently cleaved RNA at low concentrations of

MgCl₂ indicating that this could have potential as highly efficient therapeutic functioning at physiological MgCl₂ concentration (2 mM).

Cleavage reaction time courses were performed in order to assess the efficiency of DNAzymes. Total uncleaved RNA and cleavage product were measured by visualizing 5'FAM labelled RNA on a urea PAGE gel and ImageJ used to measure densitometry. DT99 was only found to cleave HPV16 RNA after 960 minutes, whereas program designed DNAzymes HPVAM-1, HPVAM-2 and HPVAM2 all show cleavage after just 30 minutes. This indicates that the computationally designed DNAzymes are indeed more efficient than DT99.

A limitation of the cleavage reactions performed is that they utilize short pieces of RNA and hence do not take into account the folding associated with the full-length RNA. The program does predict secondary structure and binding site accessibility, but this needs to be fully investigated in future studies. In order to further investigate the potential of each DNAzyme against full-length HPV16 RNA it would be advantageous to perform cell-free transcription and translation assays. In this way DNAzyme cleavage of the target gene could be examined by monitoring protein synthesis in the presence of the DNAzymes in question. Alternatively transfecting the DNAzymes into a cell line such as C33-A, a cervical tumour line, and performing proliferation assays with crystal violet would allow us to investigate the *in vivo* potential of DNAzymes shown to be effective *in vitro*. This would overcome the issue of short nt length RNA being used in *in vitro* cleavage reactions.

Another DNAzyme against HPV16 has been tested in recent years. Dz1023-434 is a 29 nt 10-23 DNAzyme with the usual 15 nt catalytic core but substrate binding arms of only 7 nt in length (Reyes-Gutierrez and Alvarez-Salas, 2009). The cleavage efficiency of this DNAzyme

was shown to be substantial. Longer substrate binding arms are known to confer a more stable hybridization with the target RNA and therefore increases activity/cleavage efficiency and specificity (Kurreck *et al.*, 2002). Interestingly, the program did identify a DNAzyme that binds to the same region of HPV16 as Dz1023-434, binding at nts 428-446. However, the program predicted this DNAzyme would be inefficient at cleaving the target RNA due to only possessing two accessible sites and low binding energy (delta G value of -18.17). It would be beneficial to investigate the cleavage efficiency of this DNAzyme in our own cleavage reactions as well as in comparison to the HPV DNAzymes we have already tested.

3.3.2 The computer model and software can be used to design efficient DNAzymes against AR RNA

It was observed that DNAzymes designed initially by hand were present in the output file of rejected DNAzymes by the program. These were DNAzymes the program predicted would not cleave AR RNA efficiently, which in our initial experiments we confirmed to be the case. All DNAzymes predicted by the program to be effective against AR RNA performed successfully.

A total of five DNAzymes against the AR were tested in this study and all proved to be efficient at cleaving RNA to varying degrees. AM-3 cleaved AR RNA completely within 5 minutes in the presence of 40 mM MgCl₂ and after 30 minutes at physiological (2 mM) concentration of MgCl₂. After just 10 minutes in the presence of the physiological concentration of MgCl₂, AM-3 cleaved approximately 50% of AR RNA. This indicates that AM-3 could be a viable DNAzyme for use as a therapeutic as it successfully cleaves target RNA even at physiological relevant concentrations of MgCl₂.

To test the efficiency of AM-3 *in vivo*, it was transfected into the AR positive PCa cell line LNCaP both in the presence of mibolerone and just in full media. In full media AM-3 inhibited proliferation by approximately 50%, however we also saw that AM-3 was able to completely abolish androgen induced growth in the presence of mibolerone. This is a considerable level of inhibition for a DNAzyme even though the DNAzyme does not contain any modified sequences in order to stabilise it in serum or biofluids. Several modifications can be made to enhance DNAzyme stability such as inverted bases (as described previously), or LNA (locked nucleic acid) whereby a O2'- to C4'- linked analogue with a C3'-endo sugar conformation proves ideal for RNA recognition and increases binding affinity of the DNAzyme to target RNA (Petersen and Wengel, 2003). It would be advantageous to incorporate LNA monomers in the binding arms of DNAzymes being transfected into cells. Studies have shown that these monomers can vastly improve DNAzymes (Vester *et al.*, 2006; Vester *et al.*, 2004). The inclusion of five LNA monomers in the substrate binding arms increases cleavage activity as they confer the ability to unfold complex RNA structures (Fluiter *et al.*, 2005; Vester *et al.*, 2002).

3.4 Summary

It was discovered that the DNAzymes designed by the program did have different efficiencies, but these did not necessarily correlate with the program's efficiency ranking. For this reason, we examined the properties of these DNAzymes per the software parameters to understand why certain ones cleave more efficiently than others. This analysis however did not point to any one parameter being able to strongly predict the efficiency of the DNAzymes. This indicates that although the program is useful in predicting DNAzymes, it is not able to predict which will be the most efficient.

The data suggests that DNAzymes can be used to down-regulate the AR and could therefore be a useful therapeutic strategy for PCa. They would be expected to be effective where current therapies would be predicted to fail, as the AR continues to drive growth in CRPC i.e. in the case of AR mutations and variants (Brooke and Bevan, 2009). Further work would be needed to assess their suitability as a treatment option for cancer for example, in order to complement cell proliferation assays it would be necessary to perform flow cytometry in order to analyse cell death/apoptosis. This would confirm if the biological effects being imposed on the cells is due to the catalytic activity of the DNAzyme rather than an off target effect. Animal model studies and delivery methods would also need to be addressed. Other DNAzymes that have entered into clinical trials such as hdg40 and DZ1 (NIH, 2012; NIH, 2014a; NIH, 2014b) have overcome these issues successfully so this provides a confident outlook for the future of DNAzymes as a potential therapeutic for PCa and CRPC.

Chapter 4: Finding novel metabolic targets for the treatment of CRPC

4.1 Introduction

PCa is typically dependent on androgen signalling in order to grow and progress. This means that patients are often initially responsive to androgen depletion therapies, however these therapies often fail within 1-3 years (Katsogiannou *et al.*, 2015). This often leads to tumours progressing to the aggressive castrate resistant stage (CRPC) for which there is limited treatments available and survival at this stage of the disease is just 13.5 months (Hirst *et al.*, 2012). For this reason, there is much need for novel targets to be investigated as possible therapeutic options for the treatment of CRPC.

4.1.1 Targeting metabolic proteins for the treatment of CRPC

Cancer cells are known to have a substantially different metabolic program to that of normal cells. Cancer cells rely more heavily on processes such as aerobic glycolysis, fatty acid synthesis and glutaminolysis than that of their normal counterparts in order to proliferate (Vander Heiden *et al.*, 2009). Studies have shown that proteins involved in metabolism are regulated in response to androgen. Since the CRPC remains reliant upon AR signalling, inhibition of advanced aggressive PCa growth could be achieved by targeting these key proteins downstream of the AR (Brooke *et al.*, 2015; Massie *et al.*, 2011).

4.2 Results

4.2.1 Optimisation of an siRNA screen to identify novel metabolic targets for the treatment of prostate cancer

An siRNA screen was carried out targeting genes involved in metabolism and cell traffic. A total of 711 different siRNAs were assessed (excluding controls) examining 237 different

genes (3 different siRNAs per gene). It is hypothesised that targeting these genes will identify novel strategies to inhibit PCa cell growth.

4.2.1.1 Optimisation of Positive Control for use in siRNA screen

Prior to completion of the siRNA knock-down screen, proliferation assays were carried out in order to observe the effect of AR knock-down which acted as a positive control for the screen. LNCaP cells were seeded in the absence of hormone and transfected with siRNA targeting AR or non-targeting control (NTC) and treated with the synthetic androgen Mibolerone (MIB) or vehicle (ethanol, EtOH). Successful knock-down was confirmed at the protein level (Figure 4.2i). As expected siRNA knock-down of AR abolishes androgen-induced growth (Figure 4.2ii and iii).

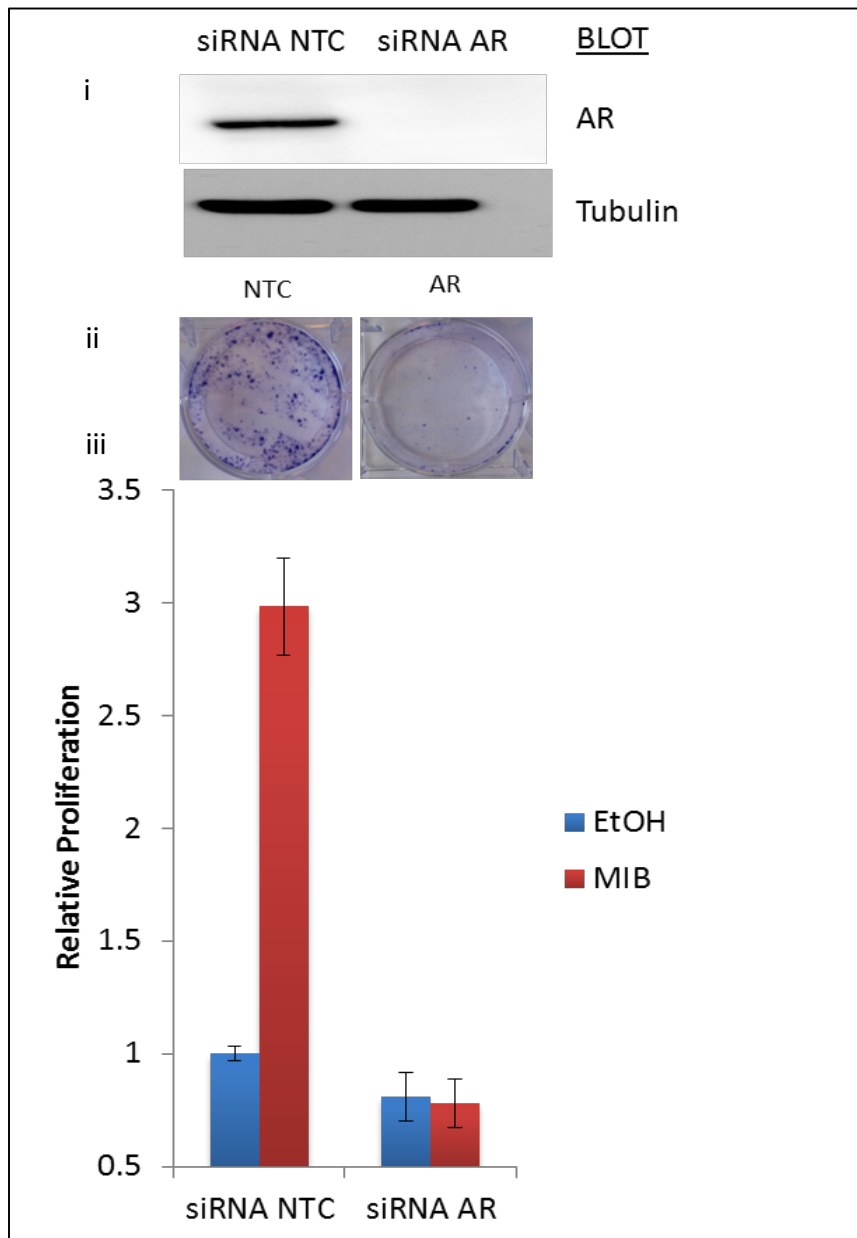


[Figure 4.1- Knock-down of AR in LNCaP cells blocks androgen-induced proliferation.](#)

LNCaP cells were transfected with siRNA targeting the AR or non-targeting control (NTC) and i) Western blotting performed to confirm successful knockdown. Crystal violet used to stain cells and imaged via light microscopy (ii) (iii) Cells were stained with crystal violet and resolubilised with 10% acetic acid, absorbance read at 490 nm to investigate LNCaP proliferation. 1 repeat, 6 technical replicates. Mean \pm 1 SE.

4.2.2 Identification of metabolic targets using an siRNA Screen

Upon completion of the siRNA screen, genes were identified that increased and decreased LNCaP cell growth (Figure 4.2). Only one gene was found to increase growth across all 3

siRNAs beyond that of 75% of the NTC, that gene being protein disulphide isomerase-like protein of the testes (PDILT). A total of 10 other genes increased proliferation beyond that of the NTC. At the opposite end of the spectrum multiple siRNA duplexes were identified that reduced LNCaP growth. Potential targets were identified when all three siRNAs decreased cell growth more than 75%, compared to the NTC control (shown in Figure 4.3 and listed in Table 4.1). The largest inhibition of cell proliferation was seen by syntaxin 8 (STX8) and fatty acid synthase (FASN), both indicating over a 90 % decrease in proliferation across all 3 siRNAs. There also appears to be specific pathways that when targeted can reduce proliferation considerably; the fatty acid and polyamine biosynthesis pathways both contain targets that decrease proliferation up to 90 % across 3 siRNAs.

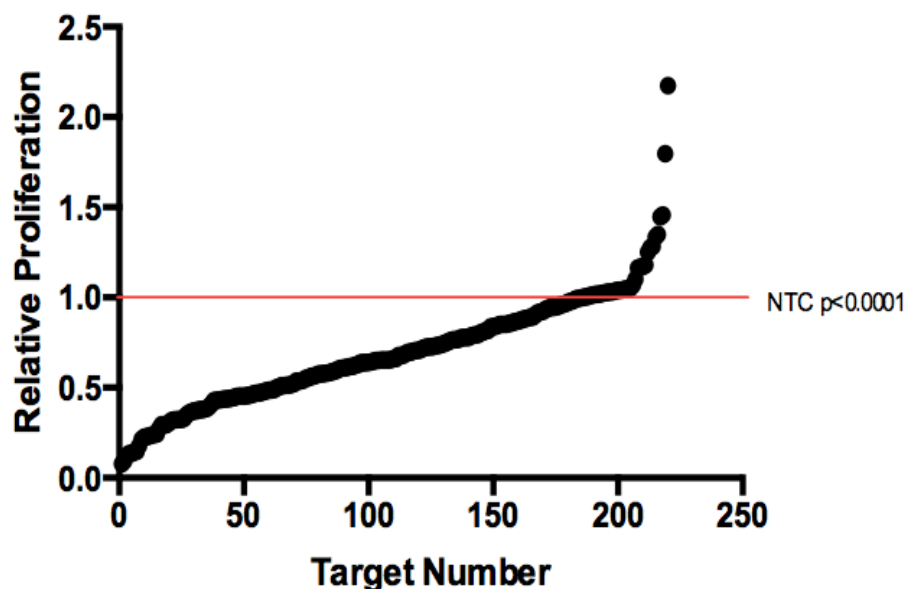


[Figure 4.2 – Average of 3 siRNAs across all genes from siRNA knock-down screen.](#)

LNCaP cells were transfected in triplicate with three siRNAs targeting various genes responsible for metabolism and cell traffic. Cell growth was measured by crystal violet assay on day 6 of growth.

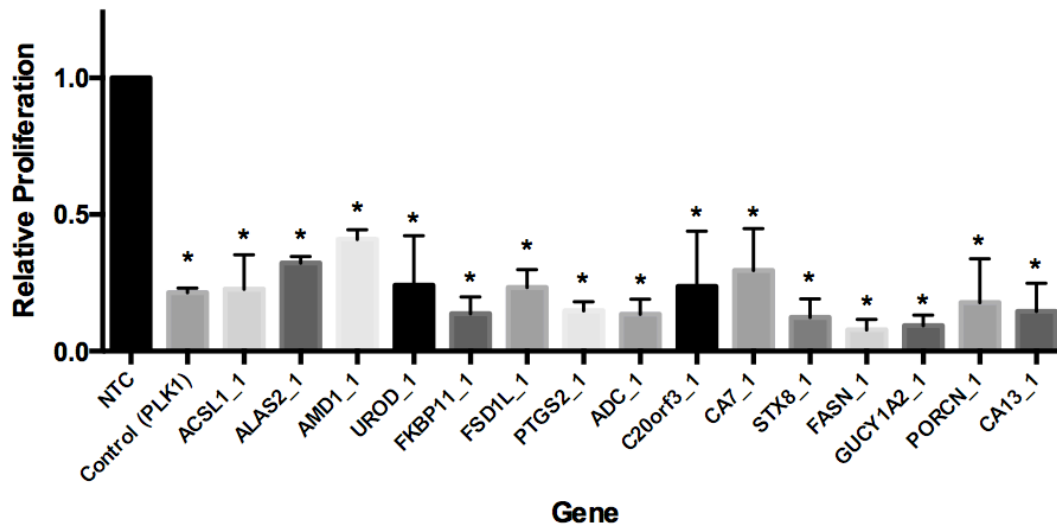


Figure 4.3 – Target genes of interest from siRNA knock-down screen.

LNCaP cells were transfected in triplicate with three siRNAs targeting various genes responsible for metabolism and cell traffic. Cell growth was measured by crystal violet assay on day 6 of growth. All genes are significant compared to the NTC (* $p < 0.0001$) mean ± 1 SE.

Table 4.1 – Target genes of Interest indicated by siRNA knock-down screen results.

Symbol (symbol in screen)	Gene Description	Pathway	Inhibition of Relative Proliferation
ACSL1	Acyl-CoA Synthetase Long-Chain Family Member 1	Fatty Acid Synthesis/Metabolism	70-90%
ALAS2	5'-Aminolevulinat Synthase 2	Links Glycine Metabolism to Porphyrin Biosynthesis	70%
AMD1	Adenosylmethionine Decarboxylase 1	Polyamines Biosynthesis (spermine & spermidine), Cysteine & Methionine Metabolism	55-60%
UROD	Uroporphyrinogen Decarboxylase	Porphyrin & Chlorophyll Metabolism	60-90%
FKBP11	FK506 Binding Protein 11	Protein Folding	80-90%
FSD1L	Fibronectin Type III And SPRY Domain Containing 1 Like	Unknown	70-85%
COX2 (PTGS2)	Prostaglandin-Endoperoxide Synthase 2	Arachidonic Acid Metabolism & Prostaglandin Synthesis	90%
AZIN2 (ADC)	Antizyme Inhibitor 2	Polyamine Biosynthesis, Arginine & Proline Metabolism	90%

APMAP (C20orf3)	Adipocyte Plasma Membrane Associated Protein	Adipocytes	60-99%
CA7 & CA13	Carbonic Anhydrase 7 & 13	Multiple Pathways	50-80% & 80-95%
STX8	Syntaxin 8	SNARE interactions in vesicular transport	90-99%
FASN	Fatty Acid Synthase	Fatty Acid Biosynthesis	90-95%
GUCY1A2	Guanylate Cyclase 1, Soluble, Alpha 2	Multiple Pathways	90%
PORCN	Porcupine Homolog	Wnt & GPCR Signalling	65-95%

4.3 Discussion

The increased metabolism and altered metabolic signalling of cells is a known hallmark of cancer (Ward and Thompson, 2012). Increased proliferation of cells means there is a heightened demand for amino acids, nucleic acids and lipids in tumours. After completing the siRNA screen several potential target genes/pathways of interest involved in metabolism and cell traffic were identified (Table 4.1).

4.3.1 Fatty Acid Biosynthesis

4.3.1.1 The fatty acid biosynthesis pathway

Fatty acids are vital for cell growth and are an essential component of cell membranes (Currie *et al.*, 2013), however in adult mammalian cells most fatty acids are acquired from dietary sources (Santos *et al.*, 2016). Fatty acids can be synthesized *de novo* however this mainly occurs in the liver, adipocytes and lactating breast tissue (Santos *et al.*, 2016).

Figure 4.4 (taken from (Currie *et al.*, 2013)) indicates the pathway of fatty acid biosynthesis. Citrate, an intermediate of the Krebs cycle, feeds into fatty acid biosynthesis thereby connecting glucose metabolism to the process. Two targets, ACSL1 and FASN, indicated by red boxes in Figure 4.4, were found to inhibit the proliferation of LNCaP's in our study related to fatty acid biosynthesis. Both enzymes are required to convert carbons from citrate to bioactive fatty acids (Currie *et al.*, 2013). FASN is a 270 kDa protein that forms a

dimer in the cytoplasm. One FASN dimer can process one acetyl-CoA and seven malonyl-CoA molecules to produce palmitate (Currie *et al.*, 2013; Santos *et al.*, 2016).

In order for fatty acids to enter into the bioactive pool, they must first be activated by enzymes. These enzymes form a family known as acyl-CoA synthetases (ACS) of which in mammals there are five isoforms (ACSL1, 3, 4, 5 & 6) (Currie *et al.*, 2013). ACSL1 is expressed in lipid droplets, microsomes and mitochondria. It is responsible for the high levels of unsaturated fatty acids in oleate and linoleate (Kanter *et al.*, 2012) and is associated with glucose homeostasis (Li *et al.*, 2015). Interestingly another gene that scored just below the cut off point for our criteria, acyl-CoA synthetase medium chain family member 1 (ACSM1) is another such enzyme in the same family as ACSL1. It therefore appears that this pathway is important in LNCaP proliferation.

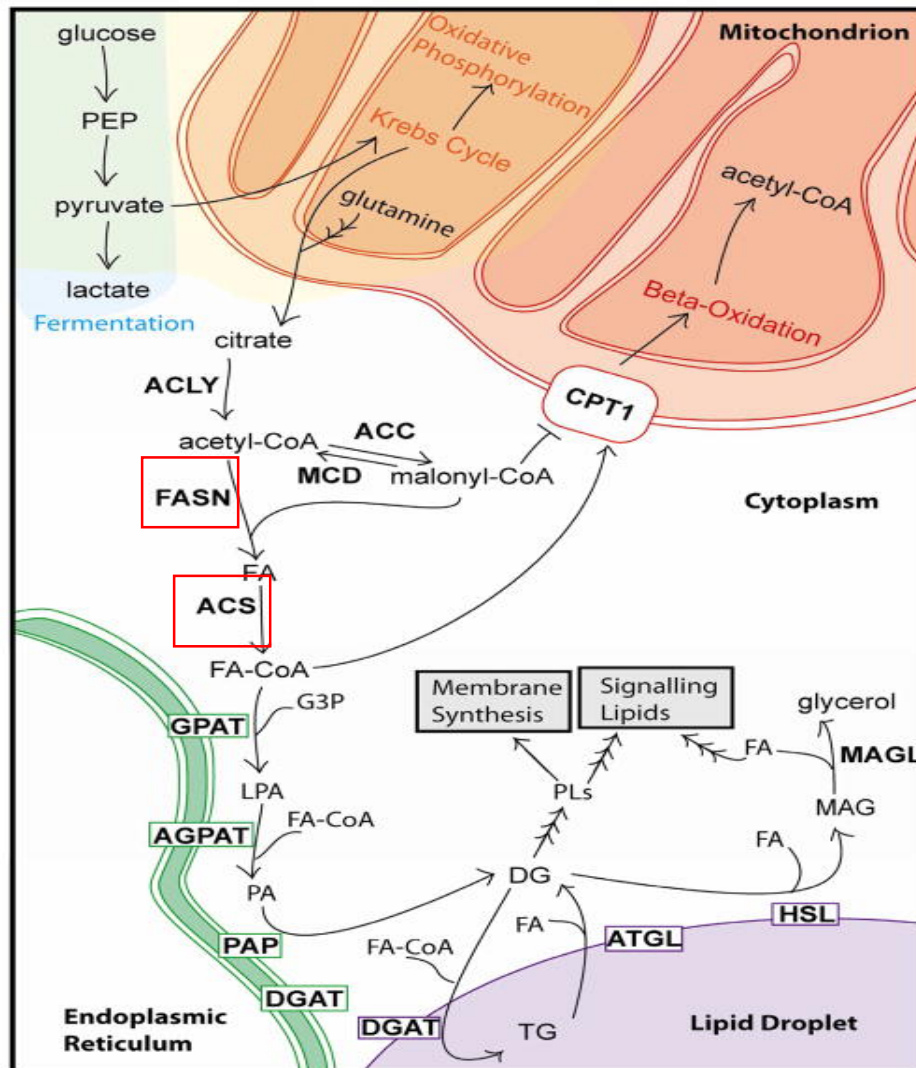


Figure 4.4 – The fatty acid biosynthesis pathway.

The synthesis of fatty acids relies heavily on enzymes such as ACSL1 and FASN (in red boxes) in order to convert the carbon in citrate from glucose metabolism into bioactive fatty acids (taken from (Currie *et al.*, 2013)).

4.3.1.2 The role of fatty acid biosynthesis in cancer

The deregulation of fatty acid synthesis has been observed in many cancers resulting in increased proliferation, progression and metastasis (Currie *et al.*, 2013). Altered fatty acid synthesis is now recognized as a marker of cancer as elevated *de novo* fatty acid synthesis is required to meet the increased energy demands and sustain cellular processes of cancer

cells (Chen *et al.*, 2016). In PCa, in particular, it has been shown that tumour cells favour lipid metabolism rather than aerobic glycolysis as their primary energy source (Ackerstaff *et al.*, 2001).

Fatty acids are in greater demand due to their role in the biosynthesis of cell membranes and signalling molecules, than energy. This results in carbon being directed away from energy production into fatty acid biosynthesis (Currie *et al.*, 2013) and tumours favour fatty acid synthesis (Figure 4.4) rather than relying on exogenous sources. Looking more towards PCa and CRPC in particular, Massie *et al.* has shown that the AR induces anabolic activity via the upregulation of various enzymes, some of which are involved in fatty acid biosynthesis (Massie *et al.*, 2011). Further, it has also been shown that androgens enhance *de novo* lipid biosynthesis (Moon *et al.*, 2011).

FASN has been shown to be upregulated in the early stages of PCa and increases during the progression of the disease (Hamada *et al.*, 2014). It has also been shown that FASN expression decreases initially in LNCaP tumours in mice following acute castration, however under long-term castration FASN levels resume and continually rise (Huang *et al.*, 2003). In order to investigate the levels of FASN in patient samples examination of immunohistochemistry staining from the Human Protein Atlas was performed. Expression of FASN in normal prostate versus low and high grade prostate adenocarcinoma supports that levels of expression increase in PCa development (Figure 4.5) (Universitet, 2016b).

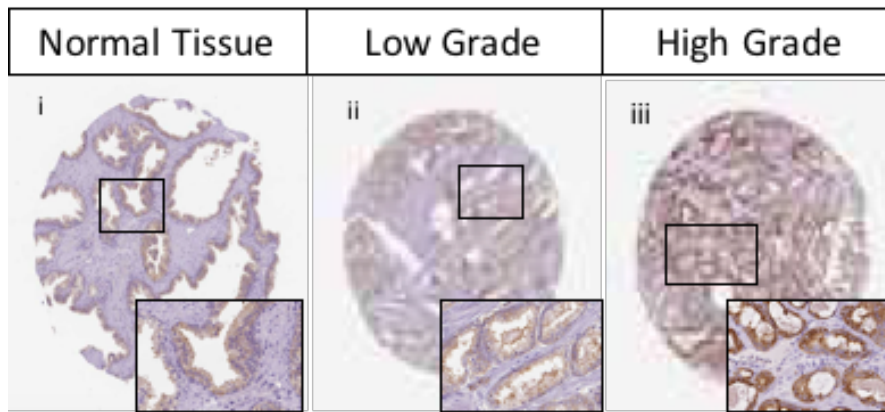


[Figure 4.5 – FASN levels appear to be increased in PCa.](#)

i) Normal prostate tissue stained using immunohistochemistry for FASN antibody (HPA006461). **ii)** Low grade prostate adenocarcinoma tissue. **iii)** High grade prostate adenocarcinoma tissue. (images taken from (Universitet, 2016b)).

The role and expression of ACSL1 appears to be tumour dependent. A recent study by Chen *et al.* assessed all of the ACS family members for their roles in cancer and attempted to determine the biological function of these enzymes (Chen *et al.*, 2016). ACSL1 was linked with breast, colon, lung, brain, cervical, esophageal, head and neck, leukemia, liver, and sarcoma cancers however, expression differed between them. Chen *et al.* found that in colon cancer ACSL1 is upregulated but in all others, it is down-regulated. In breast and colorectal cancer higher expression of ACSL1 is associated with poor survival, however in lung cancer it is associated with better survival (Chen *et al.*, 2016). It was determined that ACSL1 plays a potentially oncogenic role in colorectal and breast cancer by inhibiting proliferation, migration and anchorage-independent growth, but acts as a tumour suppressor in lung cancer (Chen *et al.*, 2016).

[4.3.1.3 Blocking Fatty Acid Synthesis via inhibition of FASN & ACSL1](#)

Inhibition of fatty acid biosynthesis could be a viable option to inhibit cancer and many inhibitors have been investigated in the hope of finding new treatments, however as yet no

inhibitor has reached the clinic (Cervantes-Madrid *et al.*, 2016). It was theorized by Currie *et al.* that inhibitors of fatty acid biosynthesis enzymes would have minimal effects on non-cancer cells, as normal cells rely on an exogenous supply of fatty acids rather than the *de novo* synthesis of them (Currie *et al.*, 2013), however this has not been the case.

The first inhibitor of FASN was C75, which was based on the natural product cerulenin and proved to be cytotoxic against a number of cancer cell lines *in vitro* (Kuhajda *et al.*, 2000) including PCa (Chen *et al.*, 2012; Pizer *et al.*, 2001). Although C75 does inhibit tumour growth, it was also found to cause substantial weight loss in mice demonstrating some side-effects (Pizer *et al.*, 2000). The studies indicated that the inhibition of FASN promotes cancer cell death (Pizer *et al.*, 2000). However the mechanism of how this promotes cell death remains unclear and may be due to the lack of fatty acids or due to the accumulation of malonyl-CoA being toxic in the cells (Pizer *et al.*, 2000). Another interesting factor is that FASN levels can be detected in the blood of cancer patients (Kuhajda, 2006). This could mean that FASN could possibly be used in conjunction with another PCa biomarker such as PSA in order to stage disease or monitor disease progression.

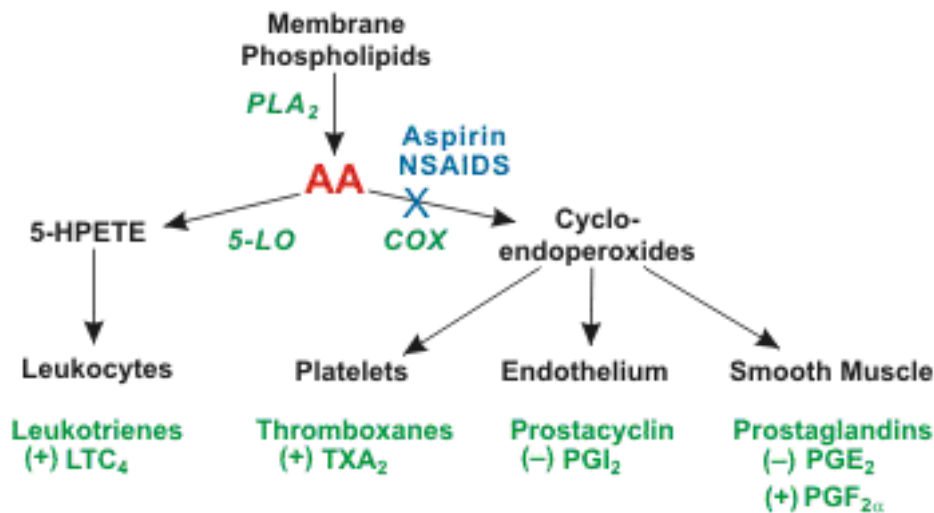
Triacsin C is a chemical inhibitor of ACSL1 and it has been shown to cause apoptotic cell death in lung, colon, and brain cancer cells (Mashima *et al.*, 2005), therefore it could be a potential inhibitor to ACSL1 in PCa cells. The issue with inhibitors against ACSL1 is that as previously stated, there are 4 other isoforms of the enzyme. This means that inhibitors to one isoform may have cross-reactivity with the others, as is the case with Triacsin C that also inhibits ACSL3 & 4 (Kim *et al.*, 2001). These variants of ACSL were not part of our study so without knowing the significance of other isoforms in PCa, targeting ACSL1 using this inhibitor could lead to undesired side-effects.

4.3.2 Arachidonic Acid & Prostaglandin Biosynthesis

4.3.2.1 *The arachidonic acid & prostaglandin bioynthesis pathway*

The arachidonic acid pathway (Figure 4.6) is important in many physiological functions (Yarla *et al.*, 2016). In this pathway various metabolic enzymes, such as cyclooxygenases (COXs) and phospholipase A2s (PLA2s) function along with their products to initiate various cellular processes (Wang and Dubois, 2010; Yarla *et al.*, 2016). PLA2s are the initial step in the arachidonic pathway and they serve to hydrolyse bonds in membrane bound phospholipids and form the free fatty acids; arachidonic acid and lipoprotein lipases (LPLs) (Yarla *et al.*, 2016).

Arachidonic acids generate eicosanoids, which are key mediators of the inflammatory response (Greene *et al.*, 2011). Prostaglandins are one of the three groups of eicosanoids. Prostaglandins are generated by COX enzymes 1 and 2: COX-1 is constitutively expressed whereas COX-2 is inducible by inflammatory factors, cytokines, growth factors and tumour promoters (Yang *et al.*, 2012). Prostaglandins transduce downstream signalling, activate transcription or induce inflammatory responses via their transmembrane receptors, E-type prostaglandin receptor (EPs) or via the nuclear receptor peroxisome-proliferator-activated receptor gamma (PPAR γ) (Bieniek *et al.*, 2014).



Abbreviations: AA, arachidonic acid; PLA₂, phospholipase A₂; PLC, phospholipase C; COX, cyclooxygenase; NSAIDS, non-steroidal anti-inflammatory drugs; +, vasoconstriction; -, vasodilation.

Figure 4.6 – The arachidonic acid biosynthesis pathway.

The synthesis of prostaglandins relies heavily on enzymes such as PLAs and COXs in order to hydrolyse membrane bound phospholipids and convert arachidonic acid to cyclo-endoperoxides prior to conversion to prostaglandins (taken from (Klabunde, 2016)).

4.3.2.2 The role of arachidonic acid & prostaglandin bioynthesis in cancer

It has been demonstrated that prostaglandin biosynthesis and the arachidonic acid pathway are important in the development of many cancers including PCa (Yang *et al.*, 2012). Arachidonic acids are n-6 fatty acids which have been found to promote cell proliferation (Yang *et al.*, 2012), and they are converted to prostaglandin H₂ (PGH₂) by the enzyme COX-2 (Bieniek *et al.*, 2014). COX-2 expression is associated with inflammation, cell growth, proliferation, angiogenesis, invasion, metastasis and apoptosis (Kirschenbaum *et al.*, 2001), and has been linked with the development of many cancers including PCa (Cohen *et al.*, 2016; Wang *et al.*, 2005). There has also been a positive correlation demonstrated between PCa tumour grade and COX-2 expression (Madaan *et al.*, 2016).

4.3.2.3 Blocking prostaglandin bioynthesis via COX-2 inhibitors

COX-2 has already been identified as a potential therapeutic target for the inhibition of PCa progression and metastasis (Garcia *et al.*, 2014; Lieberman, 2002). Knockout of the COX-2 gene and chemical inhibition has also been shown to reduce cancer growth and development in preclinical models of breast and colon cancer (Xu *et al.*, 2014). COX-2 inhibitors such as celecoxib, rofecoxib and the chemotherapeutic podophyllotoxin have been evaluated in pre-clinical trials for their effect and efficiency at inhibiting COX-2 in PCa. These studies found that COX-2 inhibitors show promise as agents in the chemoprevention of PCa (Basler and Piazza, 2004; Hernandez *et al.*, 2004; Srinath *et al.*, 2003).

These studies highlight the correlation between the results of this study and previously identified targets for PCa, such as COX-2. However, a recent study by Flamiatos *et al.* indicated that Celecoxib did not induce apoptosis and did not alter prostaglandin or AR levels in cancerous or benign prostate tissues (Flamiatos *et al.*, 2016). This highlights a need for further evaluation and characterization of this enzyme and even the investigation of alternative inhibitors of COX-2. There are many alternative inhibitors of COX-2, such as apigenin (a flavonoid found widely in plants) has been shown to downregulate COX-2 expression in breast cancer cells (Yi Lau and Leung, 2010)). Berberin (also found in plants) has been shown to possess anticancer activities and is currently undergoing clinical trials for colorectal, oral and breast cancer (Liu *et al.*, 2015; Yarla *et al.*, 2016)).

4.3.3 Polyamine Biosynthesis

4.3.3.1 The polyamine biosynthesis pathway

The screen identified two genes involved in the polyamine biosynthesis pathway, AZIN2 and AMD1. AZIN2 is a regulator of polyamine synthesis and AMD1 is the second rate limiting

step in polyamine biosynthesis, it provides the necessary aminopropyl donor required for the synthesis of both spermine and spermidine (Casero and Marton, 2007). Polyamines are organic polycations known to be involved in the regulation of many cellular functions such as; proliferation, differentiation, malignant transformation and apoptosis (Pegg, 2006; Seiler and Raul, 2005). There are three main polyamines: spermidine, spermine and putrescine (Rasila *et al.*, 2016). The most important role of polyamines is their involvement in regulating the proliferation of both normal and cancer cells (Casero and Marton, 2007).

Antizyme inhibitors (AZINs) inhibit antizymes (AZ) whose role is to bind monomers of the enzyme ornithine decarboxylase (ODC) (Kahana, 2009). ODC is the first rate-limiting enzyme involved in polyamine biosynthesis (Figure 4.7). ODC is often found in elevated levels in rapidly proliferating cells, therefore it is often tightly regulated (Pegg, 2006). When AZ's bind ODC they sequester it. AZINs can reverse this since AZIN binding to AZ releases ODC, allowing ODC to form catalytically active dimers (Wallace *et al.*, 2003). AZIN2 is found most abundantly in differentiated resting cells or in cells with a slow turnover such as those in the brain and testis (Rasila *et al.*, 2016). This is somewhat surprising as it plays such a crucial role in the release of ODC when cells proliferate. This could indicate another role for either: AZIN2, ODC or AZ's in cancer of which we are unaware.

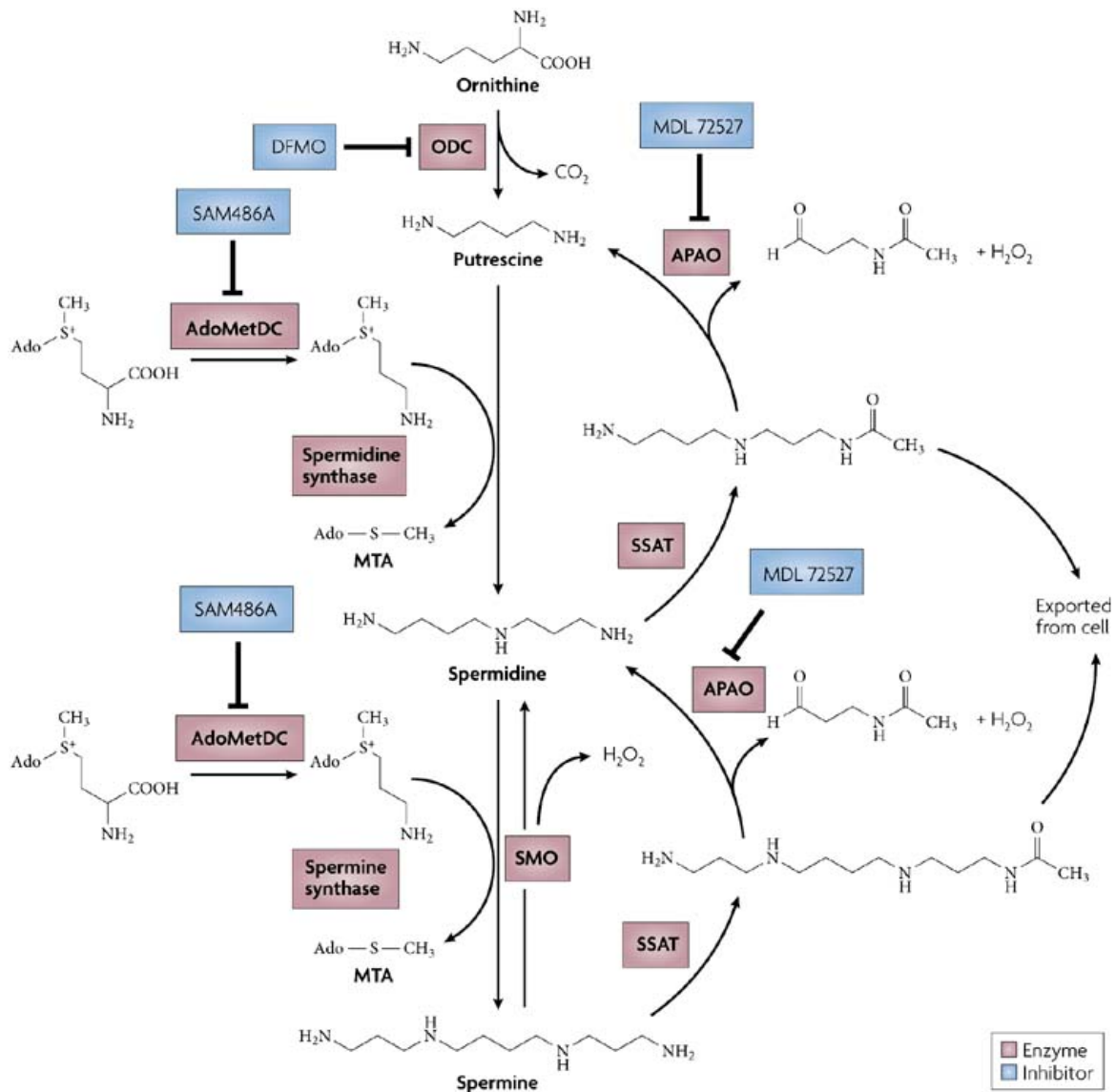
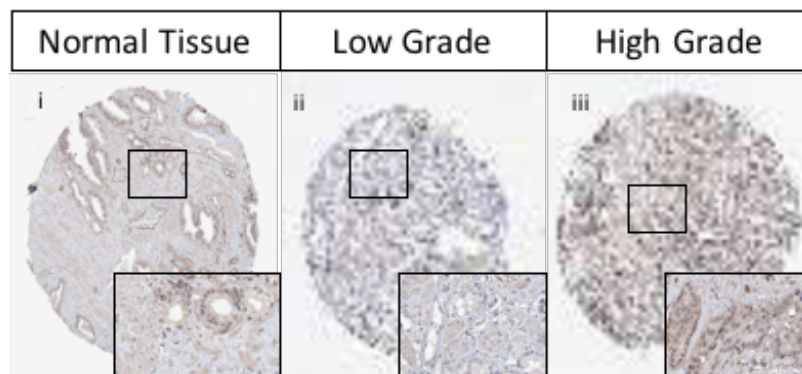


Figure 4.7 – The polyamine biosynthesis pathway.

Ornithine decarboxylase (ODC) produces putrescine and is the first rate-limiting step in polyamine biosynthesis. It is regulated at multiple steps and is inhibited by AMD1 (shown here as AdoMetDC), the activity of which provides the aminopropyl donor for the synthesis of both spermidine and spermine, which can be prevented by the inhibitor SAM486A. Spermine oxidase (SMO) is an inducible oxidase and N¹-acetylpolyamine oxidase (APAO) is a constitutively expressed, peroxisomal oxidase; both of these enzymes can be inhibited by MDL 72527. Spermidine/spermine N¹-acetyltransferase (SSAT) is an enzyme crucial for the maintenance of polyamine homeostasis (image taken from (Casero and Marton, 2007)).

4.3.3.2 The role of polyamine biosynthesis in cancer and its inhibition

The crucial role that AMD1 plays in polyamine synthesis has made it an attractive target for therapeutics against various malignancies with an inhibitor, SAM486A, having undergone clinical trials for multiple cancers but not PCa (Eskens *et al.*, 2000; Millward *et al.*, 2005; Pless *et al.*, 2004; van Zuylen *et al.*, 2004). The Human Protein Atlas provides immunostaining of AMD1 in normal prostate versus low and high grade adenocarcinoma indicating overexpression in PCa (Universitet, 2016a) (Figure 4.8). It would prove interesting to trial SAM486A as an inhibitor of PCa.



[Figure 4.8 – AMD1 levels appear to be increased in PCa.](#)

i) Normal prostate tissue stained using immunohistochemistry for AMD1 antibody (HPA029281). **ii)** Low grade prostate adenocarcinoma tissue. **iii)** High grade prostate adenocarcinoma tissue. (images taken from (Universitet, 2016a)).

It is also interesting to note that a downstream enzyme (Figure 4.7) to AMD1, spermidine synthase (SRM) did not provide as great an inhibitory effect on LNCaP proliferation as it's upstream counterpart. The inhibitory effect of SRM was only 10-20 % across two of the siRNA's, however in the third it did provide 60% inhibition of proliferation. In future, it

would be important to confirm the knock-down efficiency of the different siRNAs to correlate this with the effects upon proliferation.

4.3.4 Other Targets Identified in the siRNA Screen

4.3.4.1 FK506 Binding Protein 11 (FKBP11)

FKBP11 is a member of the FKBP family of isomerases which catalyse the folding of proline containing polypeptides (LIN *et al.*, 2013). FKBP11 was first described by Rulten *et al.* in 2006. It is a 19 kDa protein which gives it its alternate name of FKBP19. *FKBP11* mRNA is found predominantly in secretory tissues, such as the prostate (Rulten *et al.*, 2006).

In a study by Lin *et al.* it was discovered that FKBP11 was a potential early marker for hepatocellular carcinoma, and that expression of FKBP11 gradually increased as the disease progressed in mice models (LIN *et al.*, 2013). This could also be the case in prostate tumours and should be investigated to see if FKBP11 could be a potential marker for the onset of the disease, as well as a therapeutic target.

4.3.4.2 Guanylate Cyclase 1, Soluble, Alpha 2 (GUCY1A2)

GUCY1A2 is an alpha subunit of a heterodimeric protein known as guanylate cyclase (GC) that is activated by nitric oxide (NO) and catalyses the conversion of GTP to 3',5''-cyclic GMP (cGMP) and pyrophosphate (NCBI, 2016a). NO and cGMP are both signalling molecules with diverse functions (Krumenacker *et al.*, 2004). NO is known to play a role in cancer by regulating cell death and survival pathways often depending on cGMP and the activation of GC (Bonavida *et al.*, 2006).

Another family member, GUCY1A3 has already been targeted in PCa. Gao *et al.* designed the peptide A-8R to target GUCY1A3 (Gao *et al.*, 2013), after a previous study showed that it

was an important mediator of PCa cell proliferation (Cai *et al.*, 2007). The peptide was shown to halt tumour growth in xenograft models of both hormone-dependent and independent PCa (Gao *et al.*, 2013).

4.3.4.3 Adipocyte Plasma Membrane Associated Protein (APMAP)/C20orf3

APMAP is a 46kDa membrane protein that was characterized in 2008 by Ilhan *et al.* (Ilhan *et al.*, 2008). Little is known about the protein but it is involved in adipocyte function (Ma *et al.*, 2016). APMAP is upregulated in human adipogenic cell models as well as in a genetic model for obesity in mice (Bogner-Strauss *et al.*, 2010). Although this does not prove an upregulation in PCa, there is a well-known association between PCa and obesity, with adipocytes surrounding the prostate, in the periprostatic adipose tissue (PPAT), supporting the direct migration of PCa cells (Laurent *et al.*, 2016). Our study indicated that there is a relationship between APMAP and PCa and so this protein should be investigated further in this context.

4.3.4.4 Syntaxin 8 (STX8)

This gene like all the Syntaxin family, mediate vesicle fusion in vesicular transport processes in conjunction with N-ethylmaleimide-sensitive factor (NSF) attachment protein receptors (SNAREs) and with the cytoplasmic NSF and soluble NSF attachment proteins (SNAP) (Zhang *et al.*, 2009). Syntaxin 8 has been found to be upregulated during oxidative stress in dopaminergic cells and has been related to the molecular mechanisms of Parkinson's disease (Yoo *et al.*, 2003). There is however very little known link between STX8 and cancer. It would be beneficial to investigate the role of STX8 in PCa as our study demonstrated a 90-99% inhibition in LNCaP proliferation across the three siRNA's targeting STX8.

4.3.4.5 Porcupine Homolog (PORCN)

The PORC gene family encode endoplasmic reticulum proteins and are involved in the processing of Wnt proteins (NCBI, 2016b) such as Wnt-11 which has been previously connected to PCa progression to CRPC (Koushyar *et al.*, 2016; Rapa *et al.*, 2013; Uysal-Onganer *et al.*, 2010). PORCN has been connected with cancer and in a study by Covey *et al.* it was found that knockdown of PORCN reduced the growth of established cancers in xenograft mice, however the reduction in proliferation was independent of Wnt signalling (Covey *et al.*, 2012). They therefore hypothesized that PORCN was actually involved in an entirely different oncogenic signalling pathway. It is also interesting to note that inhibition of PORCN by its inhibitor IWP did not have the same effect (Covey *et al.*, 2012). It would be interesting to see if in LNCaP cells the inhibitor IWP had any effect on growth in order to determining which signalling pathway is being effected.

4.3.4.6 Fibronectin type III and SPRY domain containing 1 like (FSD1L)

The *FSD1L* gene is located on chromosome 9 and mostly found within neural tissues (Talluri and Shete, 2015). The gene codes for type 2 cystatins, which regulate the activity of cysteine proteinases known as cathepsin. The cathepsin enzymes are involved in the migration, invasion and metastasis of tumour cells. (Sloane *et al.*, 1990). However, very little is known about the role of FSD1L in PCa.

4.3.4.7 5'-Aminolevulinic Acid Synthase 2 (ALAS2) & Uroporphyrinogen Decarboxylase (UROD)

ALAS2 is the first enzyme in the heme biosynthesis pathway. It only has one substrate, glycine, which it catalyses the reaction between this and succinyl-CoA to give 2-aminoketone, 5 aminolevulinic acid (Shoolingin-Jordan *et al.*, 2003). The exact role that ALAS2 would play in PCa or any form of cancer is unknown as cancer cells are known to

switch away from oxidative phosphorylation despite the availability of sufficient oxygen at times (Hooda *et al.*, 2013). It has been shown in recent studies however that the altered metabolic state of cancer cells is such that even at low oxygen levels (1%), cancer cells can maintain a substantial rate of oxidative phosphorylation (Frezza *et al.*, 2011). With this being the case, heme biosynthesis would still be a vital metabolic process for cancer cells to maintain and the enzymes involved could certainly be expected to play a crucial role.

UROD is another enzyme in the heme biosynthesis pathway. It catalyses the conversion of uroporphyrinogen to coproporphyrinogen (Yip *et al.*, 2014). UROD has been linked to head and neck cancers (Ito *et al.*, 2011a; Ito *et al.*, 2011b) whereby studies from Ito *et al.* discovered that UROD was significantly upregulated in some cancers and that lower levels of UROD could serve as a marker for better patient disease-free survival (Ito *et al.*, 2011b). There is however no published link between UROD and PCa.

4.3.4.8 Carbonic Anhydrases

The reversible conversion of carbon dioxide to bicarbonate and proton are catalyzed by the carbonic anhydrase metalloenzymes (Alterio *et al.*, 2012). Carbonic anhydrases form a family of at least 15 isozymes that are involved in numerous processes such as gluconeogenesis, lipid biosynthesis, ureagenesis (Supuran, 2008). The screen identified two of these isozymes as potential targets, CA7 and CA13. Carbonic anhydrase 13 (CA13) has been linked with colorectal carcinoma (Kummola *et al.*, 2005) however, in this setting it was found that CA13 was down-regulated in tumour cells and appears to act as a tumour suppressor (Kummola *et al.*, 2005). This would be in stark contrast to the results of our study whereby the knockdown of CA13 inhibited PCa cell proliferation (75-95% reduction in growth across all 3 siRNAs) when compared to that of the control. This could be due to the

role played by this enzyme in prostate tissue being different to that in the colon, however this would need further investigation.

Carbonic anhydrase 7 (CA7) has more recently been found to also be an important suppressor in normal and colorectal carcinoma tissue (Chu *et al.*, 2014) and that when down-regulated it acts as an important predictor of poor prognosis in colorectal carcinoma patients (Yang *et al.*, 2015). However, upregulated CA7 has also been linked with poor prognosis for patients with astrocytomas (a type of brain tumour) (Bootorabi *et al.*, 2011). It could be presumed that the role played by CA7, much like CA13, is different depending on the tissue in which it is found and this is cause for the different outcome of up or down-regulation in various cancers.

Inhibiting the action of CAs could be potentially a very simple task as over 25 clinically used drugs exist that possess significant CA inhibitory properties (Supuran, 2011). However, the number of different isoforms of CAs make targeting one specific CA a very challenging task. Interestingly one such drug that inhibits CA7 is celecoxib, the COX-2 inhibitor (Supuran, 2011), however, it also has inhibitory action on all other CAs as well (Supuran, 2011). The lack of specificity is probably the reason that it has not been used to inhibit CA7 or indeed CA13 in relation to cancer.

4.3.5 Protein disulphide isomerase-like protein of the testes (PDILT)

PDILT is a protein found to be expressed in the testes. It is involved in the disulphide bond formation necessary for the folding of the protein ADAM3, a sperm membrane protein critical for sperm migration from the uterus into the oviduct and for sperm primary binding. There is currently no evidence to support PDILT playing a role in PCa, however our study

appears to show that it could function as a tumour suppressor as knockdown of this target significantly increased LNCaP growth.

4.4 Summary

The identification of COX-2, GUCY1A2 and FASN, known targets in PCa, validates the findings of this screen. Other proteins such as ACSL1, FKBP11, PORCN, FSD1L, CA7, CA13, UROD and AMD1 have also been shown to be important in other cancers indicating the scope and potential in further investigating these in relation to PCa based upon our results. It is also important to note that several novel targets, where there has been no previous link to cancer, have been identified: AZIN2, STX8, ALAS2, as well as the identification of PDILT as a possible tumour suppressor in PCa.

Chapter 5: Conclusion

Current therapeutics for advanced PCa primarily target the androgen-signalling axis by directly interfering with AR function. Resistance to therapeutics remains the main issue with treatment and the development and progression of the disease to the castrate resistant stage remains the biggest factor contributing to poor prognosis and decreased patient survival.

The introduction of a tool, such as the computer model and software used to design DNAzymes, will have a significant impact on DNAzyme design and could promote the use of these potential therapeutics in line with current methods of RNA and protein inhibition. The tool can reduce time spent designing DNAzymes by hand as well as reduce costs and time spent analyzing the efficiency of each individual molecule. DNAzymes have been identified that can effectively target *AR* RNA and reduce PCa cell proliferation, highlighting the potential of this strategy as a novel therapeutic approach for this disease.

The siRNA screen performed identified novel metabolic targets, although more work would be needed to investigate these further. This study offers hope for the development of novel methods to target the AR signalling axis, either directly or further downstream. The results of this study may also prove relevant in other diseases whereby DNAzymes could be used to target other oncogenes, or even to improve upon current DNAzymes targeting RNA such as HPV16. The screen results could also serve as relevant in other cancers whereby the metabolism in tumours is altered similarly to that of in PCa.

Bibliography

- Ackerstaff, E., Pflug, B. R., Nelson, J. B. and Bhujwala, Z. M. (2001) Detection of Increased Choline Compounds with Proton Nuclear Magnetic Resonance Spectroscopy Subsequent to Malignant Transformation of Human Prostatic Epithelial Cells.
- Alterio, V., Di Fiore, A., D'Ambrosio, K., Supuran, C. T. and De Simone, G. (2012) Multiple binding modes of inhibitors to carbonic anhydrases: how to design specific drugs targeting 15 different isoforms? *Chem Rev*, **112**, 4421-68.
- Alvarez-Salas, L. M., Arpawong, T. E. and DiPaolo, J. A. (1999) Growth inhibition of cervical tumor cells by antisense oligodeoxynucleotides directed to the human papillomavirus type 16 E6 gene. *Antisense Nucleic Acid Drug Dev*, **9**, 441-50.
- Alvarez-Salas, L. M., Cullinan, A. E., Siwkowski, A., Hampel, A. and DiPaolo, J. A. (1998) Inhibition of HPV-16 E6/E7 immortalization of normal keratinocytes by hairpin ribozymes. *Proc Natl Acad Sci U S A*, **95**, 1189-94.
- Ammannagari, N. and George, S. (2016) Anti-Androgen Therapies for Prostate Cancer: A Focused Review. *American Journal of Hematology / Oncology*[®], **11**.
- Antonarakis, E. S., Lu, C., Wang, H., Lubner, B., Nakazawa, M., Roeser, J. C., Chen, Y., Mohammad, T. A., Fedor, H. L., Lotan, T. L., Zheng, Q., De Marzo, A. M., Isaacs, J. T., Isaacs, W. B., Nadal, R., Paller, C. J., Denmeade, S. R., Carducci, M. A., Eisenberger, M. A. and Luo, J. (2014) AR-V7 and resistance to enzalutamide and abiraterone in prostate cancer. *N Engl J Med*, **371**, 1028-38.
- Babunageswararao, K. R., R.; Kumar, P. D. Kamal; Sameer, Syed (2011) DNAzymes as Novel Therapeutics. *International Journal of Pharma & Bio Sciences*, **Vol. 2**, 161.
- Basler, J. W. and Piazza, G. A. (2004) Nonsteroidal anti-inflammatory drugs and cyclooxygenase-2 selective inhibitors for prostate cancer chemoprevention. *J Urol*, **171**, S59-62; discussion S62-3.
- Beale, G., Hollins, A. J., Benboubetra, M., Sohail, M., Fox, S. P., Benter, I. and Akhtar, S. (2003) Gene silencing nucleic acids designed by scanning arrays: anti-EGFR activity of siRNA, ribozyme and DNA enzymes targeting a single hybridization-accessible region using the same delivery system. *J Drug Target*, **11**, 449-56.
- Berthold, D. R., Pond, G. R., Soban, F., de Wit, R., Eisenberger, M. and Tannock, I. F. (2008) Docetaxel plus prednisone or mitoxantrone plus prednisone for advanced prostate cancer: updated survival in the TAX 327 study. *J Clin Oncol*, **26**, 242-5.
- Bianchini, D., Omlin, A., Pezaro, C., Lorente, D., Ferraldeschi, R., Mukherji, D., Crespo, M., Figueiredo, I., Miranda, S., Riisnaes, R., Zivi, A., Buchbinder, A., Rathkopf, D. E., Attard, G., Scher, H. I., de Bono, J. and Danila, D. C. (2013) First-in-human Phase I study of EZN-4176, a locked nucleic acid antisense oligonucleotide to exon 4 of the androgen receptor mRNA in patients with castration-resistant prostate cancer. *Br J Cancer*, **109**, 2579-86.
- Bieniek, J., Childress, C., Swatski, M. D. and Yang, W. (2014) COX-2 inhibitors arrest prostate cancer cell cycle progression by down-regulation of kinetochore/centromere proteins. *Prostate*, **74**, 999-1011.
- Bogner-Strauss, J. G., Prokesch, A., Sanchez-Cabo, F., Rieder, D., Hackl, H., Duszka, K., Krogdams, A., Di Camillo, B., Walenta, E., Klatzer, A., Lass, A., Pinent, M., Wong, W. C., Eisenhaber, F. and Trajanoski, Z. (2010) Reconstruction of gene association

- network reveals a transmembrane protein required for adipogenesis and targeted by PPARgamma. *Cell Mol Life Sci*, **67**, 4049-64.
- Bonavida, B., Khineche, S., Huerta-Yepe, S. and Garban, H. (2006) Therapeutic potential of nitric oxide in cancer. *Drug Resist Updat*, **9**, 157-73.
- Bootorabi, F., Haapasalo, J., Smith, E., Haapasalo, H. and Parkkila, S. (2011) Carbonic anhydrase VII—a potential prognostic marker in gliomas. *Health*, **03**, 6.
- Boulikas, T. and Hancock, R. (1981) A highly sensitive technique for staining DNA and RNA in polyacrylamide gels using silver. *J Biochem Biophys Methods*, **5**, 219-28.
- Breaker, R. R. and Joyce, G. F. (1994) A DNA enzyme that cleaves RNA. *Chem Biol*, **1**, 223-9.
- Brooke, G. N. and Bevan, C. L. (2009) The role of androgen receptor mutations in prostate cancer progression. *Curr Genomics*, **10**, 18-25.
- Brooke, G. N., Gamble, S. C., Hough, M. A., Begum, S., Dart, D. A., Odontiadis, M., Powell, S. M., Fioretti, F. M., Bryan, R. A., Waxman, J., Wait, R. and Bevan, C. L. (2015) Antiandrogens act as selective androgen receptor modulators at the proteome level in prostate cancer cells. *Mol Cell Proteomics*, **14**, 1201-16.
- Brooke, G. N., Powell, S. M., Lavery, D. N., Waxman, J., Buluwela, L., Ali, S. and Bevan, C. L. (2014) Engineered repressors are potent inhibitors of androgen receptor activity. *Oncotarget*, **5**, 959-69.
- Cai, C., Chen, S. Y., Zheng, Z., Omwancha, J., Lin, M. F., Balk, S. P. and Shemshedini, L. (2007) Androgen regulation of soluble guanylyl cyclase α 1 mediates prostate cancer cell proliferation. *Oncogene*, **26**, 1606-15.
- Cairns, M. J., Hopkins, T. M., Witherington, C., Wang, L. and Sun, L.-Q. (1999) Target site selection for an RNA-cleaving catalytic DNA. *Nature Biotechnology*, **17**, 480-486.
- Casero, R. A., Jr. and Marton, L. J. (2007) Targeting polyamine metabolism and function in cancer and other hyperproliferative diseases. *Nat Rev Drug Discov*, **6**, 373-90.
- Cervantes-Madrid, D., Division of Basic Research, I. N. d. C., Mexico City, Tlalpan 14080, Mexico, Dueñas-González, A. and Instituto de Investigaciones Biomédicas, U. N. A. d. M. U. I. N. d. C., Mexico City, Tlalpan 14080, Mexico (2016) Antitumor effects of a drug combination targeting glycolysis, glutaminolysis and de novo synthesis of fatty acids. *Oncology Reports*, **34**, 1533-1542.
- Chan, S. C., Selth, L. A., Li, Y., Nyquist, M. D., Miao, L., Bradner, J. E., Raj, G. V., Tilley, W. D. and Dehm, S. M. (2015) Targeting chromatin binding regulation of constitutively active AR variants to overcome prostate cancer resistance to endocrine-based therapies. *Nucleic Acids Res*.
- Chen, H.-W., Chang, Y.-F., Chuang, H.-Y., Tai, W.-T. and Hwang, J.-J. (2012) Targeted therapy with fatty acid synthase inhibitors in a human prostate carcinoma LNCaP cell-bearing animal model. *Prostate Cancer and Prostatic Diseases*, **15**, 260-264.
- Chen, W. C., Wang, C. Y., Hung, Y. H., Weng, T. Y., Yen, M. C. and Lai, M. D. (2016) Systematic Analysis of Gene Expression Alterations and Clinical Outcomes for Long-Chain Acyl-Coenzyme A Synthetase Family in Cancer. *PLoS One*, **11**.
- Chng, K. R. and Cheung, E. (2013) Sequencing the transcriptional network of androgen receptor in prostate cancer. *Cancer Lett*, **340**, 254-60.
- Chu, C. M., Yao, C. T., Chang, Y. T., Chou, H. L., Chou, Y. C., Chen, K. H., Terng, H. J., Huang, C. S., Lee, C. C., Su, S. L., Liu, Y. C., Lin, F. G., Wetter, T. and Chang, C. W. (2014) Gene expression profiling of colorectal tumors and normal mucosa by microarrays meta-analysis using prediction analysis of microarray, artificial neural network, classification, and regression trees. *Dis Markers*, **2014**, 634123.

- Clegg, N. J., Wongvipat, J., Joseph, J. D., Tran, C., Ouk, S., Dilhas, A., Chen, Y., Grillot, K., Bischoff, E. D., Cai, L., Aparicio, A., Dorow, S., Arora, V., Shao, G., Qian, J., Zhao, H., Yang, G., Cao, C., Sensintaffar, J., Wasielewska, T., Herbert, M. R., Bonnefous, C., Darimont, B., Scher, H. I., Smith-Jones, P., Klang, M., Smith, N. D., De Stanchina, E., Wu, N., Ouerfelli, O., Rix, P. J., Heyman, R. A., Jung, M. E., Sawyers, C. L. and Hager, J. H. (2012) ARN-509: a novel antiandrogen for prostate cancer treatment. *Cancer Res*, **72**, 1494-503.
- Cohen, B. L., Department of Urology, M. S. o. M., University of Miami, Miami, FL, USA, Gomez, P., Department of Urology, M. S. o. M., University of Miami, Miami, FL, USA, Omori, Y., Department of Urology, M. S. o. M., University of Miami, Miami, FL, USA, Duncan, R. C., Epidemiology and Public Health, M. S. o. M., University of Miami, Miami, FL, USA, Civantos, F., Department of Urology, M. S. o. M., University of Miami, Miami, FL, USA, Department of Pathology, M. S. o. M., University of Miami, Miami, FL, USA, Soloway, M. S., Department of Urology, M. S. o. M., University of Miami, Miami, FL, USA, Lokeshwar, V. B., Department of Urology, M. S. o. M., University of Miami, Miami, FL, USA, Department of Cell Biology and Anatomy, M. S. o. M., University of Miami, Miami, FL, USA, Sylvester Comprehensive Cancer Center, M. S. o. M., University of Miami, Miami, FL, USA, Lokeshwar, B. L., Department of Urology, M. S. o. M., University of Miami, Miami, FL, USA, Sylvester Comprehensive Cancer Center, M. S. o. M., University of Miami, Miami, FL, USA, Department of Radiation Oncology, M. S. o. M., University of Miami, Miami, FL, USA and Department of Urology (M-800), P. O. B., Miami, FL 33101, USA (2016) Cyclooxygenase-2 (cox-2) expression is an independent predictor of prostate cancer recurrence. *International Journal of Cancer*, **119**, 1082-1087.
- Covey, T. M., Kaur, S., Tan Ong, T., Proffitt, K. D., Wu, Y., Tan, P. and Virshup, D. M. (2012) PORCN moonlights in a Wnt-independent pathway that regulates cancer cell proliferation. *PLoS One*, **7**, e34532.
- CRUK (2014a) *About hormone therapy for prostate cancer* [Online]: <http://www.cancerresearchuk.org/about-cancer/type/prostate-cancer/treatment/hormone/about-hormone-therapy-for-prostate-cancer-hormadv>. Cancer Research UK.
- CRUK (2014b) *Cancer mortality for common cancers* [Online]: <http://www.cancerresearchuk.org/cancer-info/cancerstats/mortality/cancerdeaths/>. Cancer Research UK. Last accessed 6/11/14.
- Currie, E., Schulze, A., Zechner, R., Walther, T. C. and Farese, R. V. (2013) Cellular Fatty Acid Metabolism and Cancer. *Cell Metab*, **18**, 153-61.
- Dart, A. D., Waxman, J., Aboagye, E. O., Bevan, C. L (2013) PLOS ONE: Visualising Androgen Receptor Activity in Male and Female Mice. *PLOS One*.
- Dass, C. R., Choong, P. F. and Khachigian, L. M. (2008) DNAzyme technology and cancer therapy: cleave and let die. *Mol Cancer Ther*, **7**, 243-51.
- Dass, C. R., Saravolac, E. G., Li, Y. and Sun, L. Q. (2002) Cellular uptake, distribution, and stability of 10-23 deoxyribozymes. *Antisense Nucleic Acid Drug Dev*, **12**, 289-99.
- de Bono, J. S., Oudard, S., Ozguroglu, M., Hansen, S., Machiels, J. P., Kocak, I., Gravis, G., Bodrogi, I., Mackenzie, M. J., Shen, L., Roessner, M., Gupta, S. and Sartor, A. O. (2010) Prednisone plus cabazitaxel or mitoxantrone for metastatic castration-resistant prostate cancer progressing after docetaxel treatment: a randomised open-label trial. *Lancet*, **376**, 1147-54.

- de Vere White, R., Meyers, F., Chi, S. G., Chamberlain, S., Siders, D., Lee, F., Stewart, S. and Gumerlock, P. H. (1997) Human androgen receptor expression in prostate cancer following androgen ablation. *Eur Urol*, **31**, 1-6.
- Dicke, T., Pali-Scholl, I., Kaufmann, A., Bauer, S., Renz, H. and Garn, H. (2012) Absence of unspecific innate immune cell activation by GATA-3-specific DNazymes. *Nucleic Acid Ther*, **22**, 117-26.
- Dinh, J. A., Baker, D. and Chahal, M. (2016) Therapy Update for Metastatic Castration-Resistant Prostate Cancer. *Consult Pharm*, **31**, 581-592.
- Dyson, N., Howley, P. M., Munger, K. and Harlow, E. (1989) The human papilloma virus-16 E7 oncoprotein is able to bind to the retinoblastoma gene product. *Science*, **243**, 934-7.
- Eskens, F. A., Greim, G. A., van Zuylen, C., Wolff, I., Denis, L. J., Planting, A. S., Muskiet, F. A., Wanders, J., Barbet, N. C., Choi, L., Capdeville, R., Verweij, J., Hanauske, A. R. and Brunsch, U. (2000) Phase I and pharmacological study of weekly administration of the polyamine synthesis inhibitor SAM 486A (CGP 48 664) in patients with solid tumors. European Organization for Research and Treatment of Cancer Early Clinical Studies Group. *Clin Cancer Res*, **6**, 1736-43.
- Evans, R. M. (1988) The steroid and thyroid hormone receptor superfamily. *Science*, **240**, 889-95.
- Feldman, B. J. and Feldman, D. (2001) The development of androgen-independent prostate cancer. *Nat Rev Cancer*, **1**, 34-45.
- Flamiatos, J. F., Beer, T. M., Graff, J. N., Eilers, K. M., Tian, W., Sekhon, H. S. and Garzotto, M. (2016) Cyclooxygenase-2 (COX-2) inhibition for prostate cancer chemoprevention: double-blind randomised study of pre-prostatectomy celecoxib or placebo. *BJU Int*.
- Fluiter, K., Frieden, M., Vreijling, J., Koch, T. and Baas, F. (2005) Evaluation of LNA-modified DNazymes targeting a single nucleotide polymorphism in the large subunit of RNA polymerase II. *Oligonucleotides*, **15**, 246-54.
- Frezza, C., Zheng, L., Tennant, D. A., Papkovsky, D. B., Hedley, B. A., Kalna, G., Watson, D. G. and Gottlieb, E. (2011) Metabolic profiling of hypoxic cells revealed a catabolic signature required for cell survival. *PLoS One*, **6**, e24411.
- Gao, S., Hsieh, C. L., Bhansali, M., Kannan, A. and Shemshedini, L. (2013) A peptide against soluble guanylyl cyclase alpha1: a new approach to treating prostate cancer. *PLoS One*, **8**, e64189.
- Garcia, M., Velez, R., Romagosa, C., Majem, B., Pedrola, N., Olivan, M., Rigau, M., Guiu, M., Gomis, R. R., Morote, J., Reventos, J. and Doll, A. (2014) Cyclooxygenase-2 inhibitor suppresses tumour progression of prostate cancer bone metastases in nude mice. *BJU Int*, **113**, E164-77.
- Giovannucci, E., Liu, Y., Platz, E. A., Stampfer, M. J. and Willett, W. C. (2007) Risk factors for prostate cancer incidence and progression in the health professionals follow-up study. *Int J Cancer*, **121**, 1571-8.
- Gleave, M. E. and Monia, B. P. (2005) Antisense therapy for cancer. *Nat Rev Cancer*, **5**, 468-79.
- Goktas, S. and Crawford, E. D. (1999) Optimal hormonal therapy for advanced prostatic carcinoma. *Semin Oncol*, **26**, 162-73.
- Greene, E. R., Huang, S., Serhan, C. N. and Panigrahy, D. (2011) Regulation of Inflammation in Cancer by Eicosanoids. *Prostaglandins Other Lipid Mediat*, **96**, 27-36.

- Guo, Z. and Qiu, Y. (2011) A new trick of an old molecule: androgen receptor splice variants taking the stage?! *Int J Biol Sci*, **7**, 815-22.
- Hamada, S., Horiguchi, A., Kuroda, K., Ito, K., Asano, T., Miyai, K. and Iwaya, K. (2014) Increased fatty acid synthase expression in prostate biopsy cores predicts higher Gleason score in radical prostatectomy specimen. *BMC Clin Pathol*, **14**, 3.
- Harris, W. P., Mostaghel, E. A., Nelson, P. S. and Montgomery, B. (2009) Androgen deprivation therapy: progress in understanding mechanisms of resistance and optimizing androgen depletion. *Nat Clin Pract Urol*, **6**, 76-85.
- Heidenreich, A., Bastian, P. J., Bellmunt, J., Bolla, M., Joniau, S., van der Kwast, T., Mason, M., Matveev, V., Wiegel, T., Zattoni, F. and Mottet, N. (2014) EAU guidelines on prostate cancer. Part II: Treatment of advanced, relapsing, and castration-resistant prostate cancer. *Eur Urol*, **65**, 467-79.
- Hernandez, J., Basler, J. W. and Thompson, I. M. (2004) The potential role of cyclooxygenase-2 inhibitors and 5alpha-reductase inhibitors in the prevention of urologic conditions. *Urol Clin North Am*, **31**, 213-8.
- Hirst, C. J., Cabrera, C. and Kirby, M. (2012) Epidemiology of castration resistant prostate cancer: A longitudinal analysis using a UK primary care database. *Cancer Epidemiology*, **36**.
- Hooda, J., Cadinu, D., Alam, M. M., Shah, A., Cao, T. M., Sullivan, L. A., Brekken, R. and Zhang, L. (2013) Enhanced heme function and mitochondrial respiration promote the progression of lung cancer cells. *PLoS One*, **8**, e63402.
- Huang, H., Zegarra-Moro, O. L., Benson, D. and Tindall, D. J. (2003) Androgens repress Bcl-2 expression via activation of the retinoblastoma (RB) protein in prostate cancer cells. *Oncogene*, **23**, 2161-2176.
- Ilhan, A., Gartner, W., Nabokikh, A., Daneva, T., Majdic, O., Cohen, G., Bohmig, G. A., Base, W., Horl, W. H. and Wagner, L. (2008) Localization and characterization of the novel protein encoded by C20orf3. *Biochem J*, **414**, 485-95.
- Ito, E., Yip, K. W. and Liu, F. F. (2011a) Uroporphyrinogen decarboxylase: optimizing radiotherapy for head and neck cancer. *Future Oncol*, **7**, 595-7.
- Ito, E., Yue, S., Moriyama, E. H., Hui, A. B., Kim, I., Shi, W., Alajez, N. M., Bhogal, N., Li, G., Datti, A., Schimmer, A. D., Wilson, B. C., Liu, P. P., Durocher, D., Neel, B. G., O'Sullivan, B., Cummings, B., Bristow, R., Wrana, J. and Liu, F. F. (2011b) Uroporphyrinogen decarboxylase is a radiosensitizing target for head and neck cancer. *Sci Transl Med*, **3**, 67ra7.
- Jiang, M. and Milner, J. (2002) Selective silencing of viral gene expression in HPV-positive human cervical carcinoma cells treated with siRNA, a primer of RNA interference. *Oncogene*, **21**, 6041-8.
- Kahana, C. (2009) Regulation of cellular polyamine levels and cellular proliferation by antizyme and antizyme inhibitor. *Essays Biochem*, **46**, 47-61.
- Kanter, J. E., Tang, C., Oram, J. F. and Bornfeldt, K. E. (2012) Acyl-CoA synthetase 1 is required for oleate and linoleate mediated inhibition of cholesterol efflux through ATP-binding cassette transporter A1 in macrophages. *Biochim Biophys Acta*, **1821**, 358-64.
- Katsogiannou, M., Ziouziou, H., Karaki, S., Andrieu, C., Henry de Villeneuve, M. and Rocchi, P. (2015) The hallmarks of castration-resistant prostate cancers. *Cancer Treat Rev*.

- Kim, J. H., Lewin, T. M. and Coleman, R. A. (2001) Expression and characterization of recombinant rat Acyl-CoA synthetases 1, 4, and 5. Selective inhibition by triacsin C and thiazolidinediones. *J Biol Chem*, **276**, 24667-73.
- Kirschenbaum, A., Department of Urology, M. S. S. o. M., New York, New York, USA, Liu, X.-H., Department of Medicine (Endocrinology), M. S. S. o. M., New York, New York, USA, Yao, S., Department of Medicine (Endocrinology), M. S. S. o. M., New York, New York, USA, Levine, A. C., alice.levine@mssm.edu and Department of Medicine (Endocrinology), M. S. S. o. M., New York, New York, USA (2001) The role of cyclooxygenase-2 in prostate cancer. *Urology*, **58**, 127-131.
- Klabunde, R. E. (2016) *CV Physiology: Arachidonic Acid Metabolites* [Online]: <http://www.cvphysiology.com/Blood Flow/BF013.htm>. Last accessed 8 October.
- Korpala, M., Korn, J. M., Gao, X., Rakiec, D. P., Ruddy, D. A., Doshi, S., Yuan, J., Kovats, S. G., Kim, S., Cooke, V. G., Monahan, J. E., Stegmeier, F., Roberts, T. M., Sellers, W. R., Zhou, W. and Zhu, P. (2013a) An F876L mutation in androgen receptor confers genetic and phenotypic resistance to MDV3100 (enzalutamide). *Cancer Discov*, **3**, 1030-43.
- Korpala, M., Korn, J. M., Gao, X., Rakiec, D. P., Ruddy, D. A., Doshi, S., Yuan, J., Kovats, S. G., Kim, S., Cooke, V. G., Monahan, J. E., Stegmeier, F., Roberts, T. M., Sellers, W. R., Zhou, W. and Zhu, P. (2013b) An F876L Mutation in Androgen Receptor Confers Genetic and Phenotypic Resistance to MDV3100 (Enzalutamide).
- Koushyar, S., Grant, G. H. and Uysal-Onganer, P. (2016) The interaction of Wnt-11 and signalling cascades in prostate cancer. *Tumour Biol*.
- Krumenacker, J. S., Hanafy, K. A. and Murad, F. (2004) Regulation of nitric oxide and soluble guanylyl cyclase. *Brain Res Bull*, **62**, 505-15.
- Kuhajda, F. P. (2006) Fatty Acid Synthase and Cancer: New Application of an Old Pathway.
- Kuhajda, F. P., Pizer, E. S., Li, J. N., Mani, N. S., Frehywot, G. L. and Townsend, C. A. (2000) Synthesis and antitumor activity of an inhibitor of fatty acid synthase.
- Kummola, L., Hamalainen, J. M., Kivela, J., Kivela, A. J., Saarnio, J., Karttunen, T. and Parkkila, S. (2005) Expression of a novel carbonic anhydrase, CA XIII, in normal and neoplastic colorectal mucosa. *BMC Cancer*, **5**, 41.
- Kurreck, J., Bieber, B., Jahnel, R. and Erdmann, V. A. (2002) Comparative study of DNA enzymes and ribozymes against the same full-length messenger RNA of the vanilloid receptor subtype I. *J Biol Chem*, **277**, 7099-107.
- Lamb, A. D., Massie, C. E. and Neal, D. E. (2014) The transcriptional programme of the androgen receptor (AR) in prostate cancer. *BJU Int*, **113**, 358-66.
- Lan, T. and Lu, Y. (2012) Metal ion-dependent DNAzymes and their applications as biosensors. *Met Ions Life Sci*, **10**, 217-48.
- Laurent, V., Guerard, A., Mazerolles, C., Le Gonidec, S., Toulet, A., Nieto, L., Zaidi, F., Majed, B., Garandeau, D., Socrier, Y., Golzio, M., Cadoudal, T., Chaoui, K., Dray, C., Monsarrat, B., Schiltz, O., Wang, Y. Y., Couderc, B., Valet, P., Malavaud, B. and Muller, C. (2016) Periprostatic adipocytes act as a driving force for prostate cancer progression in obesity. *Nat Commun*, **7**, 10230.
- Lee, J. H., Isayeva, T., Larson, M. R., Sawant, A., Cha, H. R., Chanda, D., Chesnokov, I. N. and Ponnazhagan, S. (2015) Endostatin: A novel inhibitor of androgen receptor function in prostate cancer. *Proc Natl Acad Sci U S A*, **112**, 1392-7.

- Li, J., Zheng, W., Kwon, A. H. and Lu, Y. (2000) In vitro selection and characterization of a highly efficient Zn(II)-dependent RNA-cleaving deoxyribozyme. *Nucleic Acids Res*, **28**, 481-8.
- Li, L. O., Grevengoed, T. J., Paul, D. S., Ilkayeva, O., Koves, T. R., Pascual, F., Newgard, C. B., Muoio, D. M. and Coleman, R. A. (2015) Compartmentalized Acyl-CoA Metabolism in Skeletal Muscle Regulates Systemic Glucose Homeostasis. *Diabetes*, **64**, 23-35.
- Li, Y., Chan, S. C., Brand, L. J., Hwang, T. H., Silverstein, K. A. and Dehm, S. M. (2013) Androgen receptor splice variants mediate enzalutamide resistance in castration-resistant prostate cancer cell lines. *Cancer Res*, **73**, 483-9.
- Lieber, A. and Strauss, M. (1995) Selection of efficient cleavage sites in target RNAs by using a ribozyme expression library. *Mol Cell Biol*, **15**, 540-51.
- Lieberman, R. (2002) Chemoprevention of prostate cancer: current status and future directions. *Cancer Metastasis Rev*, **21**, 297-309.
- LIN, I.-Y., YEN, C.-H., LIAO, Y.-J., LIN, S.-E., MA, H.-P., CHAN, Y.-J. and CHEN, Y.-M. A. (2013) Identification of FKBP11 as a Biomarker for Hepatocellular Carcinoma.
- Liu, X., Ji, Q., Ye, N., Sui, H., Zhou, L., Zhu, H., Fan, Z., Cai, J. and Li, Q. (2015) Berberine Inhibits Invasion and Metastasis of Colorectal Cancer Cells via COX-2/PGE2 Mediated JAK2/STAT3 Signalling Pathway. *PLoS One*, **10**, e0123478.
- Lonergan and Lonergan PE, T. D. (2011) Androgen receptor signalling in prostate cancer development and progression.
- Lonergan, P. E. and Tindall, D. J. (2011) Androgen receptor signalling in prostate cancer development and progression. *J Carcinog*, **10**, 20.
- Lu, Z. X., Ma, X. Q., Yang, L. F., Wang, Z. L., Zeng, L., Li, Z. J., Li, X. N., Tang, M., Yi, W., Gong, J. P., Sun, L. Q. and Cao, Y. (2008) DNazymes targeted to EBV-encoded latent membrane protein-1 induce apoptosis and enhance radiosensitivity in nasopharyngeal carcinoma. *Cancer Lett*, **265**, 226-38.
- Ma, Y., Gao, J., Yin, J., Gu, L., Liu, X., Chen, S., Huang, Q., Lu, H., Yang, Y., Zhou, H., Wang, Y. and Peng, Y. (2016) Identification of a Novel Function of Adipocyte Plasma Membrane-Associated Protein (APMAP) in Gestational Diabetes Mellitus by Proteomic Analysis of Omental Adipose Tissue. *J Proteome Res*, **15**, 628-37.
- Madaan, S., Surgery, I. C. S. o. M., Hammersmith Hospital Campus, London and, Abel, P. D., Surgery, I. C. S. o. M., Hammersmith Hospital Campus, London and, Chaudhary, K. S., and, D. o. H., Hewitt, R., and, D. o. H., Stott, M. A., Department of Urology, R. D. a. E. H., Exeter, UK, Stamp, G. W. H., and, D. o. H., Lalani, E. N. and and, D. o. H. (2016) Cytoplasmic induction and over-expression of cyclooxygenase-2 in human prostate cancer: implications for prevention and treatment. *BJU International*, **86**, 736-741.
- Mahajan, K., Challa, S., Coppola, D., Lawrence, H., Luo, Y., Gevariya, H., Zhu, W., Chen, Y. A., Lawrence, N. J. and Mahajan, N. P. (2010) Effect of Ack1 tyrosine kinase inhibitor on ligand-independent androgen receptor activity. *Prostate*, **70**, 1274-85.
- Mashima, T., Oh-hara, T., Sato, S., Mochizuki, M., Sugimoto, Y., Yamazaki, K., Hamada, J., Tada, M., Moriuchi, T., Ishikawa, Y., Kato, Y., Tomoda, H., Yamori, T. and Tsuruo, T. (2005) p53-defective tumors with a functional apoptosome-mediated pathway: a new therapeutic target. *J Natl Cancer Inst*, **97**, 765-77.
- Massie, C. E., Lynch, A., Ramos-Montoya, A., Boren, J., Stark, R., Fazli, L., Warren, A., Scott, H., Madhu, B., Sharma, N., Bon, H., Zecchini, V., Smith, D. M., Denicola, G. M., Mathews, N., Osborne, M., Hadfield, J., Macarthur, S., Adryan, B., Lyons, S. K., Brindle, K. M., Griffiths, J., Gleave, M. E., Rennie, P. S., Neal, D. E. and Mills, I. G.

- (2011) The androgen receptor fuels prostate cancer by regulating central metabolism and biosynthesis. *Embo j*, **30**, 2719-33.
- Meehan, K. L. and Sadar, M. D. (2004) Quantitative profiling of LNCaP prostate cancer cells using isotope-coded affinity tags and mass spectrometry. *Proteomics*, **4**, 1116-34.
- Millward, M. J., Joshua, A., Kefford, R., Aamdal, S., Thomson, D., Hersey, P., Toner, G. and Lynch, K. (2005) Multi-centre Phase II trial of the polyamine synthesis inhibitor SAM486A (CGP48664) in patients with metastatic melanoma. *Invest New Drugs*, **23**, 253-6.
- Moon, J.-S., Jin, W.-J., Kwak, J.-H., Kim, H.-J., Yun, M.-J., KIM, J.-W. and Kim, K.-S. (2011) Androgen stimulates glycolysis for de novo lipid synthesis by increasing the activities of hexokinase 2 and 6-phosphofructo-2-kinase/fructose-2,6-bisphosphatase 2 in prostate cancer cells.
- Morris, M. A., Dawson, C. W. and Young, L. S. (2009) Role of the Epstein-Barr virus-encoded latent membrane protein-1, LMP1, in the pathogenesis of nasopharyngeal carcinoma. *Future Oncol*, **5**, 811-25.
- Mostaghel, E. A., Plymate, S. R. and Montgomery, B. (2014) Molecular pathways: targeting resistance in the androgen receptor for therapeutic benefit. *Clin Cancer Res*, **20**, 791-8.
- Munger, K., Phelps, W. C., Bubb, V., Howley, P. M. and Schlegel, R. (1989) The E6 and E7 genes of the human papillomavirus type 16 together are necessary and sufficient for transformation of primary human keratinocytes. *J Virol*, **63**, 4417-21.
- Muruve, N. A. (2015) *Prostate Anatomy* [Online]: <http://emedicine.medscape.com/article/1923122-overview-aw2aab6b3>. Last accessed 04/02/15.
- Myung, J.-K., Banuelos, C. A., Fernandez, J. G., Mawji, N. R., Wang, J., Tien, A. H., Yang, Y. C., Tavakoli, I., Haile, S., Watt, K., McEwan, I. J., Plymate, S., Andersen, R. J. and Sadar, M. D. (2013) An androgen receptor N-terminal domain antagonist for treating prostate cancer.
- NCBI (2016a) *GUCY1A2 guanylate cyclase 1 soluble subunit alpha 2 [Homo sapiens (human)] - Gene - NCBI* [Online]: <https://www.ncbi.nlm.nih.gov/pubmed/>. Pubs. Last accessed 4 October.
- NCBI (2016b) *PORCN porcupine homolog (Drosophila) [Homo sapiens (human)] - Gene - NCBI* [Online]: <https://www.ncbi.nlm.nih.gov/pubmed/>. Pubs. Last accessed 5 October.
- NCI (2015) *SEER Training: Morphology & Grade* [Online]: <http://training.seer.cancer.gov/prostate/abstract-code-stage/morphology.html>. National Institute of Health. Last accessed 23/3/15.
- NICE (2014) *NICE Guidelines: Prostate cancer (metastatic, hormone relapsed, not treated with chemotherapy) - abiraterone acetate (with prednisolone)* [Online]: <http://www.nice.org.uk/guidance/gid-tag434/documents/prostate-cancer-metastatic-hormone-relapsed-not-treated-with-chemotherapy-abiraterone-acetate-with-prednisolone-id503-appraisal-consultation-document>. Last accessed 25/3/15.
- NIH (2012) ClinicalTrials.gov - Safety, Efficacy, PK, and PD Characteristics of Orally Inhaled SB010 in Male Patients With Mild Asthma (Multiple Dose). 28/11/12 ed.: NIH.
- NIH (2014a) ClinicalTrials.gov - Efficacy, Pharmacokinetics, Tolerability, Safety of SB012 Intrarectally Applied in Active Ulcerative Colitis Patients (SECURE). 30/4/14 ed.

- NIH (2014b) ClinicalTrials.gov - Efficacy, Safety, Tolerability, Pharmacokinetics and Pharmacodynamics Study of the Topical Formulation SB011 Applied to Lesional Skin in Patients With Atopic Eczema. 4/3/15 ed.: NIH.
- Njar, V. C. and Brodie, A. M. (2015) Discovery and Development of Galeterone (TOK-001 or VN/124-1) for the Treatment of All Stages of Prostate Cancer. *J Med Chem*, **58**, 2077-87.
- Oliveira, P. F., Martins, A. D., Moreira, A. C., Cheng, C. Y. and Alves, M. G. (2015) The Warburg effect revisited--lesson from the Sertoli cell. *Med Res Rev*, **35**, 126-51.
- Pegg, A. E. (2006) Regulation of ornithine decarboxylase. *J Biol Chem*, **281**, 14529-32.
- Penning, T. M. (2015) Mechanisms of Drug Resistance that Target the Androgen Axis in Castration Resistant Prostate Cancer (CRPC). *J Steroid Biochem Mol Biol*, **153**, 105-13.
- Petersen, M. and Wengel, J. (2003) LNA: a versatile tool for therapeutics and genomics. *Trends Biotechnol*, **21**, 74-81.
- Petrylak, D. P. (2003) Docetaxel for the Treatment of Hormone-Refractory Prostate Cancer. *Rev Urol*, **5**, S14-21.
- Petrylak, D. P., Tangen, C. M., Hussain, M. H., Lara, P. N., Jr., Jones, J. A., Taplin, M. E., Burch, P. A., Berry, D., Moinpour, C., Kohli, M., Benson, M. C., Small, E. J., Raghavan, D. and Crawford, E. D. (2004) Docetaxel and estramustine compared with mitoxantrone and prednisone for advanced refractory prostate cancer. *N Engl J Med*, **351**, 1513-20.
- Pine, A. (2016) Advances in genetics: widening our understanding of prostate cancer - F1000Research.
- Pirisi, L., Yasumoto, S., Feller, M., Doniger, J. and DiPaolo, J. A. (1987) Transformation of human fibroblasts and keratinocytes with human papillomavirus type 16 DNA. *J Virol*, **61**, 1061-6.
- Pizer, E. S., Pflug, B. R., Bova, G. S., Han, W. F., Udan, M. S. and Nelson, J. B. (2001) Increased fatty acid synthase as a therapeutic target in androgen-independent prostate cancer progression. *Prostate*, **47**, 102-10.
- Pizer, E. S., Thupari, J., Han, W. F., Pinn, M. L., Chrest, F. J., Frehywot, G. L., Townsend, C. A. and Kuhajda, F. P. (2000) Malonyl-Coenzyme-A Is a Potential Mediator of Cytotoxicity Induced by Fatty-Acid Synthase Inhibition in Human Breast Cancer Cells and Xenografts.
- Pless, M., Belhadj, K., Menssen, H. D., Kern, W., Coiffier, B., Wolf, J., Herrmann, R., Thiel, E., Bootle, D., Sklenar, I., Muller, C., Choi, L., Porter, C. and Capdeville, R. (2004) Clinical efficacy, tolerability, and safety of SAM486A, a novel polyamine biosynthesis inhibitor, in patients with relapsed or refractory non-Hodgkin's lymphoma: results from a phase II multicenter study. *Clin Cancer Res*, **10**, 1299-305.
- Possemato, R., Marks, K. M., Shaul, Y. D., Pacold, M. E., Kim, D., Birsoy, K., Sethumadhavan, S., Woo, H. K., Jang, H. G., Jha, A. K., Chen, W. W., Barrett, F. G., Stransky, N., Tsun, Z. Y., Cowley, G. S., Barretina, J., Kalaany, N. Y., Hsu, P. P., Ottina, K., Chan, A. M., Yuan, B., Garraway, L. A., Root, D. E., Mino-Kenudson, M., Brachtel, E. F., Driggers, E. M. and Sabatini, D. M. (2011) Functional genomics reveal that the serine synthesis pathway is essential in breast cancer. *Nature*, **476**, 346-50.
- Prostate, T. (2016a) *Staging of Prostate Cancer* [Online]: <http://www.tackleprostate.org/staging-of-prostate-cancer.php>. Last accessed 3 October.
- Prostate, T. (2016b) *The Gleason Score* [Online]: <http://www.tackleprostate.org/the-gleason-score.php>. tackleprostate.org. Last accessed 3 October.

- Proverbs-Singh, T., Feldman, J., Morris, M. J., Autio, K. and Traina, T. (2015) Targeting the androgen receptor in prostate and breast cancer: several new agents in development. *Endocr Relat Cancer*.
- Ramadan, W. H., Kabbara, W. K. and Al Basiouni Al Masri, H. S. (2015) Enzalutamide for patients with metastatic castration-resistant prostate cancer. *Onco Targets Ther*, **8**, 871-6.
- Rapa, I., Volante, M., Migliore, C., Farsetti, A., Berruti, A., Vittorio Scagliotti, G., Giordano, S. and Papotti, M. (2013) Human ASH-1 promotes neuroendocrine differentiation in androgen deprivation conditions and interferes with androgen responsiveness in prostate cancer cells. *Prostate*, **73**, 1241-9.
- Rasila, T., Lehtonen, A., Kanerva, K., Mäkitie, L. T., Haglund, C. and Andersson, L. C. (2016) Expression of ODC Antizyme Inhibitor 2 (AZIN2) in Human Secretory Cells and Tissues. *PLoS One*, **11**.
- Reyes-Gutierrez, P. and Alvarez-Salas, L. M. (2009) Cleavage of HPV-16 E6/E7 mRNA mediated by modified 10-23 deoxyribozymes. *Oligonucleotides*, **19**, 233-42.
- Roehr, B. (1998) Fomivirsen approved for CMV retinitis. *J Int Assoc Physicians AIDS Care*, **4**, 14-6.
- Ros, S., Santos, C. R., Moco, S., Baenke, F., Kelly, G., Howell, M., Zamboni, N. and Schulze, A. (2012) Functional metabolic screen identifies 6-phosphofructo-2-kinase/fructose-2,6-biphosphatase 4 as an important regulator of prostate cancer cell survival. *Cancer Discov*, **2**, 328-43.
- Rowland, J. G., Robson, J. L., Simon, W. J., Leung, H. Y. and Slabas, A. R. (2007) Evaluation of an in vitro model of androgen ablation and identification of the androgen responsive proteome in LNCaP cells. *Proteomics*, **7**, 47-63.
- Rulten, S. L., Kinloch, R. A., Tateossian, H., Robinson, C., Gettins, L. and Kay, J. E. (2006) The human FK506-binding proteins: characterization of human FKBP19. *Mamm Genome*, **17**, 322-31.
- Sahin, E., Elboga, U., Kalender, E., Basibuyuk, M., Demir, H. D. and Celen, Y. Z. (2015) Clinical significance of incidental FDG uptake in the prostate gland detected by PET/CT. *Int J Clin Exp Med*, **8**, 10577-85.
- SantaLucia, J. (1998) A unified view of polymer, dumbbell, and oligonucleotide DNA nearest-neighbor thermodynamics. *Proc Natl Acad Sci U S A*.
- Santoro, S. W. and Joyce, G. F. (1997) A general purpose RNA-cleaving DNA enzyme. *Proc Natl Acad Sci U S A*, **94**, 4262-6.
- Santos, C. R., Translational Cancer Therapeutics, C. R. U. L. R. I., UK, Schulze, A. and Gene Expression Analysis Laboratory, C. R. U. L. R. I., UK (2016) Lipid metabolism in cancer. *The FEBS Journal*, **279**, 2610-2623.
- Schalken, J. and Fitzpatrick, J. M. (2016) Enzalutamide: targeting the androgen signalling pathway in metastatic castration-resistant prostate cancer. *BJU Int*, **117**, 215-25.
- Seiler, N. and Raul, F. (2005) Polyamines and apoptosis. *J Cell Mol Med*, **9**, 623-42.
- Semenas, J., Allegrucci, C., Boorjian, S. A., Mongan, N. P. and Persson, J. L. (2012) Overcoming drug resistance and treating advanced prostate cancer. *Curr Drug Targets*, **13**, 1308-23.
- Shoolingin-Jordan, P. M., Al-Daihan, S., Alexeev, D., Baxter, R. L., Bottomley, S. S., Kahari, I. D., Roy, I., Sarwar, M., Sawyer, L. and Wang, S. F. (2003) 5-Aminolevulinic acid synthase: mechanism, mutations and medicine. *Biochim Biophys Acta*, **1647**, 361-6.

- Sloane, B. F., Moin, K., Krepela, E. and Rozhin, J. (1990) Cathepsin B and its endogenous inhibitors: the role in tumor malignancy. *Cancer Metastasis Rev*, **9**, 333-52.
- Somerville, L. L. and Wang, K. (1981) The ultrasensitive silver "protein" stain also detects nanograms of nucleic acids. *Biochem Biophys Res Commun*, **102**, 53-8.
- Sood, V., Gupta, N., Bano, A. S. and Banerjea, A. C. (2007) DNA-enzyme-mediated cleavage of human immunodeficiency virus type 1 Gag RNA is significantly augmented by antisense-DNA molecules targeted to hybridize close to the cleavage site. *Oligonucleotides*, **17**, 113-21.
- Srinath, P., Rao, P. N., Knaus, E. E. and Suresh, M. R. (2003) Effect of cyclooxygenase-2 (COX-2) inhibitors on prostate cancer cell proliferation. *Anticancer Res*, **23**, 3923-8.
- Steinestel, J., Luedeke, M., Arndt, A., Schnoeller, T. J., Lennerz, J. K., Wurm, C., Maier, C., Cronauer, M. V., Steinestel, K. and Schrader, A. J. (2015) Detecting predictive androgen receptor modifications in circulating prostate cancer cells. *Oncotarget*.
- Supuran, C. T. (2008) Carbonic anhydrases: novel therapeutic applications for inhibitors and activators. *Nat Rev Drug Discov*, **7**, 168-81.
- Supuran, C. T. (2011) Carbonic anhydrase inhibitors and activators for novel therapeutic applications. *Future Med Chem*, **3**, 1165-80.
- Takayama, K. and Inoue, S. (2013) Transcriptional network of androgen receptor in prostate cancer progression. *Int J Urol*, **20**, 756-68.
- Takayama, K., Kaneshiro, K., Tsutsumi, S., Horie-Inoue, K., Ikeda, K., Urano, T., Ijichi, N., Ouchi, Y., Shirahige, K., Aburatani, H. and Inoue, S. (2007) Identification of novel androgen response genes in prostate cancer cells by coupling chromatin immunoprecipitation and genomic microarray analysis. *Oncogene*, **26**, 4453-63.
- Talluri, R. and Shete, S. (2015) Evaluating Methods for Modeling Epistasis Networks with Application to Head and Neck Cancer. *Cancer Inform*, **14**, 17-23.
- Tan, T. M. and Ting, R. C. (1995) In vitro and in vivo inhibition of human papillomavirus type 16 E6 and E7 genes. *Cancer Res*, **55**, 4599-605.
- Tangen, C. M., Faulkner, J. R., Crawford, E. D., Thompson, I. M., Hirano, D., Eisenberger, M. and Hussain, M. (2003) Ten-year survival in patients with metastatic prostate cancer. *Clin Prostate Cancer*, **2**, 41-5.
- Tannock, I. F., de Wit, R., Berry, W. R., Horti, J., Pluzanska, A., Chi, K. N., Oudard, S., Theodore, C., James, N. D., Turesson, I., Rosenthal, M. A. and Eisenberger, M. A. (2004) Docetaxel plus prednisone or mitoxantrone plus prednisone for advanced prostate cancer. *N Engl J Med*, **351**, 1502-12.
- Taplin, M. E. (2007) Drug insight: role of the androgen receptor in the development and progression of prostate cancer. *Nat Clin Pract Oncol*, **4**, 236-44.
- Toren, P. J., Kim, S., Pham, S., Mangalji, A., Adomat, H., Guns, E. S., Zoubeydi, A., Moore, W. and Gleave, M. E. (2015) Anticancer activity of a novel selective CYP17A1 inhibitor in preclinical models of castrate-resistant prostate cancer. *Mol Cancer Ther*, **14**, 59-69.
- Tsao, C. K., Division of Hematology and Medical Oncology, T. T. C. I., Mount Sinai School of Medicine, New York, NY, USA, Galsky, M. D., Division of Hematology and Medical Oncology, T. T. C. I., Mount Sinai School of Medicine, New York, NY, USA, Small, A. C., Division of Hematology and Medical Oncology, T. T. C. I., Mount Sinai School of Medicine, New York, NY, USA, Yee, T., Division of Hematology and Medical Oncology, T. T. C. I., Mount Sinai School of Medicine, New York, NY, USA, Oh, W. K. and Division of Hematology and Medical Oncology, T. T. C. I., Mount Sinai School of Medicine,

- New York, NY, USA (2016) Targeting the androgen receptor signalling axis in castration-resistant prostate cancer (CRPC). *BJU International*, **110**, 1580-1588.
- Universitet, U. (2016a) *Expression of AMD1 in prostate cancer - The Human Protein Atlas* [Online]: <http://www.proteinatlas.org/ENSG00000123505-AMD1/cancer/tissue/prostate+cancer>. Last accessed 4 October.
- Universitet, U. (2016b) *Expression of FASN in prostate cancer - The Human Protein Atlas* [Online]: <http://www.proteinatlas.org/ENSG00000169710-FASN/cancer/tissue/prostate+cancer>. Last accessed 4 October.
- Uysal-Onganer, P., Kawano, Y., Caro, M., Walker, M. M., Diez, S., Darrington, R. S., Waxman, J. and Kypta, R. M. (2010) Wnt-11 promotes neuroendocrine-like differentiation, survival and migration of prostate cancer cells. *Mol Cancer*, **9**, 55.
- van Zuylen, L., Bridgewater, J., Sparreboom, A., Eskens, F. A., de Bruijn, P., Sklenar, I., Planting, A. S., Choi, L., Bootle, D., Mueller, C., Ledermann, J. A. and Verweij, J. (2004) Phase I and pharmacokinetic study of the polyamine synthesis inhibitor SAM486A in combination with 5-fluorouracil/leucovorin in metastatic colorectal cancer. *Clin Cancer Res*, **10**, 1949-55.
- Vander Heiden, M. G., Cantley, L. C. and Thompson, C. B. (2009) Understanding the Warburg effect: the metabolic requirements of cell proliferation. *Science*, **324**, 1029-33.
- Vashchenko, N. and Abrahamsson, P. A. (2005) Neuroendocrine differentiation in prostate cancer: implications for new treatment modalities. *Eur Urol*, **47**, 147-55.
- Vester, B., Hansen, L. H., Lundberg, L. B., Babu, B. R., Sorensen, M. D., Wengel, J. and Douthwaite, S. (2006) Locked nucleoside analogues expand the potential of DNAzymes to cleave structured RNA targets. *BMC Mol Biol*, **7**, 19.
- Vester, B., Lundberg, L. B., Sorensen, M. D., Babu, B. R., Douthwaite, S. and Wengel, J. (2002) LNAzymes: incorporation of LNA-type monomers into DNAzymes markedly increases RNA cleavage. *J Am Chem Soc*, **124**, 13682-3.
- Vester, B., Lundberg, L. B., Sorensen, M. D., Babu, B. R., Douthwaite, S. and Wengel, J. (2004) Improved RNA cleavage by LNAzyme derivatives of DNAzymes. *Biochem Soc Trans*, **32**, 37-40.
- Vias, M., Massie, C. E., East, P., Scott, H., Warren, A., Zhou, Z., Nikitin, A. Y., Neal, D. E. and Mills, I. G. (2008) Pro-neural transcription factors as cancer markers. *BMC Med Genomics*, **1**, 17.
- Wallace, H. M., Fraser, A. V. and Hughes, A. (2003) A perspective of polyamine metabolism. *Biochem J*, **376**, 1-14.
- Wang, D. and Dubois, R. N. (2010) Eicosanoids and cancer. *Nat Rev Cancer*, **10**, 181-93.
- Wang, W., Bergh, A. and Damber, J.-E. (2005) Cyclooxygenase-2 Expression Correlates with Local Chronic Inflammation and Tumor Neovascularization in Human Prostate Cancer. *Clin Cancer Res*, **11**.
- Wang, Z., Luo, F., Li, L., Yang, L., Hu, D., Ma, X., Lu, Z., Sun, L. and Cao, Y. (2010) STAT3 activation induced by Epstein-Barr virus latent membrane protein1 causes vascular endothelial growth factor expression and cellular invasiveness via JAK3 And ERK signalling. *Eur J Cancer*, **46**, 2996-3006.
- Ward, P. S. and Thompson, C. B. (2012) Metabolic Reprogramming: A Cancer Hallmark Even Warburg Did Not Anticipate. *Cancer Cell*, **21**, 297-308.
- Werness, B. A., Levine, A. J. and Howley, P. M. (1990) Association of human papillomavirus types 16 and 18 E6 proteins with p53. *Science*, **248**, 76-9.

- Wu, Y., Yu, L., McMahon, R., Rossi, J. J., Forman, S. J. and Snyder, D. S. (1999) Inhibition of bcr-abl oncogene expression by novel deoxyribozymes (DNAzymes). *Hum Gene Ther*, **10**, 2847-57.
- Xu, L., Stevens, J., Hilton, M. B., Seaman, S., Conrads, T. P., Veenstra, T. D., Logsdon, D., Morris, H., Swing, D. A., Patel, N. L., Kalen, J., Haines, D. C., Zudaire, E. and St Croix, B. (2014) COX-2 inhibition potentiates antiangiogenic cancer therapy and prevents metastasis in preclinical models. *Sci Transl Med*, **6**, 242ra84.
- Yamamoto, Y., Lorient, Y., Beraldi, E., Zhang, F., Wyatt, A. W., Nakouzi, N. A., Mo, F., Zhou, T., Kim, Y., Monia, B. P., MacLeod, A. R., Fazli, L., Wang, Y., Collins, C. C., Zoubeidi, A. and Gleave, M. (2015) Generation 2.5 Antisense Oligonucleotides Targeting the Androgen Receptor and Its Splice Variants Suppress Enzalutamide-Resistant Prostate Cancer Cell Growth. *Clin Cancer Res*.
- Yang, G. Z., Hu, L., Cai, J., Chen, H. Y., Zhang, Y., Feng, D., Qi, C. Y., Zhai, Y. X., Gong, H., Fu, H., Cai, Q. P. and Gao, C. F. (2015) Prognostic value of carbonic anhydrase VII expression in colorectal carcinoma. *BMC Cancer*.
- Yang, P., Cartwright, C. A., Li, J., Wen, S., Prokhorova, I. N., Shureiqi, I., Troncoso, P., Navone, N. M., Newman, R. A. and Kim, J. (2012) Arachidonic acid metabolism in human prostate cancer. *Int J Oncol*, **41**, 1495-503.
- Yarla, N. S., Bishayee, A., Sethi, G., Reddanna, P., Kalle, A. M., Dhananjaya, B. L., Dowluru, K. S., Chintala, R. and Duddukuri, G. R. (2016) Targeting arachidonic acid pathway by natural products for cancer prevention and therapy. *Semin Cancer Biol*.
- Yi Lau, G. T. and Leung, L. K. (2010) The dietary flavonoid apigenin blocks phorbol 12-myristate 13-acetate-induced COX-2 transcriptional activity in breast cell lines. *Food Chem Toxicol*, **48**, 3022-7.
- Yip, K. W., Zhang, Z., Sakemura-Nakatsugawa, N., Huang, J. W., Vu, N. M., Chiang, Y. K., Lin, C. L., Kwan, J. Y. Y., Yue, S., Jitkova, Y., To, T., Zahedi, P., Pai, E. F., Schimmer, A. D., Lovell, J. F., Sessler, J. L. and Liu, F. F. (2014) A Porphodimethene Chemical Inhibitor of Uroporphyrinogen Decarboxylase. *PLoS One*, **9**.
- Yoo, M. S., Chun, H. S., Son, J. J., DeGiorgio, L. A., Kim, D. J., Peng, C. and Son, J. H. (2003) Oxidative stress regulated genes in nigral dopaminergic neuronal cells: correlation with the known pathology in Parkinson's disease. *Brain Res Mol Brain Res*, **110**, 76-84.
- Zhang, L., Kang, L., Bond, W. and Zhang, N. (2009) Interaction between syntaxin 8 and HECTd3, a HECT domain ligase. *Cell Mol Neurobiol*, **29**, 115-21.
- zur Hausen, H. (1996) Papillomavirus infections--a major cause of human cancers. *Biochim Biophys Acta*, **1288**, F55-78.

